Mathematical Modelling of Ultrasensitivity in Enzyme-Mediated Reactions

by

Cailan Jeynes-Smith

Bachelor of Mathematics

School of Mathematical Sciences

Science and Engineering Faculty

Queensland University of Technology

Submitted in fulfillment of the

requirements for the degree of

Master of Philosophy

2020

Keywords: mathematical modelling; enzyme-kinetics; ultrasensitivity; chemical reaction networks; covalent-modification; network motifs; dynamical systems; stochastic simulation.

In accordance with the requirements of the degree of Master of Philosophy in the School of Mathematical Sciences, I present the following thesis entitled,

Mathematical Modelling of Ultrasensitivity in Enzyme-Mediated Reactions.

This work was performed under the supervision of Dr Robyn Araujo and Dr Pamela Burrage. The work contained in this thesis has not been previously submitted to meet requirements for an award at this or any other higher education institution. To the best of my knowledge and belief, the thesis contains no material previously submitted or written by another person except where due reference is made.

Signed,
QUT Verified Signature

Cailan Jeynes-Smith
20 November 2019

Acknowledgments

I would like to extend my deepest gratitudes for the guidance of my supervisors, Robyn and Pamela. I appreciate their support in helping me access job opportunities through the university and their direction and guidance throughout my research experience.

I would also like to acknowledge the Institute of Health and Biomedical Innovation, the School of Mathematical Sciences and ANZIAM, all of which provided me with the financial support necessary to travel to conferences. I appreciate the support greatly.

Abstract

Ultrasensitivity is a particularly interesting dose-response behaviour found in cascade structures, such as cell signalling networks (the failure of which is linked to the development of some cancers), and robust perfect adaptation mechanisms, observed in signal transduction and gene regulation. Ultrasensitivity has previously been investigated in reversible covalent-modification cycles under the assumption that the substrate concentrations exist in vast excess over the enzyme concentrations. Here we furthered this investigation by using a variety of analytic and numeric models to examine the detrimental effect on ultrasensitivity of introducing comparable concentrations of enzyme and substrate. This required us to introduce new terms to the nomenclature in order to describe the new behaviours which we observed, namely the conversion potential, mid-conversion stimulus, and mixed-sensitivity. This analysis also comprised of a thorough investigation into how the parameter regimes associated with this system effect these new behaviours and ultrasensitivity. We then proposed two novel strategies of positive autoregulation into the covalent-modification cycle to attempt and improve the dose-response profiles. Here we observed that the new models were able to improve on the ultrasensitivity and conversion potential, but at the expense of introducing the potential for bistability.

Contents

1 Introduction

The seminal work of Fischer and Krebs [40, 56] in the 1950s established a conclusive link between reversible protein phosphorylation and signal transmission in intracellular protein networks. Protein phosphorylation is an example of enzyme-mediated covalent-modification. It involves an enzyme, called a kinase, that phosphorylates (adds a phosphate to) a protein and another enzyme, called a phosphatase, that dephosphorylates (removes a phosphate from) a protein. Reversible covalent-modification by two independent enzymes gives rise to a "covalent-modification cycle" (see Figure 1a). We then typically observe the output from one cycle (e.g. phosphorylated form of the protein) acts as an enzyme (e.g. kinase) for another protein. This forms a cascade of covalent-modification cycles which Fischer and Krebs identified as a fundamental mechanism for cell signalling in the development of skeletal muscle in rabbits [56]. More recently with the complete sequencing of the human genome [22] and the advance in technologies with the capability to accurately measure protein abundance and post-translational modification, particularly in cell signalling pathways [6, 17, 57, 43], disruptions to these signalling networks have been linked to the development of particular cancers [37, 42]. Defects in these signalling pathways are in fact considered to be the underlying cause of most human diseases, and are particularly true in the case of cancers [48, 52, 38, 7]. Understanding how signalling is regulated through enzyme mediated networks could potentially have extensive applications in medical sciences, particularly when considering the development of molecular-level treatments [7].

The reversible covalent-modification cycle has already been found to exhibit sophisticated input-output responses as first revealed by the work of Goldbeter and Koshland in the early 1980s [26, 20]. The focus of this report will be to use mathematical modelling, firstly to perform a thorough review of the work by Goldbeter and Koshland on this mechanism and extend their investigation into this cycle. We later introduce variations to this system and examine their ability to obtain the same input-output responses.

Of particular interest in the reversible covalent-modification cycle is the input-output response called ultrasensitivity. This essentially describes a behaviour in which the substrate in a system is rapidly converted into its active or modified form over only a small increase in input. An example of this can be seen in Figure 1b. Ultrasensitivity is important as we find this in a number of signalling networks such as in the maturation of oocytes to form egg cells. In this system we are particularly interested in this "all-or-none" dose response which is representative of ultrasensitivity [19]. It also plays a key role in a number of larger mechanisms such as the cascade structure which is typically associated with cell signalling pathways [23, 40, 56] and in robust perfect adaptation in which ultrasensitivity-generating mechanisms are embedded into a negative feedback loop [8].

Goldbeter and Koshland were the first to identify the phenomenon of "zero-order" ultrasensitivity, which involved having a much higher concentration of substrate than the enzyme concentrations. For each of the two enzyme-mediated reactions, the rate of production of the output is independent of the substrate concentration. Hence we say that this is zero-order in the substrate, and therefore zero-order ultrasensitivity. This assumption enabled Goldbeter and Koshland to remove a dependence on intermediate complexes which resulted in obtaining an explicit analytic solution to this system. However more recent research [11] has shown that it may be unlikely to have the abundant substrate concentration required to achieve zero-order ultrasensitivity. The original report on zero-order ultrasensitivity also had a large focus on profiles obtained using rate constants that were identical for the two independent enzyme mediated reactions (such as Figure 1b). However in a real biological system, this constraint on parameters is much less likely to be able to occur [42].

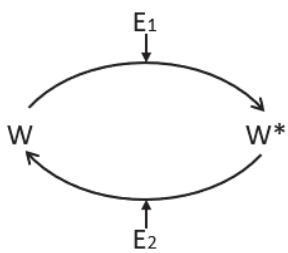

(a) Schematic of Reversible Covalent-Modification Cycle

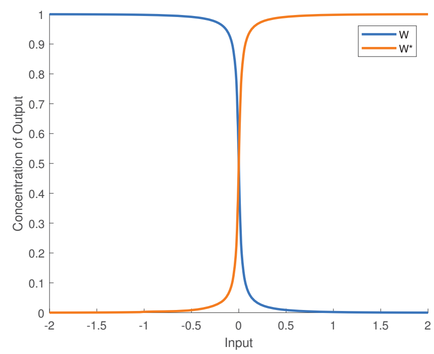

(b) Ultrasensitive Protein Concentration Profile

Figure 1: Schematic of reversible covalent-modification cycle (left) represents the modification of the unmodified substrate, W, to create W^* via a reaction with E_1. This modified substrate, W^*, can then return to the unmodified form via a reaction with E_2. The protein concentration profile (right) is an example of an ultrasensitive response. This is characterised by the rapid change in the substrate concentrations. We later consider the input to this system to be the total concentration of the E_1 enzyme. The output is also expressed as a percentage of the total substrate i.e. $W_{tot} = W + W^*$.

One of the key aims of this report is to thoroughly investigate the links between the parameter regimes that govern a covalent modification cycle and ultrasensitive responses. This work aims to extend on that done by Goldbeter and Koshland and develop other conditions on how to achieve ultrasensitivity. In order to do this we will thoroughly investigate the effect that altering the abundant substrate constraint will have on the cycle's ability to achieve ultrasensitive behaviour. In particular there is a focus on having comparable concentrations of enzyme and substrate and examining under what circumstances ultrasensitivity can still be achieved. This report also increases the focus on the intermediate complexes and the major role that these have on ultrasensitivity. To perform this analysis, it has also required a number of new terms to be introduced, in particular "conversion potential" and "mid-conversion stimulus". Here the conversion potential refers to the maximum concentration of modified substrate that a system is able to achieve for a given parameter regime. The mid-conversion stimulus (M-value) refers to the amount of input required for the concentrations of modified and unmodified substrate to be equal. These terms become essential for describing the behaviour of the systems that this report will investigate. This is particularly true when investigating the effect of altering the rate constants and examining the effect that each of these has on the behaviour of the system.

It is also of interest to investigate how ultrasensitive behaviour can be achieved in variations on the reversible covalent-modification cycle and whether these are capable of improving upon the ultrasensitivity achieved in the original cycle. In this report, we investigate implementing positive-autoregulatory mechanisms into the system. Positive-autoregulation (PAR) involves the output of a system increasing its own production. This can either occur directly or indirectly. For this report we investigate an implementation of both direct and indirect PAR. For the direct PAR this was done by including a third reaction in the system where the modified substrate acts as an enzyme and catalyses the unmodified substrate to create more modified substrate. The indirect PAR is implemented by introducing a condition on the enzyme that catalyses the unmodified substrate to create the modified substrate, whereby it must now form a complex with the modified substrate before it is able to catalyse the unmodified substrate. These are then compared with the original reversible covalent-modification cycle using similar parameter regimes to examine whether these variations are able to improve upon the ultrasensitivity achieved by the original.

Throughout this investigation this report will be using numerical deterministic and stochastic mathematical methods. Deterministic methods give an exact solution to the system based on the initial condition. This will give profiles similar to what is observed in the paper by Goldbeter and Koshland [26]. The discrete stochastic approach used allows for more realistic, integer-based simulations of a single cell's behaviour. A simulation is then repeated a large number of times and can be averaged to achieve similar profiles to the deterministic method. It is also of interest to examine the variability between the simulations. This allows for a different interpretation of ultrasensitivity. Analytic solutions are also investigated for each of the systems described.

1.1 Literature Review and Background

1.1.1 Early Mathematical Models of Biochemical Reactions

Experimental data on biological systems has provided the scientific community with tremendous amounts of information, but does not provide us with the insight required to understand the underlying mechanisms responsible for these observations [29]. Obtaining experimental data is also expensive and prone to error [36]. For this reason, being able to apply mathematics and create models that describe the functionality of such biological systems can potentially reduce the dependence on experimental data and optimise experimental processes.

One of the first attempts at describing biochemical reactions mathematically was in the form of mass-action equations. In the 1860's, Guldberg and Waage published a series of four papers [27, 28] in which they proposed the concepts of affinity between two reactant molecules in a chemical reaction. In these papers the affinity of a system was a measure of its reactive potential [45, 53], which was defined mathematically to be proportional to the concentration of the reactants [28, 45, 53]. For example, consider a system defined by the reactions

$$A + B \rightleftharpoons A' + B', \tag{1}$$

where A and B are molecules that participate in a reversible reaction to create two new molecules, A' and B'. According to an English translation and summary [54] of the first paper by Guldberg and Waage, the original equation for the affinity of a system was given by

$$\text{affinity} = \alpha[A]^a[B]^b,$$

where a, b and α are constants, and $[X]$ represents the concentration of molecule X. This form was used to match the experimental data by Guldberg and Waage. The experimental data shown in the initial reports [27] demonstrated that in all cases $a = 1$ and in the majority of cases $b \approx 1$. Since the data strongly supported the use of exponents that were approximately unity, Guldberg and Waage released a subsequent paper in 1867 [28] where the equation was given by

$$\text{affinity} = \alpha[A][B],$$

which is now the accepted form of this expression [45].

This concept led directly to the development of the Law of Mass-Action [28, 45, 53], which has become one of the most influential guiding principles in the mathematical descriptions of chemical reactions. According to the Law of Mass-Action, the rate of a reaction is proportional to the product of the concentrations of the reactants. For example, the mass-action equation related to the rate reaction for A in (1) consists of summing the affinities for the proteins removal and creation and would be written as

$$\frac{\mathrm{d}[A]}{\mathrm{d}t} = -k[A][B] + k'[A'][B'],$$

where k is the rate constant associated with the forward reaction, and k' is associated with the reverse reaction. This gives rise to an ordinary differential equation (ODE) for each molecule involved in a chemical reaction, and ultimately, a system of coupled ODEs to describe networks of interconnected chemical reactions. The mass-action equations have been extensively studied and applied. See [53] for a recent comprehensive review.

1.1.2 Modelling Enzyme Kinetics

In cellular signalling, enzyme-mediated reactions are of paramount importance [23, 40, 56]. Enzymes are special proteins that play the role of a catalyst, and are required for many biochemical reactions [45]. These enzyme catalysts reduce the energy required for the reaction to proceed, thereby speeding up the reactions, whilst being conserved in the reaction itself [34]. In 1913, Michaelis and Menten studied the basic mechanism underlying an enzyme-mediated reaction in biochemistry [29]. These investigators proposed the following basic reaction mechanism

$$E + S \underset{\mathrm{k}_2}{\overset{\mathrm{k}_1}{\rightleftharpoons}} C \overset{\mathrm{k}_3}{\rightarrow} E + P. \tag{2}$$

This mechanism involves three distinct reactions. The enzyme, E, combines with an inactive substrate, S, to form a complex, C, at rate k_1. This complex can then split without having activated the substrate, at rate k_2. Alternatively, this complex can allow for the activation of the substrate which then releases the enzyme from its bind with the activated substrate, P. This occurs at rate k_3. We often refer to the activated form of the substrate as the product.

Michaelis and Menten applied the reaction mechanism (2) to study the enzyme, invertase, in certain metabolic reactions and were able to develop an analytic expression to match their experimental results [44, 36]. Using specific conditions on experimental data, they created the well-known equation.

$$V = \frac{\mathrm{d}P}{\mathrm{d}t} = \frac{V_{\max}[S]}{K_m + [S]} \tag{3}$$

This describes the saturated behaviour of the production rate of the activated substrate as a function of its inactive form. Note that $V_{\max} = k_3 E_{tot}$, where E_{tot} is the total concentration of enzyme, represents the maximum production rate and $K_m = \frac{k_2+k_3}{k_1}$ is known as the Michaelis constant. Applying the Michaelis-Menten equation, where $V_{\max} = K_m = 1$, creates the plot as seen in Figure 2. This behaviour is referred to as being Michaelian or hyperbolic and is characterised by the distinct change in production in that these profiles require an 81-fold increase in input, $[S]$, to alter the output from 10% to 90% of their optimal value ($V_{\max}$). This can be proven mathematically as found in Appendix A.2.

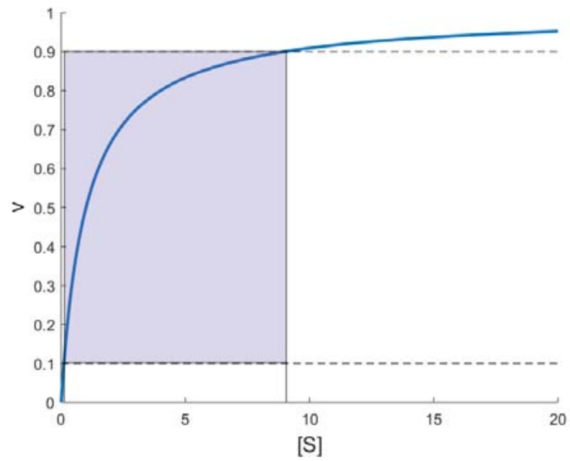

Figure 2: Profile of V with respect to $[S]$ created using the Michaelis-Menten equation with $[S] \in [0, 20]$, and $V_{\max} = K_m = 1$. Highlighted is the section of curve between 10% $V_{\max}$ and 90% $V_{\max}$. This demonstrates the 81-fold increase in input required to achieve this change in output.

The equation itself has since been derived using the full system of mass-action equations and the conservation equations that govern this system. In 1925, twelve years after Michaelis and Menten published their findings, Briggs and Haldane [12] derived the Michaelis-Menten equation using the quasi-steady state assumption. A succinct derivation can be found in Appendix A.1.

1.1.3 Sigmoidal Response Profiles

The work of Michaelis and Menten simplified the modelling of biochemical reactions under certain simplifying conditions and highlighted the phenomenon of enzyme saturation, which could produce the hyperbolic profile shown in Figure 2. In 1910 A. V. Hill had proposed a model for cooperative biochemical reactions, specifically the binding of oxygen and haemoglobin [31]. Cooperative behaviour occurs when an enzyme allows for multiple bindings of substrate i.e. multiple substrate molecules can bind to a single enzyme. Positive cooperativity, as was observed by Hill, requires that, once the enzyme is bound by a substrate, the new complex is easier to bind to by the next substrate, and so on. The equation was given by

$$y = \frac{Kx^n}{1 + Kx^n},$$

where x and y are the concentrations of the input, unbound oxygen, and output, oxygen and haemoglobin complex, respectively [32]. K is the equilibrium constant and n is the number of binding sites on the haemoglobin molecule. This has also been applied for more general systems [24] whereby the equation is given by

$$y = y_{\max} \frac{x^{n_H}}{\mathrm{EC}_{50}^{n_H} + x^{n_H}}, \tag{4}$$

where $y_{\max}$ is the maximum output produced, EC_{50} is the amount of input required to obtain half of the maximum output and n_H is the Hill coefficient. The Hill coefficient is given by

$$n_H = \frac{\log_{10}(81)}{\log_{10}\left(\frac{\mathrm{EC}_{90}}{\mathrm{EC}_{10}}\right)},$$

where the EC_{90} and EC_{10} are the amounts of input required for the output to be 90% and 10% of the maximum output respectively [20, 5].

To demonstrate the effect of the Hill coefficient, the Hill equation shown in equation (4) has been plotted with $y_{\max} = \mathrm{EC}_{50} = 1$ and $n_H = 1, 2, 5$ (Figure 3). It can be seen that as n_H increases, the amount of input required to change the output from 10% to 90% of the maximum output, decreases. It should also be noted that when $n_H = 1$ the Hill equation takes the form of the Michaelis-Menten equation when $V_{\max} = y_{\max}$ and $K_m = \mathrm{EC}_{50}$ [3] and requires an 81-fold increase in x to change the output of y from 10% to 90%. This behaviour has allowed the Hill equation to be used as a method of measuring the sensitivity of profiles [39].

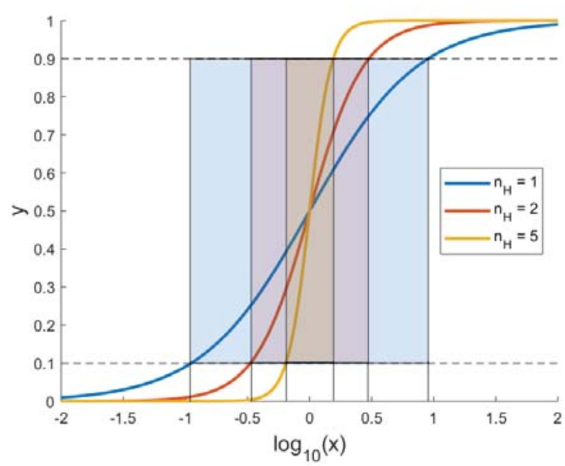

Figure 3: Profiles of the output, y, with respect to the input, x using the Hill equation, with $y_{\max} = \mathrm{EC}_{50} = 1$. The highlighted sections, associated with the colours of the curves, represent the amount of input required to alter the output from $0.1y_{\max}$ to $0.9y_{\max}$. This shows that as the Hill coefficient increases, the change in input required to make this change in output, decreases. As shown, Hill coefficients greater than unity ($n_H > 1$) give rise to ultrasensitive profiles where an increase from $0.1y_{\max}$ to $0.9y_{\max}$ is achieved with less than an 81-fold increase in input (x).

Whilst the Hill equation has been highly influential on modelling the binding of oxygen and haemoglobin, improved models have since been produced. By using concepts from the works of Adair [2] and Pauling [47], Koshland et al. [39] created a model which improves upon the accuracy of the Hill equation and relates the model to the geometry of the problem. The binding of oxygen and haemoglobin is referred to as a cooperative system and through their models, Koshland et al. were able to identify the conditions under which this mechanism displayed sigmoidal behaviour.

1.1.4 Ultrasensitivity

As previously discussed, the Hill equation is closely related to the Michaelis-Menten equation, and is equivalent to the Michaelis-Menten equation when the Hill coefficient is set to unity [3]. The relationship between the Hill coefficient and the sigmoidality of the dose-response has led to the Hill coefficient being used as a measure of steepness in concentration profiles [50, 39]. It was partly also this observation that led to the definition of "ultrasensitivity" in 1981 by Goldbeter and Koshland [26]. Ultrasensitivity was defined by Goldbeter and Koshland as "an output response that is more sensitive to change in stimulus than the hyperbolic (Michaelis-Menten) equation" [26]. In essence, ultrasensitivity is achieved when a system requires less than the 81-fold increase in input to increase from 10% to 90% maximal output. This concept is illustrated in Figure 3 where several ultrasensitive profiles (i.e. with Hill coefficients greater than unity) are compared to a Michaelian (Hill coefficient of unity) profile.

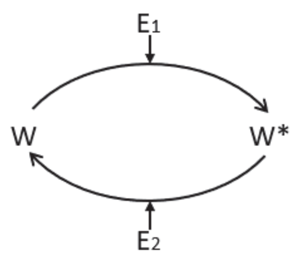

Figure 4: Schematic of the reversible covalent-modification system used by Goldbeter and Koshland. The forward and backward reactions of this system are as described by Michaelis and Menten in their original work, as previously discussed. Note that in this system, E_1 is the enzyme that catalyses the modification of W, creating W^*, whilst E_2 catalyses the unmodification of W^* back to W. Note that the modified forms of the proteins are represented by the addition of an asterisk.

Goldbeter and Koshland were interested in investigating a cycle of covalent-modification reactions, whereby the enzyme-mediated reaction used by Michaelis and Menten, in (2), could be reversed by a second, independent, enzyme as seen in the schematic, Figure 4. Here W and W^* are the unmodified and modified forms, respectively, of the protein substrate and E_1 and E_2 are the two independent respective enzymes. This covalent-modification cycle [26] is the building block of the cascade structures associated with intracellular communication pathways as discussed by Fischer and Krebs [40, 56] in their fundamental work, whereby the enzymes are kinase, for E_1, and phosphatase, for E_2.

We can represent this system with the following set of reactions. These highlight the fact that we have two different enzymes at work in this cycle. The enzyme E_1 binds to W to create the intermediate complex, C_1. Once complexed with W, E_1 catalyses the formation of W^* - the activated (e.g. phosphorylated) form. Similarly E_2 binds to W^*, then catalyses conversion of W^* back to W. These reactions occur independently, with different rate constants for each reaction.

$$W + E_1 \underset{\mathrm{d}_1}{\overset{\mathrm{a}_1}{\rightleftharpoons}} C_1 \overset{\mathrm{k}_1}{\rightarrow} W^* + E_1, \tag{5}$$

$$W^* + E_2 \underset{\mathrm{d}_2}{\overset{\mathrm{a}_2}{\rightleftharpoons}} C_2 \overset{\mathrm{k}_2}{\rightarrow} W + E_2. \tag{6}$$

Goldbeter and Koshland were then specifically interested in the scenario in which there is an abundance of substrate in comparison to the concentrations of enzymes. They were able to define how this system can achieve ultrasensitivity as a function of the magnitude of the non-dimensionalised Michaelis constants for the reactions, $K_1 = \frac{d_1+k_1}{a_1 W_{tot}}$ and $K_2 = \frac{d_2+k_2}{a_2 W_{tot}}$. Their key finding was that when we have very small values of K_1 and K_2 we achieve an ultrasensitive system as seen in Figure 5b. When these values are increased it approaches a Michaelian profile as seen in Figure 5a. This will be discussed in detail in Chapter 2.2.

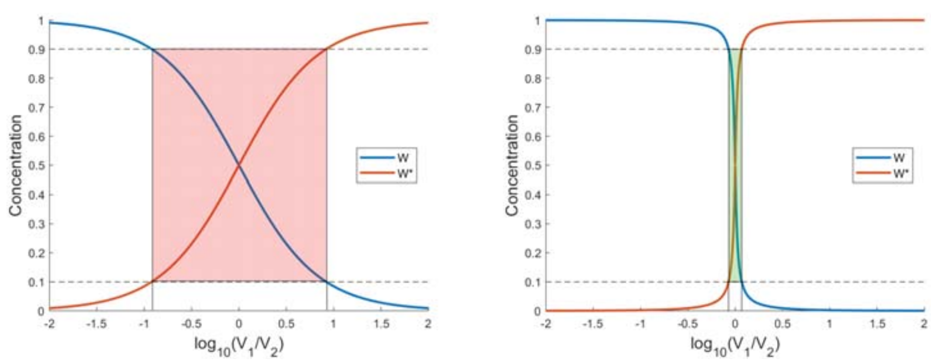

(a) Michaelian protein concentration profile. **(b)** Ultrasensitive protein concentration profile

Figure 5: These profiles were created using the analytic solution created by Goldbeter and Koshland when assuming negligible complex concentrations [26]. The constants were set such that $W_{tot} = 100$ and $\frac{V_1}{V_2} \in \{10^{-2}, 10^2\}$. For a) the non-dimensionalised Michaelis constants are given by $K_1 = K_2 = 1$, whilst for b) the Michaelis constants are given by $K_1 = K_2 = 0.02$. The highlighted sections demonstrate the input required to change the output concentration of W^* from 0.1 to 0.9. In a) it can be seen that this requires an approximate 81-fold increase and is therefore approximately Michaelian, whereas b) required much less than an 81-fold increase and is therefore ultrasensitive.

Goldbeter and Koshland also investigated the effect of reducing enzyme saturation using an analytic solution that included the proteins and complexes. This led to the finding that as the abundance of enzymes approached the abundance of protein substrate, the concentrations of the free, modified and unmodified substrates approached zero.

1.1.5 Alternative Ultrasensitivity-Generating Mechanisms

Since the discovery of zero-order ultrasensitivity by Goldbeter and Koshland, several other mechanisms for generating ultrasensitivity have been explored. A detailed review by Ferrell and Ha [18] discuss a variety of alternative mechanisms that can produce this response. A few of the systems considered in their analysis included reciprocal regulation, feed-forward regulation, stoichiometric inhibitors, competing substrates, and positive feedback loops. The analysis carried out by Ferrell and Ha is predominantly analytical with a few exceptions. However in a number of these solutions, in order to create the analytic solutions, Ferrell and Ha, have introduced a number of simplifying assumptions for each system.

Reciprocal Regulation

Ultrasensitive dose-responses can be created using reciprocal regulation [18]. Reciprocal regulation, as discussed by Ferrell and Ha [18], involves an input both activating the forward reaction and inhibiting the backward reaction of a reversible covalent-modification system. The example investigated by Ferrel and Ha can be seen in Figure 6. This involves the input to the system converting the inactive form of E_1 and creating its active form which can then be used to catalyse the forward reaction. The input also removes the active form E_2 by converting it into its inactive form. This behaviour has been found in skeletal muscle cells, whereby reciprocal regulation increases the production of insulin [1]. Ferrell and Ha created an analytic solution using the mass-action equations to obtain the following expression for the concentration of the modified substrate, W^*.

$$\frac{XP}{X_{tot}} = \frac{K_2 input + input^2}{K_1 K_2 K_3 + (K_2 + K_2 K_3) input + input^2}$$

where K_1, K_2 and K_3 are the fraction of rate constants associated with linking the enzymes E_1 and E_2 to the input and the creation of W^* from W respectively such that $K_* = \frac{k_{-*}}{k_*}$. Using this they found that the ultrasensitivity of the system is dependent on the rate constant associated with inhibition, K_1, being larger than that associated with activation, K_2. If $K_1 = K_2 = K_3 = 1$ then the system was Michaelian.

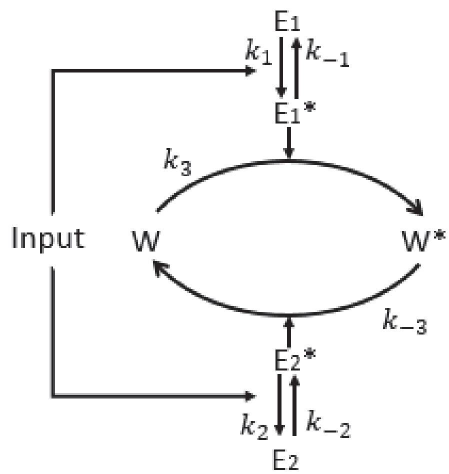

Figure 6: Schematic of a system of reactions which use a reciprocal regulation mechanism. This is built on a reversible covalent-modification system, where an input is used to activate the enzymes, E_1 and E_2, before they can be used in the modification and un-modification of W and W^* respectively. Note that the active forms of the enzymes are represented by the addition of an asterisk.

Feed-Forward Regulation

This form of reciprocal regulation, can also be seen as a form of feed-forward regulation, whereby the input to the system is both directly and indirectly contributing to the production of the output [18]. Ferrell and Ha discuss another form of feed-forward regulation found in the role of Phosphatidylinositol (3,4,5)-trisphosphate (PIP_3). PIP_3 is part of a signalling cascade found on the cell membrane [14]. This system involves an enzyme, Akt, being bound to the membrane by PIP_3. Akt is then activated by PIP_3 bound $Pdk1$ (See Figure 7). PIP_3 is therefore contributing directly to the activation of Akt by bringing it to the $Pdk1$ and indirectly by binding the $Pdk1$ as well. Ferrell and Ha investigated this system by creating an analytic solution to describe its behaviour. From this they found that if the constants for binding Akt and $Pdk1$ to PIP_3 are much stronger than the activation of Akt, then ultrasensitivity can be achieved.

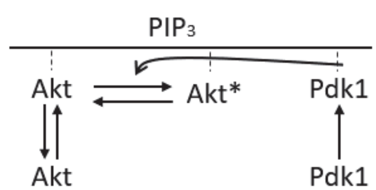

Figure 7: Schematic of a system of reactions which use a feed-forward regulation mechanism. This system represents the activation of Akt by $Pdk1$. PIP_3 works at directly and indirectly activating Akt. PIP_3 attaches Akt and $Pdk1$ to the membrane, where $Pdk1$ is then used to catalyse the activation of Akt. Adapted from Figure 7 in [18]

Stoichiometric Inhibitors

Another mechanism for generating ultrasensitivity has been found in systems with stoichiometric inhibitors [18]. Ferrell and Ha describe an example whereby a reversible covalent-modification system has the addition of an inhibitor which binds to the enzyme that activates the substrate, as seen in Figure 8. Ferrell and Ha [18] developed another analytic model to investigate this system. However modelling this was very complex and required assuming the exclusion of a term for the concentration of E_2. However making this assumption led them to find that ultrasensitivity was dependent on the rate constant for the creation of the inhibitor complex being greater than the rate constant for the activation of the substrate. This combination results in a threshold where the inhibitor binding to the enzyme slows the creation of enzyme-substrate complexes. It is only when this complex is greater than the concentration of the inhibitor that the substrate begins to be activated at a rapid rate, causing the ultrasensitive profile. When the aforementioned relationship between rate constants does not hold, the profile of the activated substrate appears hyperbolic.

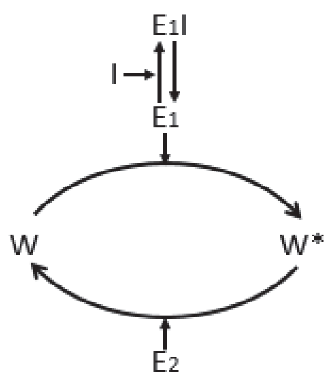

Figure 8: Schematic of a system of reactions which include a stoichiometric inhibitor. The inhibitor, I, attaches to the enzyme, E_1, to form a complex which cannot be used to catalyse the forward reaction of the reversible covalent-modification system.

Competing Substrates

Much like the inhibitor system above, systems with competing substrates can also obtain ultrasensitive responses [18]. However instead of a separate protein in the form of the inhibitor, there is now a reversible covalent-modification system that uses the same enzyme to catalyse the forward reaction (see Figure 9). It has been shown [18] that if there is a dominant system with a larger total substrate and a higher affinity (larger rate constants for the forward reaction), the activated substrate for the less dominant system will have an ultrasensitive profile. This works in much the same way as the inhibitor system whereby the dominant system will originally use the majority of the enzyme, but as it approaches its steady state, the enzyme becomes available for the other system, which uses this at a rapid rate.

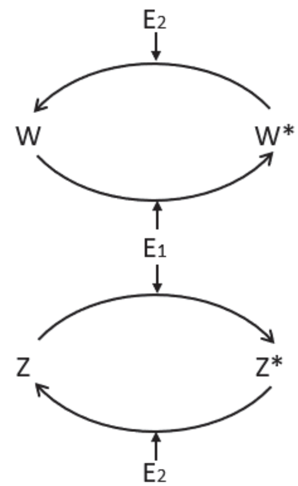

Figure 9: Schematic of a system of reactions that demonstrate competitive substrate behaviour. Pictured are two reversible covalent-modification systems that use the same enzyme, E_1 to modify the different substrates, W and Z.

Cascades

The analytic solution that Goldbeter and Koshland derived for zero-order ultrasensitivity in a reversible covalent-modification cycle was also applied to a bi-cyclic cascade format [26] (see Figure 10). This showed that as the "signal" passes down the cascade, the protein profiles increase in sensitivity. This assumes however that the input to the second loop of the system is the steady state value of the output of the first loop. This essentially results in the assumption that the steady states of the two systems are independent, which has not been found to be the case [51].

The sensitivity of cascades had been examined prior to the work of Goldbeter and Koshland. The works of Chock and Stadtman [49, 13] were aimed at creating mathematical models for mono-cyclic and bi-cyclic cascades. For example, Figure 10 demonstrates the form of a bi-cyclic cascade whereby the output of the upper loop is used to catalyse the substrate in the lower loop. The analysis of these systems was based on analytical solutions created using quasi-steady state assumptions of the mass-action equations that described the systems. The work of Fischer and Krebs [23, 40, 56] has also pushed the need to understand cascade structures. Analytical studies by Ferrell [21] have used the Hill equation when the Hill coefficient is greater than two to demonstrate that the input to a cascade structure is amplified as a signal passes down the cascade. Alternatively, the signal diminishes if the coefficient is less than two and remains unchanged if it is equal. Similar analytic studies by Huang and Ferrell [35] have demonstrated that the output becomes more sensitive as it passes down the cascade as well. This demonstrated that zero-order ultrasensitivity was a contributing factor to the sensitivity of the cascade.

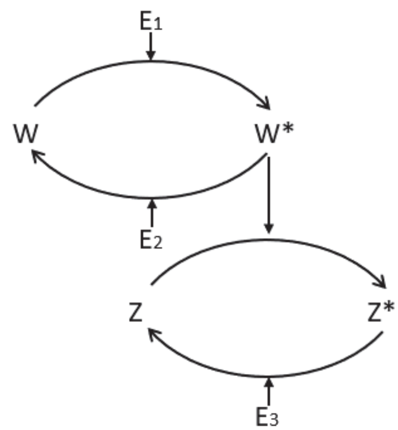

Figure 10: Schematic of a system of reactions in a bi-cyclic cascade format. This cascade is made up of two reversible covalent-modification systems with two different substrates. The systems are connected by the output of the upper system, W^*, being used as the enzyme that modifies the substrate in the lower system, Z.

1.2 Research Objectives and Thesis Structure

This project will investigate two main objectives centered around ultrasensitivity in reversible covalent-modification cycles.

The first objective involves a thorough analysis of the Goldbeter and Koshland mechanism (Chapter 2). As discussed by Goldbeter and Koshland [26], a reversible covalent modification cycle can achieve zero-order ultrasensitivity under conditions of enzyme saturation, which can be readily obtained when the substrates for each of the two reactions in the cycle exist in vast excess over the corresponding enzyme. Consistent with this finding, our preliminary work has suggested that increases in substrate abundance has a negative effect on the ultrasensitivity of the system. The work of Goldbeter and Koshland [26] was theoretical when it was first introduced, and since its publication, it has been observed that the conditions they assumed in regards to excess concentration of substrate in comparison with the enzymes are not typically present in intra-cellular phosphorylation cascades [11]. It is therefore of interest to examine the conditions required to obtain an ultrasensitive response without the assumption of relative substrate abundance. For this reason the main goal of this objective is to investigate how a system with comparable concentrations of enzyme and substrate can achieve an ultrasensitive response, and investigate the role of complexes in this system.

Our analysis of the G-K mechanism investigates the effect of having different Michaelis constants for the forward and reverse reactions. We also thoroughly investigate the role of the individual rate constants as opposed to simply the Michaelis constants. This extends on the work of Goldbeter and Koshland which only focused on the role of the Michaelis constants, and typically these constants were the same for the forward and reverse reactions. In order to compare these different parameter regimes, we have also proposed new terminology which has been crucial for describing the differences in the profiles that we observe. Chapter 2 also involves re-deriving the analytic solutions created by Goldbeter and Koshland, discussing the behaviours in which these solutions can be used to describe and further investigating just how these solutions behave themselves. We also simulate the model using Gillespie's Stochastic Simulation Algorithm which allows for an investigation into how ultrasensitivity can affect the intracellular variability caused by the ultrasensitive signalling response.

The second objective of this thesis is to investigate how ultrasensitive behaviour can be achieved in variations on the reversible covalent-modification cycle, in particular, by implementing direct and indirect positive autoregulation (PAR) mechanisms (Chapter 3). To implement direct PAR a third reaction in the system is included whereby the modified substrate, W^*, acts as an enzyme and forms a complex with the unmodified substrate, W, which it catalyses and creates more W^*. The indirect PAR is implemented by introducing a condition on the E_1 enzyme whereby it may now form a complex with W^* before it then forms a complex with W to create more W^*. It is then of interest to examine how the sensitivity of these systems compare with the original reversible covalent-modification cycle, particularly when there are comparable concentrations of substrate and enzyme. As discussed by Ferrell [18] positive autoregulation can introduce bistable behaviour where a system is highly dependent on its initial condition and can switch between two possible states. This objective also investigates under what circumstances this bistability can occur. The comparison of these two proposed positive autoregulation mechanisms with the original cycle requires the use of the new terminology. In this objective we also derive analytic solutions to these systems and discuss their behaviour. And lastly, we perform a similar analysis of these systems using Gillespie's Stochastic Simulation Algorithm and compared with the results found in the first objective.

Chapter 4 of this thesis reviews the key findings and discusses possible future directions of research.

2 Goldbeter-Koshland (G-K) Mechanism

2.1 Introduction

The term ultrasensitivity was first defined by Goldbeter and Koshland in their 1981 paper [26] in which they observed this special signalling response in a reversible covalent-modification cycle under certain conditions where the protein undergoing conversion between two alternative forms was present at much higher concentrations than the inter-converting enzymes. They referred to this phenomenon as zero-order ultrasensitivity because of the high substrate concentrations saturated the modifying enzymes. In other words, each of the two opposing reactions was independent of (zero-order in) the substrate concentration. As we have previously discussed, this was associated with negligible concentrations of the enzyme-substrate complexes. These complexes however do play a major role in this system, particularly when the system has comparable concentrations of enzyme and substrate. This chapter presents a thorough analysis of this zero-order ultrasensitivity generating mechanism first proposed by Goldbeter and Koshland. We refer to this particular mechanism hereafter as the G-K mechanism to distinguish this model from the autoregulation mechanisms we consider in Chapter 3.

The work of Goldbeter and Koshland had a main focus on substrate abundance and the effect of the Michaelis constants on this system. This focused on a particular case where the Michaelis constants were equal, i.e. $K_{m1} = K_{m2}$. Their analysis then also tended to focus on these constants and not on the effect of the individual rate constants that made up these values.

We extend the analysis of Goldbeter and Koshland in two key ways. First we have focused on the effect that having different Michaelis constants have on the system. In addition to this we also investigate the effect of the individual rate constants that create the Michaelis constants. Throughout the majority of this chapter, we are particularly interested in how this system is able to achieve ultrasensitivity when we include comparable concentrations of enzyme and substrate. Furthermore we will propose some new terminology that allows us to precisely describe the new behaviours that develop under these new conditions. Lastly this chapter shall discuss some other methods for solving this system such as the analytic solutions found by Goldbeter and Koshland [26] and a stochastic method. Using a method such as Gillespie's Stochastic Simulation Algorithm allows for the investigation into how ultrasensitivity can affect the variability of a system. The analytic solutions provide a clear insight into just how the inclusion of the complexes is critical in representing accurate solutions to this system when there are comparable concentrations of enzyme and substrate.

2.2 Basic Properties of the Goldbeter and Koshland System

As noted in Chapter 1, the G-K mechanism concerns the conversion of a single protein between two alternative forms, W and W^*, through the catalytic activity of two independent enzymes, E_1 and E_2. Schematically this can be represented by the following.

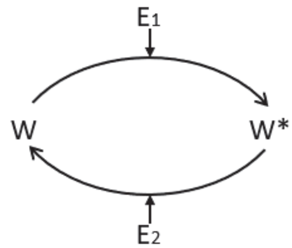

Figure 11: Schematic of the reversible covalent-modification system used by Goldbeter and Koshland. The forward and backward reactions of this system are as described by Michaelis and Menten in their original work, as previously discussed. Note that in this system, E_1 is the enzyme that catalyses the modification of W, creating W^*, whilst E_2 catalyses the unmodification of W^* back to W. Note that the modified forms of the proteins are represented by the addition of an asterisk.

In order to achieve zero-order ultrasensitivity we require that the total substrate is much larger than the Michaelis constants i.e. $W_{tot} \gg K_{m1},\ K_{m2}$. The clearest way to do this is to increase the concentration of total substrate relative to the total concentration of enzymes. We can then use the Law of Mass-Action to obtain a system of ODEs which can later be used to derive the analytic solutions used for the majority of the analysis.

$$\frac{\mathrm{d}[W]}{\mathrm{d}t} = d_1[C_1] + k_2[C_2] - a_1[W][E_1], \tag{7}$$
$$\frac{\mathrm{d}[W^*]}{\mathrm{d}t} = d_2[C_2] + k_1[C_1] - a_2[W^*][E_2], \tag{8}$$
$$\frac{\mathrm{d}[C_1]}{\mathrm{d}t} = a_1[W][E_1] - d_1[C_1] - k_1[C_1], \tag{9}$$
$$\frac{\mathrm{d}[C_2]}{\mathrm{d}t} = a_2[W^*][E_2] - d_2[C_2] - k_2[C_2], \tag{10}$$

We also require the following conservation equations.

$$W_{tot} = W + W^* + C_1 + C_2, \tag{11}$$
$$E_{1tot} = E_1 + C_1, \tag{12}$$
$$E_{2tot} = E_2 + C_2. \tag{13}$$

By making the assumption that the complexes C_1 and C_2 are negligible due to the abundance of substrate, we can rewrite equation (11) to be

$$W_{tot} = W + W^*. \tag{14}$$

By using this assumption, equations (7)-(13), and the quasi-steady state assumption Goldbeter and Koshland were able to derive an analytic solution for the steady-state concentrations of W and W^* [26]. This result can be seen below and has been verified and derived in

Appendix A.3.

$$W^* = \frac{\left[\left(\frac{V_1}{V_2}-1\right) - K_2\left(\frac{V_1}{V_2}+\frac{K_1}{K_2}\right)\right] + \sqrt{\left[\left(\frac{V_1}{V_2}-1\right) - K_2\left(\frac{V_1}{V_2}+\frac{K_1}{K_2}\right)\right]^2 + 4K_2\left(\frac{V_1}{V_2}-1\right)\frac{V_1}{V_2}}}{2\left(\frac{V_1}{V_2}-1\right)} \tag{15}$$

$$W = W_{tot} - W^* \tag{16}$$

where W and W^* and non-dimensionalised parameters, $K_1 = \frac{d_1+k_1}{a_1 W_{tot}}$, $K_2 = \frac{d_2+k_2}{a_2 W_{tot}}$, and $\frac{V_1}{V_2} = \frac{k_1 E_{1tot}}{k_2 E_{2tot}}$.

In order to analyse the result of this equation, Goldbeter and Koshland examined plots of the substrate concentrations, W and W^*, as they vary with changes in the input. They define this input as $\frac{V_1}{V_2}$ where $\frac{V_1}{V_2} = \frac{k_1 E_{1tot}}{k_2 E_{2tot}}$. An example of these profiles can be seen below.

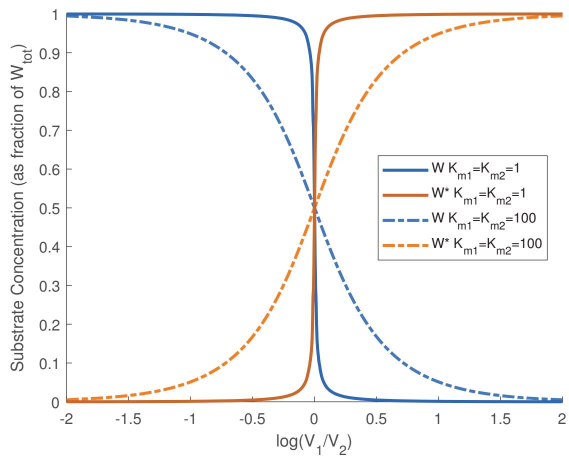

Figure 12: Proteins concentration profiles created using equations (15) and (16). This demonstrates an ultrasensitive response (solid line) and a Michaelis response (dashed line). The ultrasensitive profile was created using the base case parameter regime with $a_1 = a_2 = 2$, $d_1 = d_2 = k_1 = k_2 = 1$. The Michaelian profile was created using the base case parameter regime with $a_1 = a_2 = 0.1$, $d_1 = d_2 = k_1 = k_2 = 5$.

In this system Goldbeter and Koshland defined the sensitivity using the non-dimensionalised Michaelis constants, $K_1 = \frac{K_{m1}}{W_{tot}} = \frac{d_1+k_1}{a_1 W_{tot}}$ and $K_2 = \frac{K_{m2}}{W_{tot}} = \frac{d_2+k_2}{a_2 W_{tot}}$. To then achieve an ultrasensitive profile as seen in Figure 12, we required a very small value for the non-dimensionalised Michaelis constants, namely $0 < K_1 = K_2 \ll 1$. As we increase these values, the profile becomes more "graded" and approaches a Michaelian response when K_1 and K_2 are $\mathcal{O}(1)$. We also observe the well defined symmetric behaviour of this system when under these conditions.

2.3 New Nomenclature and Definitions

We are now interested in analysing this system further to consider how it performs when we relax the substrate abundance assumption which was a key focus of the G-K mechanism.

This is done by introducing a parameter regime in which W_{tot} is now of a comparable magnitude to E_{1tot} and E_{2tot}. We are also interested in further investigating the role of individual rate constants, rather than just the role of the Michaelis constants. We do this by altering individual rate constants while maintaining the same Michaelis constant. We are also interested in understanding the effect of having different values for the two Michaelis constants i.e. $K_{m1} \neq K_{m2}$ - an "asymmetric" reaction cycle.

In order to carry out this investigation we define a base case. This is then used in later investigations by perturbing certain parameters and comparing the effect that this has relative to the base case. We first define this to be a system with comparable concentrations of enzyme and substrate i.e. $W_{tot} = 100$, $E_{2tot} = 20$ and $E_{1tot} \in (0, 40)$. We also choose the Michaelis constants for both reactions to be equal such that $K_{m1} = K_{m2} = 1$ and are created by setting the rate constants to be $d = k = 1$ and $a = 2$. This parameter regime has been chosen as it uses equivalent parameters to those used in the above reproduction of a zero-order ultrasensitive profile seen in Figure 12, but without the substrate abundance.

For each of these investigations, we have ensured to isolate a single parameter, or parameter group, at a time, holding all others fixed. The analysis of this system is then carried out by examining figures of the modified and unmodified substrate concentrations plotted against the input, E_{1tot}. The main output of this analysis is the modified substrate, W^*, however we are also interested in examining the profiles of the unmodified substrate, W, and the intermediate enzyme-substrate complexes, C_1 and C_2. The input has also been chosen to be E_{1tot} as opposed to the ratio of inputs, $\frac{V_1}{V_2}$, as this removes the dependence on the rate constants, k_1 and k_2. It should also be noted that Goldbeter and Koshland typically used the non-dimensionalised Michaelis constants, such as $K_1 = \frac{K_{m1}}{W_{tot}}$, but the following chapters will tend to only consider the unaltered Michaelis constants, K_{m*}, as this removes the dependence on W_{tot}. Detailed results of these investigations can be found in Appendix A.5 along with a summary of the observations in Appendix B.4.

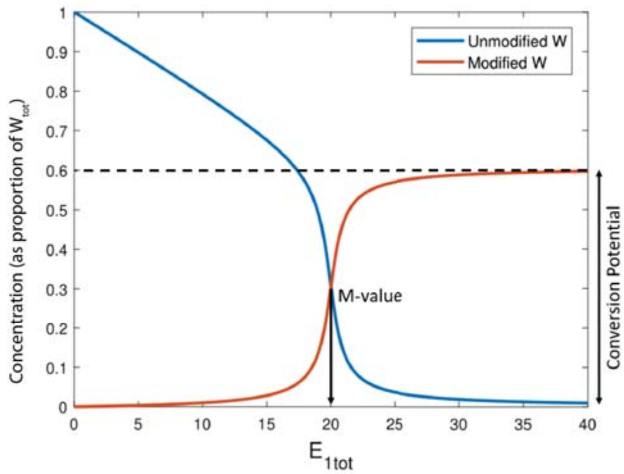

Figure 13: Base case for the G-K mechanism. This defines the reference parameter set that is used throughtout this chapter. We observe an M-value located at $E_{1tot} = 20$ and a conversion potential at 0.6. This profile does not display any mixed sensitivity. Reference parameter regime is chosen such that $a_1 = a_2 = 2$, $d_1 = d_2 = k_1 = k_2 = 1$ with $W_{tot} = 100$, $E_{2tot} = 20$, and $E_{1tot} \in [0, 40]$.

The above figure demonstrates the profiles of the two substrate forms. It is immediately clear that there is a distinct difference between this base case and the profiles seen in the zero-order ultrasensitive profile. In order to describe these differences fully, we have introduced new nomenclature, namely:

- conversion potential,
- mid-conversion stimulus (M-value),
- trivial M-value,
- and mixed sensitivity.

In the base case above, we observe a distinct lower concentration of modified substrate that is achieved as we increase the value of E_{1tot}. We refer to this concept as the "conversion potential" of a profile and it specifically describes the maximum concentration of modified substrate that a profile is able to achieve. We also introduce this concept of the "mid-conversion stimulus". This refers to the value of E_{1tot} required for the system to have equal concentrations of modified and unmodified substrate. In the above profile we can observe that the M-value point occurs when $E_{1tot} = 20$. The concepts of a trivial M-value and mixed sensitivity will be discussed in the following examples where these novel features are evident.

2.3.1 Role of Relative Substrate Abundance

The first investigation examines how altering the abundance of substrate affects the sensitivity and profile for this system. This was done by increasing the value of W_{tot} by ten fold over three simulations such that $W_{tot} = \{10^2, 10^3, 10^4\}$ in comparison with enzyme concentration, $E_{2tot} = 20$. The rate constants remained unchanged from the base case throughout this test. Simulations were run for each parameter regime and can be seen below in which the increasing total substrate concentration is represented by the line type used whereby the increasing order is solid, dashed, dotted.

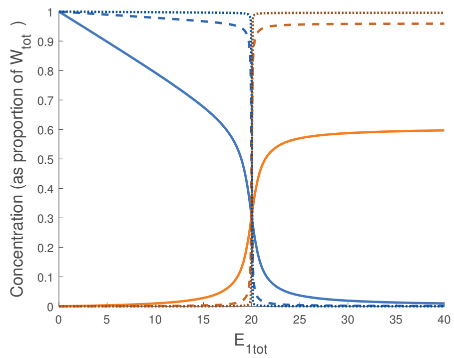

Figure 14: Investigation 1: Test 1. Parameter regime is chosen such that $a_1 = a_2 = 2$, $d_1 = d_2 = k_1 = k_2 = 1$ with $E_{2tot} = 20$, and $E_{1tot} \in [0, 40]$. The total substrate is set such that $W_{tot} = 100$ (solid line), $W_{tot} = 1000$ (dashed line), and $W_{tot} = 10000$ (dotted line).

From this it is most notable that as we increase the total substrate concentration, the conversion potential of the system also increases. In the final profile in which there is a clear abundance of substrate over the enzyme concentration, it appears as though the profile is now symmetric around the M-value. It is also worth noting that altering this parameter has also dramatically increased the sensitivity of the system whereby, when fitting a Hill function to the profile, the Hill coefficient has increased from 17.5 in the base case (solid line), to 881.1 in this last case where $W_{tot} = 10^4$ (dotted line). We also find that altering this parameter has no effect on the M-value of this system and it continues to occur at $E_{1tot} = 20$.

2.3.2 Role of Michaelis Constants

Let us now investigate the effect that the individual Michaelis constants have on the system. For this investigation we have three test regimes to examine: altering K_{m1}, K_{m2} and both K_{m1} and K_{m2}. For each of these regimes, we have comparable concentrations of enzyme and substrate i.e. $W_{tot} = 100$, and we aim to not alter as many rate constants as possible. To perform these tests then, we examine three parameter regimes for each test. These regimes are calculated by altering the value of a_* to be larger and smaller by five-fold to change the associated Michaelis constant, K_{m*}. By doing this we are able to hold the values for d_* and k_* constant so as to not confuse this as an effect that these rate constants may be having on the system themselves. The profiles created by these regimes can be seen below where for each test the increasing change in a_*, which translates to a decreasing change in K_{m*}, is represented by the line types: solid, dashed, and dotted.

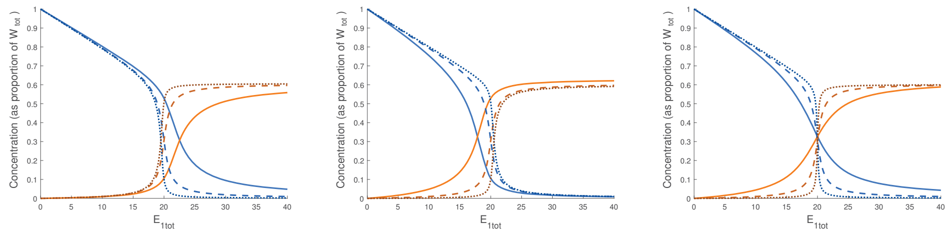

Altering K_{m1}: Test 2   Altering K_{m2}: Test 3   Altering K_{m1} and K_{m2}: Test 4

Figure 15: Investigation 2: Altering Michaelis constants. Parameter regime is chosen such that $a_1 = a_2 = 2$, $d_1 = d_2 = k_1 = k_2 = 1$ with $W_{tot} = 100$, $E_{2tot} = 20$, and $E_{1tot} \in [0, 40]$. The Michaelis constant is altered by setting $a_1 = \{0.4, 2, 10\}$ in Test 2, $a_2 = \{0.4, 2, 10\}$ in Test 3, and $a_1 = a_2 = \{0.4, 2, 10\}$ for Test 4. The increase in rate constants is represented by the line type: solid, dashed, dotted i.e. the smallest value of a is represented by a solid line and the largest value is represented by a dotted line.

From these we can now observe a change in the M-value. We find that a decrease in K_{m1} results in the M-value shifting left, whereas a decrease in K_{m2} results in it shifting right. We can then see that if both constants are changing together, the M-value is not shifted at all which supports the work produced by Goldbeter and Koshland as this was the basis of their investigation. We also begin to observe some new behaviour whereby as we approach the M-value point immediately from either side, in Tests 2 and 3, the profile is no longer symmetric. For example when $K_{m1} = \frac{1}{5}$ (dotted line) in Test 2, we can see that the profile clearly changes at a much steeper rate after the M-value than it does before. We refer to this behaviour as mixed sensitivity.

We also note that changing one Michaelis constant can alter the sensitivity and conversion potential of a profile. Here we observe that in Test 2, when K_{m1} is decreased, the level of conversion potential and sensitivity of the profile is increased. As was observed with the M-value, decreasing K_{m2} acts in the opposite way for the conversion potential, whereby conversion potential also decreases. However decreasing K_{m2} also increases sensitivity. It's also worth noting that when both Michaelis constants are decreased simultaneously, the sensitivity is increased but the conversion potential appears to be relatively unchanged.

2.3.3 Role of Individual Rate Constants

The enzyme-mediated conversion between unmodified (W) and modified (W^*) protein forms involves three rate constants: association (binding) rate constants a, dissociation (unbinding) rate constants d, and catalytic rate constants k. In order to understand how the individual rate constants affect the dose-response of the system, we first perturb a single conversion reaction. In each case we wish to keep one rate constant and the Michaelis constant of this reaction unchanged whilst altering the remaining rate constants. We then compare the altered regimes to the base case to investigate if the altered rate constants have some effect on the system. These profiles are shown below.

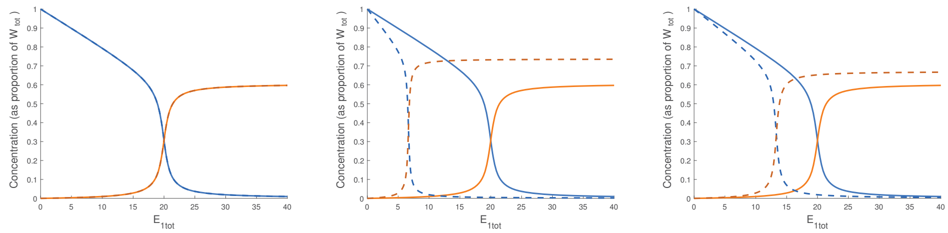

Holding k_1 constant: Test 5 | Holding d_1 constant: Test 6 | Holding a_1 constant: Test 7

Figure 16: Investigation 3: Altering rate constants for forward reaction. This shows that the protein profile is only altered when k_1 is altered. System parameters are set as $W_{tot} = 100$, $E_{2tot} = 20$, and $E_{1tot} \in [0, 40]$. We then alter the rate constants from the base case given by $a_1 = a_2 = 2$, $d_1 = d_2 = k_1 = k_2 = 1$. The altered rate constants are given by $a_1 = 4$, $d_1 = 3$, $k_1 = 1$ for Test 5, $a_1 = 2$, $d_1 = 0.5$, $k_1 = 1.5$ for Test 6, and $a_1 = 4$, $d_1 = 1$, $k_1 = 3$ for Test 7. The altered parameter set is represented by the dashed line.

While k_1 is held constant, as seen in Test 5, the profile has no change from the base case indicating that a_1 and d_1 have no effect. This is true for all possible choices of a_1 and d_1 as long as the Michaelis constant is unchanged. We do observe however that in Tests 6 and 7, the profiles vary dramatically with large shifts in the M-value and conversion potential. Since k_1 is the only rate constant changed in both of the profiles that exhibit change, this must be the cause.

Since these tests indicate that only the catalytic constant, k_1, has an effect on the profile, we can now begin to investigate this effect in a similar fashion to what was seen above in Investigation 2 by examining three test regimes: altering k_1, k_2, and both k_1 and k_2. For these tests this is done by increasing and decreasing the magnitude of all rate constants associated with the reaction of interest by two-fold. The tests are performed in this manner to ensure that the Michaelis constants are unchanged and that it is only the magnitude of the rate constants, in particular k_*, that is affecting the profile. With this in mind the Michaelis constants are kept the same as the base case i.e. $K_{m1} = K_{m2} = 1$ and the substrate abundance is unchanged i.e. $W_{tot} = 100$. The following profiles demonstrate an increasing magnitude of the rate constants using line type: solid, dashed, dotted.

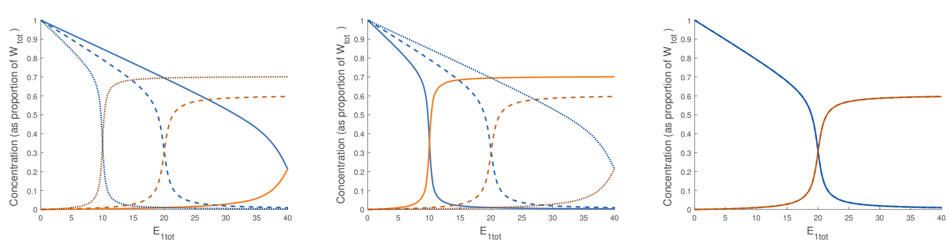

Altering k_1: Test 8 | Altering k_2: Test 9 | Altering k_1 and k_2: Test 10

Figure 17: Investigation 3: Altering all catalytic constants. System parameters are set as $W_{tot} = 100$, $E_{2tot} = 20$, and $E_{1tot} \in [0, 40]$. We then alter the rate constants from the base case given by $a_1 = a_2 = 2$, $d_1 = d_2 = k_1 = k_2 = 1$. The altered rate constants are then given by $a_1 = \{1, 2, 4\}$ and $d_1 = k_1 = \{0.5, 1, 2\}$ for Test 8, $a_2 = \{1, 2, 4\}$ and $d_2 = k_2 = \{0.5, 1, 2\}$ for Test 9, and $a_1 = a_2 = \{1, 2, 4\}$ and $d_1 = d_2 = k_1 = k_2 = \{0.5, 1, 2\}$ for Test 10. The increase in rate constants is represented by the line type: solid, dashed, dotted i.e. the smallest set of values are represented by a solid line and the largest values are represented by a dotted line.

From this we can see that altering k_1 or k_2 individually can have a large effect on the profile, but when they are altered simultaneously, there is no effect on the profile at all. When altered individually we can see that the catalytic constants have a large effect on the conversion potential and the M-value and also an effect on the sensitivity. We can see that as we increase k_1 or decrease k_2 the M-value is shifted towards the left of the domain and the conversion potential can be clearly seen to increase. We also see that when $k_1 = 0.5$ (solid line) in Test 8 or when $k_2 = 2$ (dotted line) in Test 9, the M-value occurs right at the end of the domain when $E_{1tot} = 40$. If the input is increased further we do obtain profiles that will eventually asymptote and continue with this trend to have a lower conversion potential.

When examining the sensitivity of these tests, we find that there is a slight increase in sensitivity as k_1 increases and k_2 decreases. For example in Test 8 the Hill coefficient for the base case (dashed line) compared to when $k_1 = 2$ (dotted line) increases from 17.5 to 21.6. If we also compare the profiles of Tests 8 and 9, it can be observed that when $k_1 = 2$ (dotted line) and $k_2 = 0.5$ (solid line) the profiles created are identical. This is interesting as it does not obtain the same asymmetric behaviour observed when altering the individual Michaelis constants.

It is also worth noting that in the tests above we have observed the M-value of the profile being shifted towards the left hand side of the domain i.e. when $E_{1tot} = 0$. The final new term that has been introduced refers to when the M-value occurs at the beginning of this domain and is referred to as the "trivial M-value". The occurrence of these points is not common in this system; however in later chapters this will become more prevalent. Since these profiles are created by running simulations for discrete values of E_{1tot} beginning at zero, the first point on the profile will have no change from the initial condition as the system is not able to run without any initial catalysing enzyme. The trivial M-value then refers to when the M-value occurs as soon as there is any input in the system. This point is therefore of less interest, as in a biological system we may expect to find at least some traces of input in a system initially and therefore there would be no switching behaviour that occurs. It is therefore of interest to only investigate regimes in which there is a non-trivial M-value for the system.

2.4 Discussion

After examining the effects that the rate constants, Michaelis constants and substrate abundance have on the quantative response of the system, it is now of interest to further investigate these parameter regimes and investigate why they cause these effects. In particular we are interested in investigating conversion potential, the M-value and symmetry and how these are related to ultrasensitivity in this system. These features are of particular interest as they are the key characteristics that describe the substrate profiles for this system. Implementing this cycle into a larger mechanism may require certain characteristics, such as complete conversion of the substrate into the modified form, or a specific M-value. Thus it is important to understand how these features are created and how they can be manipulated.

2.4.1 Conversion Potential

We begin by investigating the reduced conversion potential of this system. We have previously seen in the work of Goldbeter and Koshland [26] that when we assume that there is an abundant concentration of substrate in comparison to the concentration of enzymes, then we are able to achieve full conversion of our modified substrate (see Figure 5b). By making this assumption, we are also implying that the concentration of the enzyme-substrate complexes are very small in comparison with the substrate concentration and may be neglected. In our simulated models, such as what has been observed above in Figure 13, when there are comparable concentrations of enzyme and substrate, we are no longer able to achieve this complete conversion potential. One clear difference between these two solutions is the inclusion of complexes in the simulated results.

When we examine the conservation equation for the substrate that this system is subject to, we find that

$$W_{tot} = W + W^* + C_1 + C_2, \tag{17}$$

where the complexes are referred to as $C_1 = WE_1$ and $C_2 = W^*E_2$ to avoid confusion with the multiplication of concentrations of the substrate and enzyme. This demonstrates that for a given value of W_{tot} any increase in the complexes will directly result in a decrease of the substrate concentrations to maintain this equation. If we now examine the profile of the base case along with a profile of the complexes, we can see that the distinct drop in conversion potential is directly related to the increase in concentration of the complexes (see Figure 18).

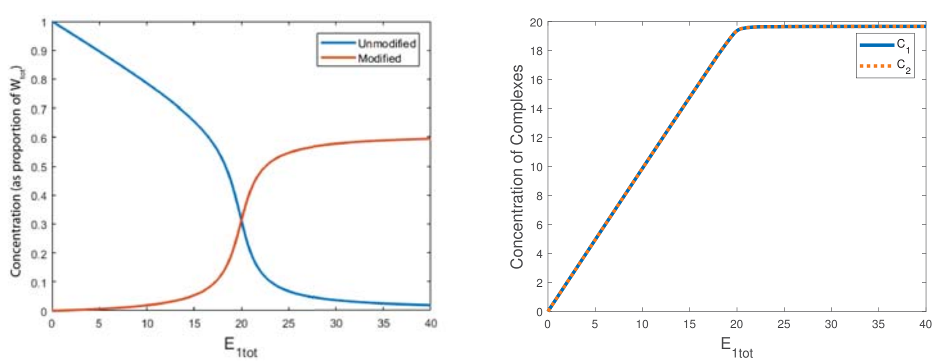

(a) Profile of Protein Concentrations

(b) Plot of Complex Concentrations

Figure 18: Ultrasensitive substrate concentration profile for base case (a) and profile of complex concentrations (b). The complexes are represented by: C_1 is the WE_1 complex (blue), and C_2 is the W^*E_2 complex (red). Parameter regime is chosen such that $a_1 = a_2 = 2$, $d_1 = d_2 = k_1 = k_2 = 1$ with $W_{tot} = 100$, $E_{2tot} = 20$, and $E_{1tot} \in [0, 40]$.

When we examine the other conservation equations that govern this system, we find that

$$E_{1tot} = E_1 + C_1, \tag{18}$$

$$E_{2tot} = E_2 + C_2. \tag{19}$$

This demonstrates that, independent to the value of W_{tot}, the complexes are never able to exceed the value of E_{1tot} and E_{2tot}.

Using this information we discover that the profile obtained when assuming substrate abundance appears to achieve complete conversion potential due to the relative low concentration of complexes and how these cannot possibly make a considerable contribution due to the limited total enzyme. When we have a system with comparable concentrations of enzyme and substrate, we are then able to observe the proportion of total substrate that consists of complexes, since the enzyme totals are now comparable in magnitude. If we are to continue this trend and set W_{tot} to be equal to E_{2tot} then we achieve a profile that has almost no modified substrate and no unmodified substrate in the system after the M-value.

Knowing that the concentrations of the complexes play such a significant role in this system, it is then of interest to investigate what controls their production and whether or not we can decrease their steady state concentration without affecting sensitivity. To do this we can first examine the mass-action equations associated with the creation of the complexes, namely,

$$\frac{\mathrm{d}C_1}{\mathrm{d}t} = a_1 W E_1 - d_1 C_1 - k_1 C_1, \tag{20}$$

$$\frac{\mathrm{d}C_2}{\mathrm{d}t} = a_2 W^* E_2 - d_2 C_2 - k_2 C_2. \tag{21}$$

This demonstrates that the creation of the complex is dependent on the ratio of the rate constants associated with the removal of complex, d_* and k_*, and the creation of complex, a_*. This ratio can therefore take the form of the Michaelis constant i.e.

$$K_{m*} = \frac{d_* + k_*}{a_*}.$$

However in order to decrease the creation of complex, we would require increasing the Michaelis constant, which has already been linked to decreasing the sensitivity of the system in the work of Goldbeter and Koshland.

When examining a Michaelian profile (see Figure 19a) associated with Michaelis constants, $K_{m1} = K_{m2} = 100$, it can be seen that we obtain a higher conversion potential of the substrate than the ultrasensitive response. This is clearly due to the concentration of the complex being smaller. When examining the concentration profile of the complexes, as seen in Figure 19b, the complexes do not exceed even half of the values achieved when the response is ultrasensitive regardless of the huge increase in input, E_{1tot}, to the system required to obtain the asymptotic behaviour in the far field. Previously the input was chosen as $E_{1tot} \in (0, 40)$ to obtain the full ultrasensitive profile. This has now been greatly increased to view the full behaviour of the Michaelian profile where $E_{1tot} \in (0, 500)$. It is also worth noting that when this Michaelian response is presented using this format it takes on a vastly different form to that observed in Figure 12 when using the same format as Goldbeter and Koshland. By plotting against a linear input, as opposed to the logged input used by Goldbeter and Koshland, we no longer observe the subsensitive region to the left of the M-value. However this response still requires the 81 fold increase in input to alter the output from 10% to 90% of the conversion potential, which is characteristic of a Michaelian response.

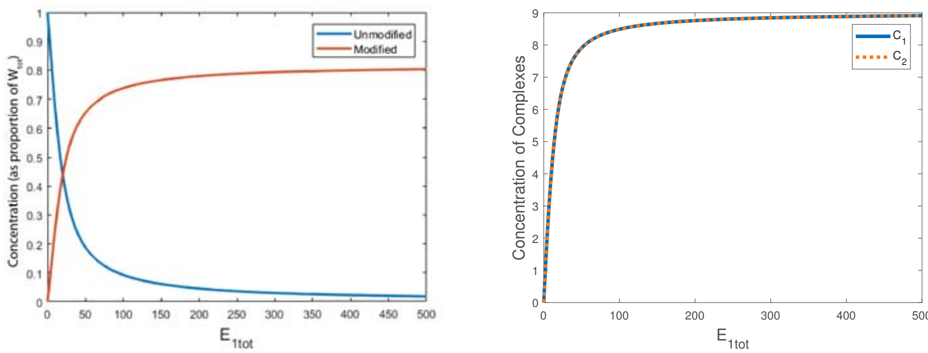

(a) Profile of Protein Concentrations

(b) Plot of Complex Concentrations

Figure 19: Michaelian substrate concentration profile (a) and profile of complex concentrations (b). The complexes are represented by: C_1 is the WE_1 complex (blue), and C_2 is the W^*E_2 complex (red). Parameter regime is chosen such that $a_1 = a_2 = 0.1$, $d_1 = d_2 = k_1 = k_2 = 5$ with $W_{tot} = 100$, $E_{2tot} = 20$, and $E_{1tot} \in [0, 500]$.

It is worth noting that whilst decreasing both Michaelis constants results in an increased conversion potential, when we examine the results from Figure 15, this is not always true. When increasing K_{m2} individually, we find that the conversion potential increases, however increasing K_{m1} decreases the conversion potential. When we examine the substrate profiles we find that as we increase the input to the system, the unmodified substrate is no longer going to zero. Therefore, whilst the complexes are still decreased in concentration because of a larger Michaelis constant, there is still a decreased conversion potential. This is most likely a result of the unbalanced affinity toward creating more W through the second reaction.

This provides some explanation as to how altering the Michaelis constants not only alters the sensitivity of a system but also affects the conversion potential of the modified substrate.

We can also further examine the mass-action equations that govern this system by combining and rearranging Equations (7) and (9) at steady state to obtain,

$$k_1 C_1 = k_2 C_2. \tag{22}$$

Using this formula we can begin to investigate the role that k_1 and k_2 have on conversion potential. Linking back to what was observed in Figures 17 and 18, we can see that when $k_1 = k_2$ we obtain a profile with incomplete conversion potential that achieves a modified substrate concentration of approximately 0.6. When we consider that in these simulations we had set $E_{2tot} = 20$ and that when $k_1 = k_2$, Equation (22) becomes

$$C_1 = C_2,$$

we know that both C_1 and C_2 could have a concentration of at most $E_{2tot} = 20$. Using Equation (17) we can confirm what was found in Figure 18 and explain how we achieve the level of conversion potential since rearranging and solving for W^* gives,

$$W^* = W_{tot} - W - C_1 - C_2 \leq W_{tot} - 2E_{2tot} = 60.$$

If we now examine the profiles created by only altering k_1 or k_2 in Figure 17, we see that we are able to achieve a higher conversion potential for larger k_1 and smaller k_2 and we achieve a lower conversion potential when k_1 is smaller and k_2 is larger. If we link this back to Equation (22) we see that a larger k_1 or smaller k_2 means that $C_1 < C_2$. Since we have found that C_2 tends to approach E_{2tot} in an ultrasensitive system, we know that $C_1 < C_2 \leq E_{2tot}$ and we can therefore achieve a higher conversion potential. When k_1 is smaller or k_2 is larger, then $C_1 > C_2$, and since the domain of our input requires $E_{1tot} \in (0, 40)$ then we can obtain that $E_{2tot} < C_1 \leq E_{1tot}$ and hence the profile has a lower conversion potential. The relationship between the complexes in Equation (22) clearly defines how the catalytic constants, k_1 and k_2, can affect the conversion potential of the system.

Finally, we want to link these two concepts of the Michaelis constants and the catalytic constants together by reiterating some concepts as to how the complexes form as seen in Figures 18 and 19. As discussed in Section 1.1.2, we can link the ratio of rate constants associated with the removal and creation of the complexes to the Michaelis constant. We have found that decreasing the value of the Michaelis constant requires increasing the production of complex relative to their removal. In particular a smaller Michaelis constant results in a higher total complex concentration at steady state. This behaviour can be observed in Figures 18 and 19 where there is less concentration of the complexes created in the Michaelian profile. This can also be observed in Figure 15 whereby, when altering only K_{m1} or K_{m2}, we observe slight differences in conversion potential since one Michaelis constant has a different magnitude to the other and therefore a larger affinity to create more complex. We also observe, particularly in Figure 19, that larger Michaelis constants require a larger input to achieve the asymptotic behaviour that indicates the maximum conversion potential of this system but this doesn't translate to increased complexes.

We can also describe how the two complexes form relative to each other by examining Equation 22. In Figure 18 the concentrations of C_1 and C_2 increase at the same rate as each other, since $k_1 = k_2$, with respect to the input (E_{1tot}). Since this parameter regime includes small Michaelis constants, there is a high affinity to create more complex, and C_1 and C_2 increase linearly with the input since C_1 is bounded by E_{1tot} and cannot increase any further. When E_{1tot} surpasses $E_{2tot} = 20$, the value of C_2 is then bounded by E_{2tot} and both complexes stop increasing. As we increase the Michaelis constant, however, we find this behaviour changes as the complex no longer increases to its maximum capacity as the input is increased. In the case of Figure 19 we see that the complexes form at equal rates, since $k_1 = k_2$, but have a hyperbolic profile.

In general the behaviour of these systems also holds true when $k_1 \neq k_2$. However in the case of an ultrasensitive system we find that C_1 and C_2 will now grow at different rates so that C_2 approaches E_{2tot} and C_1 approaches $\frac{k_2}{k_1}E_{2tot}$ and these level out at the M-value, rather than when $E_{1tot} = E_{2tot}$. To fully understand this behaviour, we then need to investigate when the M-value occurs.

2.4.2 The Mid-Conversion Stimulus (M-value)

We wish to consider how the M-value is influenced by system parameters. We therefore use Equations (7) and (9) to calculate the value of E_{1tot} for which $W = W^*$ at steady state. We obtain the following analytical expression. The full derivation can be found in Appendix A.6

$$k_1 E_{1tot}(K_{m2} + W) = k_2 E_{2tot}(K_{m1} + W) \tag{23}$$

In the special case where $K_{m1} = K_{m2}$, this may be further simplified to give

$$E_{1tot} = \frac{k_2}{k_1} E_{2tot}. \tag{24}$$

This function now states that when the Michaelis constants are equal, we are able to analytically define the M-value (the value of E_{1tot}). For example in the base case for this system, seen in Figure 13, we have that $k_1 = k_2 = 1$ and therefore the M-value occurs at $E_{1tot} = E_{2tot} = 20$.

Thus we see that when $K_{m1} = K_{m2}$, only the ratio of the catalytic constants, $\frac{k_2}{k_1}$ and the concentration of the second enzyme, can affect where the M-value occurs. This is also very similar in behaviour as the relationship that governs the concentration of complexes (Equation 22) in that an increase in k_1 or a decrease in k_2 will shift the M-value left, and an increase in k_2 or a decrease in k_1 will shift the M-value towards the right. The M-value is also completely unaffected by the total substrate abundances when $K_{m1} = K_{m2}$.

However when we relax the assumption that $K_{m1} = K_{m2}$, we cannot explicitly determine an expression for the M-value. This is due to the function's dependence on the unmodified substrate and the implicit expression of this variable which shall be discussed later in this chapter. However there are still a number of observations that we can make about what affects the M-value in this case. To better analyse the behaviour, Equation (23) can be rewritten as

$$E_{1tot} = E_{2tot} \frac{k_2}{k_1} \frac{(K_{m1} + W)}{(K_{m2} + W)}. \tag{25}$$

Once again larger k_1 or smaller k_2 will result in shifting the M-value left. We can also get some idea of how the Michaelis constants can effect the M-value. Much like the catalytic constants we now have $\frac{K_{m1}}{K_{m2}}$ and so an increase in K_{m2} or a decrease in K_{m1} should shift the M-value left. This behaviour matches what was found in Figure 15.

However it is also important to keep in mind that altering the catalytic constants or the Michaelis constants will also affect the concentration of the unmodified substrate, so these will have secondary effects on the M-value by also altering the value of W. We also introduce a dependence on W_{tot}, which was not present when $K_{m1} = K_{m2}$, since this can also effect the concentration of W. Since we have shown that W_{tot} improves sensitivity and conversion potential, increasing the value of W_{tot} can increase the value of W. We then find that when $K_{m1} < K_{m2}$, then increasing W_{tot} will decrease the M-value as $\frac{(K_{m1}+W)}{(K_{m2}+W)}$ decreases. Similarly, when $K_{m1} > K_{m2}$ the M-value is shifted right as demonstrated below.

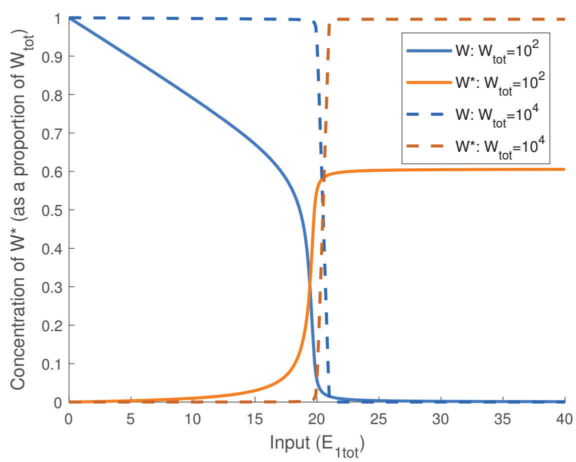

Figure 20: The effect of substrate abundance on the M-value. This demonstrates that when $K_{m1} > K_{m2}$, an increase in W_{tot} increases the M-value. The concentration of unmodified substrate is represented by the blue lines and the concentration of modified substrate is represented by the orange lines. Parameter regime is chosen such that $a_1 = 20$, $a_2 = 2$, $d_1 = d_2 = k_1 = k_2 = 1$ with $E_{2tot} = 20$, and $E_{1tot} \in [0, 40]$. The substrate abundance altered from $W_{tot} = 100$ (solid line) to $W_{tot} = 10000$ (dashed line).

When the Michaelis constants are not equal we have demonstrated the M-value's dependence on the steady state concentration of the unmodified substrate, which itself is dependent on conversion potential and sensitivity. In order to better understand how the M-value behaves, let us now investigate the capacity for ultrasensitivity of this system.

2.4.3 Capacity for Ultrasensitivity

We have now seen how sensitivity can be linked to the regulation of the M-value and the conversion potential in our profiles. However understanding sensitivity itself is directly linked with the behaviour of the profile and is far too complex to directly link to any particular parameter regime using some form of analytic expression. We discuss this more later when examining analytic solutions to this system. We can however link this behaviour to certain parameter regimes through observation. As we have previously seen, W_{tot}, the Michaelis constants and the catalytic constants all have some effect on the sensitivity of the profile.

Goldbeter and Koshland focussed on the role of the Michaelis constants in driving ultrasensitivity, whereby smaller Michaelis constants result in a more ultrasensitive system. This has been confirmed throughout this investigation (see Figure 15 for example). We have also observed that when the two Michaelis constants are altered individually, this relationship still holds true, but we begin to obtain "mixed sensitivity", where the dose-response has a different ultrasensitivity on either side of the M-value. We consider the effect of the Michaelis constants to be linked to the creation of the complex. When we acquire smaller Michaelis constants, it requires that the rate constant associated with the creation of the complex, a, is comparable or larger than the constants associated with the removal of the complex, d and k. We could then think of the increased creation of complex to be linked to the increase in sensitivity, as it allows for more modification of the substrate.

Similarly we have observed that modifying the catalytic constants, whilst not altering the Michaelis constants, can also increase sensitivity. For example we observed that increases in k_1 or decreases in k_2 can increase the sensitivity (see, for example, Figure 17). This could be explained by the increased affinity for the forward reaction, relative to the reverse reaction. This is linked to the increase in C_1 relative to C_2, as highlighted by Equation (22).

We have also observed that increasing the total substrate can improve sensitivity (see, for example, Figure 14). This too could be linked to an increased affinity for the reactions, but without having as large of an effect on the M-value as altering the catalytic constants.

2.4.4 Mixed Sensitivity

As discussed above, altering the Michaelis constants individually introduces an interesting behaviour to the profile, which we refer to as "mixed sensitivity". As seen in Figure 15 making one Michaelis constant larger than the other results in a different sensitivity on either side of the M-value. Having an inconsistent sensitivity could then have a siginificant effect when implementing this system into a larger mechanism. For example, if we consider a cascade made of these cycles whereby the output of one cycle acts as the enzyme for the next, we may be more interested in only acquiring a small, but rapid, increase in the output as only a small input may be required for the next cycle. In this scenario a profile that has a more sensitive profile prior to the M-value may be ideal, as we are less interested for what occurs later on in the profile. This provides just one example that motivates why this behaviour is important to understand.

It is also worth noting that when we compare profiles when altering the Michaelis constants individually, the Hill coefficient no longer captures this difference in behaviour. When comparing the behaviour of this model when $K_{m1} = \frac{1}{5}$ (dashed line) to when $K_{m2} = \frac{1}{5}$ (dotted line) in Figure 21, we obtain a considerably different profile. We can observe that when we decrease K_{m1} the profile is more sensitive after the M-value, which is shifted left, while when altering K_{m2} the profile is more sensitive prior to the M-value and the M-value is shifted further to the right. Despite the differences in the profiles they have fairly similar Hill coefficients, 27.5 for K_{m1} and 29.2 for K_{m2}. We can also compare these to another profile, when $K_{m1} = K_{m2} = \frac{4}{7}$. This profile is less sensitive than the small K_{m2} profile before the M-value, and less sensitive than the small K_{m1} profile after the M-value. Yet this profile is able to achieve a Hill coefficient of 28.4. This demonstrates that the Hill coefficient may not be an accurate measurement of sensitivity as it does not take into account the mixed sensitivity characteristics of a profile.

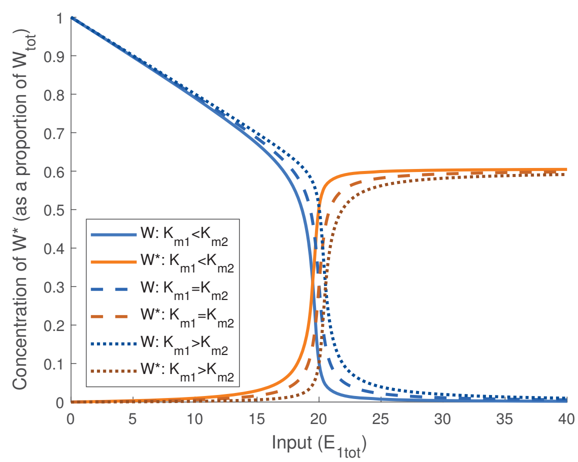

Figure 21: The effect of substrate abundance on the M-value. The concentration of unmodified substrate is represented by the blue lines and the concentration of modified substrate is represented by the orange lines. Parameter regime is chosen such that $a_1 = a_2 = 2$, $d_1 = d_2 = k_1 = k_2 = 1$ with $W_{tot} = 100$, $E_{2tot} = 20$, and $E_{1tot} \in [0, 40]$. The Michaelis constants were changed from the base case by setting $a_1 = a_2 = \frac{7}{2}$ (solid line), $a_1 = 10$ (dashed line), and $a_2 = 10$ (dotted line).

2.5 Analytic Solutions

We can now derive analytic solutions for the substrate concentrations at steady steady state for this system in order to try and obtain further insight into how this system behaves. As we have previously discussed, Goldbeter and Koshland derived two analytic solutions for the reversible covalent-modification cycle. The first of these is a quadratic whose positive root provides an explicit expression for the concentration of W^* (as a proportion of W_{tot}) as a function of the input, E_{1tot}. The second analytic solution is a cubic in W, whose roots provide the concentrations of W at steady state (as a proportion of W_{tot}). The difference between the solutions is that the quadratic is based on the assumption that the intermediate substrate-enzyme complexes, C_1 and C_2, are negligible. As noted earlier, this assumption may be valid when $W_{tot} \gg E_{1tot}, E_{2tot}$, but is not applicable to parameter regimes in which $W_{tot} \approx E_{1tot}, E_{2tot}$ (see, for example, Figure 22). By constrast, including these complexes gives rise to a more complicated cubic expression. A full derivation of each solution can be found in Appendix A.3 and A.4 respectively. For the quadratic the solutions for W and W^* at steady state as a proportion of W_{tot} are given by

$$W^* = \frac{\left[\left(\frac{V_1}{V_2}-1\right) - K_2\left(\frac{V_1}{V_2}+\frac{K_1}{K_2}\right)\right] + \sqrt{\left[\left(\frac{V_1}{V_2}-1\right) - K_2\left(\frac{V_1}{V_2}+\frac{K_1}{K_2}\right)\right]^2 + 4K_2\left(\frac{V_1}{V_2}-1\right)\frac{V_1}{V_2}}}{2\left(\frac{V_1}{V_2}-1\right)},$$

$$W = W_{tot} - W^*,$$

where $K_1 = \frac{d_1+k_1}{a_1 W_{tot}}$ and $K_2 = \frac{d_2+k_2}{a_2 W_{tot}}$ are the non-dimensionalised Michaelis constants, and $\frac{V_1}{V_2} = \frac{k_1 E_{1tot}}{k_2 E_{2tot}}$. The cubic equation can be solved to obtain the concentration of W at steady state and then used to calculate the concentrations of C_1, C_2, and W^* as a proportion of W_{tot} by using,

$$W^3\{1-\alpha\} + W^2\{(K_1+K_2\alpha) + (1-\alpha)(K_1+\epsilon_1+\epsilon_2\alpha-1)\} \tag{26}$$

$$+ K_1 W\{(K_1+K_2\alpha) + (\alpha-2) + (\epsilon_1+\epsilon_2\alpha)\} - K_1^2 = 0, \tag{27}$$

$$C_1 = \frac{\epsilon_1 W}{K_1 + W}, \tag{28}$$

$$C_2 = \frac{k_1}{k_2} C_1, \tag{29}$$

$$W^* = 1 - W - C_1 - C_2, \tag{30}$$

where $\alpha = 1 - \frac{k_1 E_{1tot}}{k_2 E_{2tot}}$, $\epsilon_1 = \frac{E_{1tot}}{W_{tot}}$, $\epsilon_2 = \frac{E_{2tot}}{W_{tot}}$, and $K_1 = \frac{d_1+k_1}{a_1 W_{tot}}$ and $K_2 = \frac{d_2+k_2}{a_2 W_{tot}}$ are the non-dimensionalised Michaelis constants.

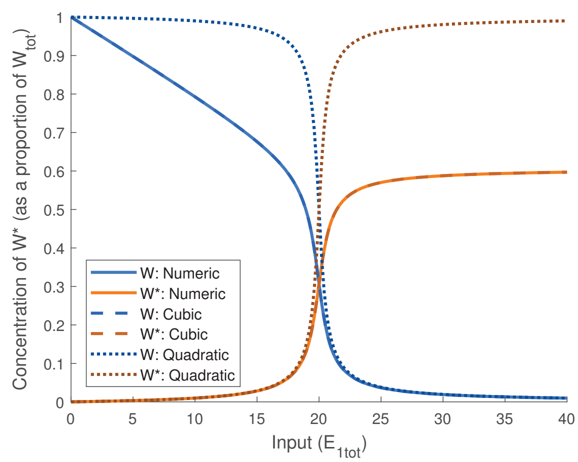

Figure 22: Comparison of analytic solutions with the simulated results. The concentration of unmodified substrate is represented by the blue lines and the concentration of modified substrate is represented by the orange lines. Simulated results (solid line) were created using the base case parameter regime with $a_1 = a_2 = 2$, $d_1 = d_2 = k_1 = k_2 = 1$ and system parameters $W_{tot} = 100$, $E_{2tot} = 20$, and $E_{1tot} \in [0, 40]$. The analytic solutions were created using the cubic solution (dashed line) and the quadratic solution (dotted) originally derived by Goldbeter and Koshland using the same parameter regime as the simulated profile.

Since the cubic gives W implicitly, it is difficult to identify how the various parameters affect the substrate profiles, so this expression gives limited insight as to how the system may be effected by different parameter regimes.

When solving for the roots numerically we found this cubic does not always have a negative discriminant which would allow us to split the solution into an irreducible form with complex roots that would simply leave one real root remaining. In fact, in the majority of cases, we found that all three roots of this polynomial were real. To eliminate invalid roots of the cubic we run a number of tests to ensure that the solutions do not disagree with physical constraints, i.e. W must be between zero and unity, and the conservation equations hold for all proteins (equations (11)-(13)). If any of the above tests fail, then the root is no longer considered valid and is removed.

After these tests we found that there was strictly one valid root for any given value of E_{1tot}. We also performed a linear stability analysis for this system. We demonstrated that all valid roots are stable nodes as seen in Figure 23 of the single valid root in each case. Here a solid circle represents a stable root. This provides us with some insight into how the numerical methods create the given profiles as it is only able to find the valid, stable roots of the system.

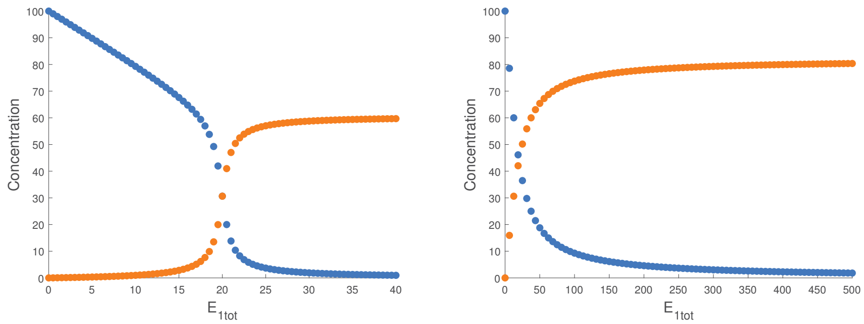

(a) Ultrasensitive profile

(b) Michaelian profile

Figure 23: Results of linear stability analysis profiles using equation (27) where solid circles represent a stable root of the solution (i.e. associated with all negative eigenvalues). The concentration of unmodified substrate is represented by the blue markers and the concentration of modified substrate is represented by the orange markers. The ultrasensitive profile is created using the base case parameter regime with $a_1 = a_2 = 2$, $d_1 = d_2 = k_1 = k_2 = 1$ and system parameters $W_{tot} = 100$, $E_{2tot} = 20$, and $E_{1tot} \in [0, 40]$. The Michaelian profile is created using the parameter regime with $a_1 = a_2 = 0.1$, $d_1 = d_2 = k_1 = k_2 = 5$ and system parameters $W_{tot} = 100$, $E_{2tot} = 20$, and $E_{1tot} \in [0, 500]$.

2.6 Stochastic Simulations

By using deterministic methods, we consider concentrations of molecules under the assumption that reactions occur continuously, and that the concentrations themselves exist on a continuum. For ergodic systems, deterministic solutions thus approach the "expected" concentrations for the molecules in a single cell. By using stochastic methods, on the other hand, we can consider the discrete nature of reaction timings and molecular abundances. We can thus simulate the time-evolution of molecular concentrations in individual cells and examine the cell-to-cell variabilities in concentrations for a population of cells. Here we use Gillespie's Stochastic Simulation Algorithm (SSA), which uses uniformly distributed random numbers to determine the occurrence of individual reactions, and to determine time intervals between reactions, as a function of reaction affinities [25]. We assume here that reactions at the level of a single cell are "well-mixed" and occur in a single cellular compartment, being a strictly time-dependent (non-spatial) problem. Performing large numbers of simulations in this manner allows us to obtain a normally-distributed sample of concentrations for each protein at a specified end time. Gillespie's SSA thus allows us to examine the relationship between the sensitivity of the system and the variability in the concentrations of the output of the system (W^*). Note that all parameters used to obtain the following figures can be found in the figure captions.

Before examining variability, we first confirm that the stochastic simulations predict an average behaviour that closely matches the solution to the deterministic model (equations (7)-(13)). To obtain solutions for this system we implement the reaction equations (5)-(6) into Gillespie's SSA. 250 simulations were then recorded at twenty input values in a neighbourhood of the M-value. In Figure 24 we compare the solutions under the ultrasensitive base case (defined in Section 2.3). This demonstrates that the stochastic simulations provide results that accurately matched those of the deterministic solver.

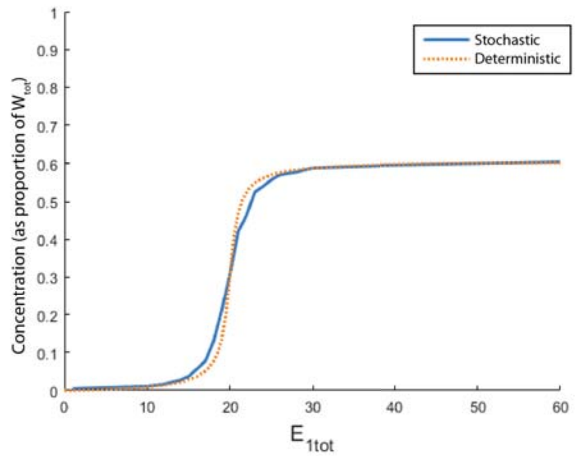

Figure 24: Protein concentration profile for the modified substrate, W^* using Gillespie's Stochastic Simulation Algorithm and Matlab's *ode23s* numerical solution to equations (7)-(13). For both simulations the system parameters were set as $W_{tot} = 100$, $E_{2tot} = 20$ and $E_{1tot} \in [1, 10, 12, 14, 15, 16, 17, 18, 19, 20, 21, 22, 23, 24, 25, 26, 28, 30, 39, 60]$ with the reference parameter set, $a_1 = a_2 = 2$, $d_1 = d_2 = k_1 = k_2 = 1$. The SSA was averaged over 250 simulations to $T = 1000$. Matlab's ODE solver was used over the same domain but with uniform spacing at much finer values.

In Figure 25 we examine the response variability of a Michaelian modified substrate profile with an emphasis on the values of input in the neighbourhood of the M-value. It can be seen that in all three cases we achieve a distribution that is fairly consistent as the input increases from slightly below the M-value to above it. This demonstrates that for a Michaelian profile, there is no clear variability in the distributions of modified substrate.

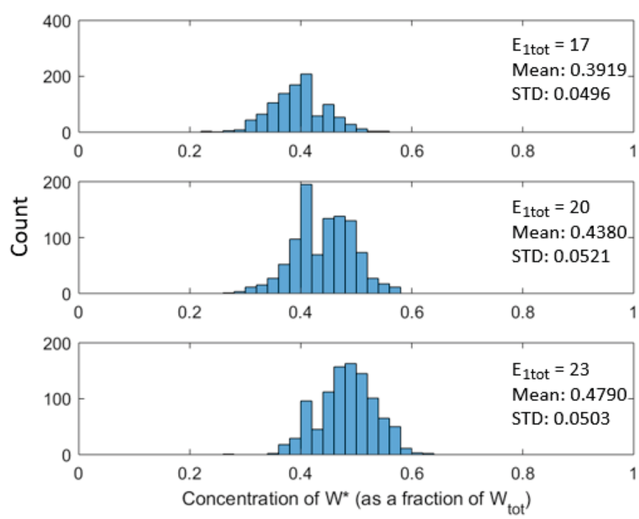

Figure 25: Histogram for a Michaelian response using Gillespie's SSA. As shown, the variability remains fairly constant. Distribution simply moves to the right as E_{1tot} increases. This result was obtained by running 1000 simulations for an increasing input centered around the M-value ($E_{1tot} \approx 20$). This was created using the Michaelian regime with parameters given by $a_1 = a_2 = 0.1$, $d_1 = d_2 = k_1 = k_2 = 5$. Note that the M-value occurs at $E_{1tot} = 20$.

In comparison when examining an ultrasensitive response, see Figure 26, the variability changes quite dramatically as we vary the amount of input. It can be seen that on either side of the M-value the distribution begins to display some skewing behaviour towards the center of the domain. At the M-value itself we observe a distribution that covers the whole domain of possible values when taking into account the decreased conversion potential. This demonstrates that not only does the distribution move to the right as E_{1tot} increases, but the variability increases dramatically as E_{1tot} approaches the M-value. Therefore over a number of systems, we would expect to observe many variations on an ultrasensitive profile, even when under the same constraints on parameters.

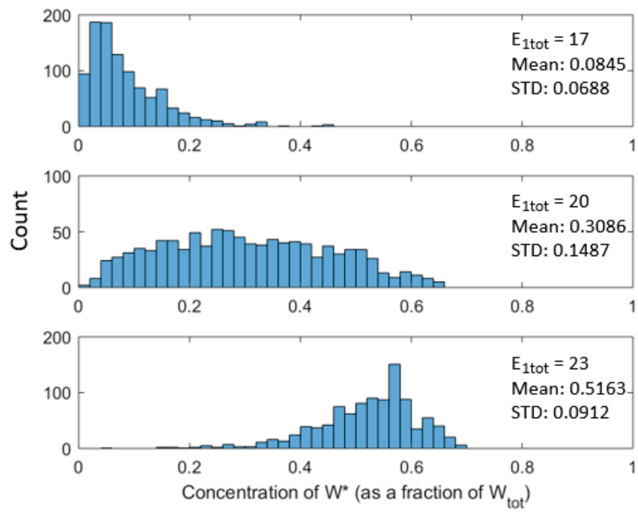

Figure 26: Histogram for an ultrasensitive response using Gillespie's SSA. As shown the variability increases drastically as E_{1tot} passes through the M-value. This result was obtained by running 1000 simulations for an increasing input centered around the M-value ($E_{1tot} \approx 20$). This was created using the base case parameter regime with $a_1 = a_2 = 2$, $d_1 = d_2 = k_1 = k_2 = 1$. Note that the M-value occurs at $E_{1tot} = 20$.

2.7 Summary

In this chapter we have presented a thorough investigation of the G-K mechanism and explored beyond the original analysis of Goldbeter and Koshland. In particular we have thoroughly investigated how the system achieves ultrasensitivity and incomplete conversion potential, how a system is able to achieve a certain M-value, and how we can obtain mixed sensitivity in the dose response profiles. These features can play a key role in how this cycle performs when incorporated into a larger system. We have demonstrated clear links between how the individual rate constants, namely the catalytic constants, can be altered to shift the M-value, and increase conversion potential and sensitivity. We have also seen how altering the Michaelis constants can not only increase sensitivity, but can also have some effect on decreasing conversion potential, shifting the M-value, and introducing mixed sensitivity into the profile. The role of the substrate abundance has also been linked to the incomplete conversion potential of a system and decreases in sensitivity, particularly when we have comparable concentrations of enzyme and substrate, and has also been linked to a shift in the M-value in certain parameter regimes. We have also examined analytic solutions for this system, which have been too complex to provide insight into exactly how the system behaves, but have provided us with insight into the solutions found by our numerical methods. Using stochastic simulation methods, we have also seen how increasing sensitivity, dramatically increases the variability in a system's response which could have large implications in this systems ability to perform when integrated into larger mechanisms.

These results have demonstrated just how difficult it may be to achieve an ultrasensitive response with certain features, particularly when the concentrations of enzymes and substrate are comparable. For this reason, the next chapter introduces two novel examples of positive autoregulation into the reversible covalent-modification cycle, in order to try and improve upon the performance of this system.

3 Positive Autoregulation in the G-K Mechanism

3.1 Introduction

Here we introduce two novel models for enzyme-mediated covalent-modification which may have a significant capacity for ultrasensitivity.

Both of these new models extend the G-K mechanism by including some form of positive autoregulation (PAR). We particularly wished to examine whether these new models might offer improvements in sensitivity when we have comparable concentrations of enzyme and substrate i.e. $W_{tot} = E_{1tot}, E_{2tot}$. Our preliminary analysis of the effect of PAR on ultrasensitivity is given in Appendix B.1, providing a motivation for the detailed study of PAR presented in this chapter. Positive autoregulation refers to a mechanism in which an output of a system either directly or indirectly increases its own production. We propose two possible reaction mechanisms that incorporate PAR. One of them is created by introducing a third reaction to the G-K mechanism, whereby W^* now acts an enzyme to create a complex, C_2, with W which catalyses to create more W^*. We call this direct PAR and will later refer to this as System 2. The second system extends on the G-K mechanism by including two new reactions. We first introduce a reactions which allows W^* to now form a complex with E_1 called C_3. This complex can then form a complex, C_4, with W which catalyses to create W^*. We call this indirect PAR and will later refer to this system as System 3. These systems can be represented by the schematics and reaction equations seen below.

$$W + E_1 \underset{\mathrm{d_1}}{\overset{\mathrm{a_1}}{\rightleftharpoons}} C_1 \overset{\mathrm{k_1}}{\rightarrow} W^* + E_1, \tag{31}$$

$$W^* + E_2 \underset{\mathrm{d_2}}{\overset{\mathrm{a_2}}{\rightleftharpoons}} C_2 \overset{\mathrm{k_2}}{\rightarrow} W + E_2, \tag{32}$$

$$W + W^* \underset{\mathrm{d_3}}{\overset{\mathrm{a_3}}{\rightleftharpoons}} C_3 \overset{\mathrm{k_3}}{\rightarrow} W^* + W^*. \tag{33}$$

$$W + E_1 \underset{\mathrm{d_1}}{\overset{\mathrm{a_1}}{\rightleftharpoons}} C_1 \overset{\mathrm{k_1}}{\rightarrow} W^* + E_1, \tag{34}$$

$$W^* + E_2 \underset{\mathrm{d_2}}{\overset{\mathrm{a_2}}{\rightleftharpoons}} C_2 \overset{\mathrm{k_2}}{\rightarrow} W + E_2, \tag{35}$$

$$W^* + E_1 \underset{\mathrm{d_3}}{\overset{\mathrm{a_3}}{\rightleftharpoons}} C_3, \tag{36}$$

$$W + C_3 \underset{\mathrm{d_4}}{\overset{\mathrm{a_4}}{\rightleftharpoons}} C_4 \overset{\mathrm{k_4}}{\rightarrow} W^* + C_3. \tag{37}$$

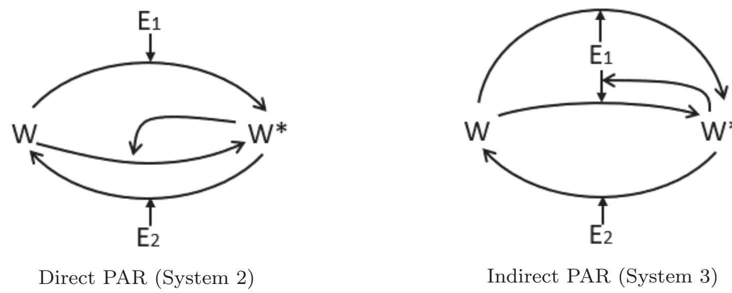

Figure 27: Reaction equations and schematics associated with Systems 2 and 3. System 2 is based on the G-K mechanism where E_1 is the enzyme that catalyses the modification of W, creating W^*, and E_2 catalyses the unmodification of W^* back to W. The third reaction now allows W^* to act as an enzyme and modify W. System 3 uses the same forward and reverse reactions of the G-K mechanism. We then include a third reaction which allows W^* and E_1 to form a complex. This complex is then used in the fourth reaction to modify W and create more W^*.

In order to examine how these systems behave we can use numeric solutions to the mass-action equations associated with each system. For System 2, the mass-action equations derived from reactions (31)-(33) are:

$$\frac{\mathrm{d}W}{\mathrm{d}t} = d_1C_1 + d_3C_3 + k_2C_2 - a_1WE_1 - a_3WW^*, \tag{38}$$
$$\frac{\mathrm{d}W^*}{\mathrm{d}t} = d_2C_2 + d_3C_3 + k_1C_1 + 2k_3C_3 - a_2W^*E_2 - a_3WW^*, \tag{39}$$
$$\frac{\mathrm{d}E_1}{\mathrm{d}t} = d_1C_1 + k_1C_1 - a_1WE_1, \tag{40}$$
$$\frac{\mathrm{d}E_2}{\mathrm{d}t} = d_2C_2 + k_2C_2 - a_2W^*E_2, \tag{41}$$
$$\frac{\mathrm{d}C_1}{\mathrm{d}t} = a_1WE_1 - d_1C_1 - k_1C_1, \tag{42}$$
$$\frac{\mathrm{d}C_2}{\mathrm{d}t} = a_2W^*E_2 - d_2C_2 - k_2C_2, \tag{43}$$
$$\frac{\mathrm{d}C_3}{\mathrm{d}t} = a_3WW^* - d_3C_3 - k_3C_3. \tag{44}$$

For System 3, the mass-action equations derived from reactions (34)-(37) are:

$$\frac{\mathrm{d}W}{\mathrm{d}t} = d_1C_1 + k_2C_2 + d_4C_4 - a_1WE_1 - a_4WC_3, \tag{45}$$
$$\frac{\mathrm{d}W^*}{\mathrm{d}t} = k_1C_1 + d_2C_2 + d_3C_3 + k_4C_4 - a_2W^*E_2 - a_3W^*E_1, \tag{46}$$
$$\frac{\mathrm{d}E_1}{\mathrm{d}t} = d_1C_1 + k_1C_1 + d_3C_3 - a_1WE_1 - a_3W^*E_1, \tag{47}$$
$$\frac{\mathrm{d}E_2}{\mathrm{d}t} = d_2C_2 + k_2C_2 - a_2W^*E_2, \tag{48}$$
$$\frac{\mathrm{d}C_1}{\mathrm{d}t} = a_1WE_1 - d_1C_1 - k_1C_1, \tag{49}$$
$$\frac{\mathrm{d}C_2}{\mathrm{d}t} = a_2W^*E_2 - d_2C_2 - k_2C_2, \tag{50}$$
$$\frac{\mathrm{d}C_3}{\mathrm{d}t} = a_3W^*E_1 + d_4C_4 + k_4C_4 - d_3C_3 - a_4WC_3, \tag{51}$$
$$\frac{\mathrm{d}C_4}{\mathrm{d}t} = a_4WC_3 - d_4C_4 - k_4C_4. \tag{52}$$

We then obtain steady state solutions to the systems by solving the set of equations numerically with Matlab's built-in ODE solver, *ode23s*. These systems are also subject to the following conservation equations which can be used to check that the numeric solutions are performing correctly and later used for analytic solutions;

$$W_{tot} = W + W^* + C_1 + C_2 + C_3, \tag{53}$$

$$E_{1tot} = E_1 + C_1, \tag{54}$$

$$E_{2tot} = E_2 + C_2, \tag{55}$$

for System 2 and,

$$W_{tot} = W + W^* + C_1 + C_2 + C_3 + C_4, \tag{56}$$

$$E_{1tot} = E_1 + C_1 + C_3 + C_4, \tag{57}$$

$$E_{2tot} = E_2 + C_2, \tag{58}$$

for System 3.

We are now interested in examining the role of substrate abundance, Michaelis constants, and the individual rate constants in these modified systems. We are also interested in directly comparing these new systems with the G-K mechanism when under similar parameter regimes. We also derive analytic solutions for these systems and produce stochastic simulations to explore the variability of these systems.

3.2 Numeric Simulations

Since the modified systems have a different set of reactions than the G-K mechanism, we need to define a base case in which we can clearly compare the effect of adding PAR. To do this we considered the scenario in which all rate constants were set to unity. For the G-K mechanism, this was very similar to the base case discussed in the previous chapter and obtains an ultrasensitive profile with incomplete conversion potential (Figure 13). However when we examine the two new systems under this regime we find that both profiles are very different (Figure 28). System 2 is associated with a profile with a trivial M-value and a lower conversion potential. We also observe that System 3 is associated with a profile that has a very low conversion potential and the concentration of modified substrate rapidly declines after achieving the conversion potential. Since we are interested in using these profiles as base cases for later investigations, we ideally want a profile that does not have a trivial M-value and a similar conversion potential to the base case in the G-K mechanism.

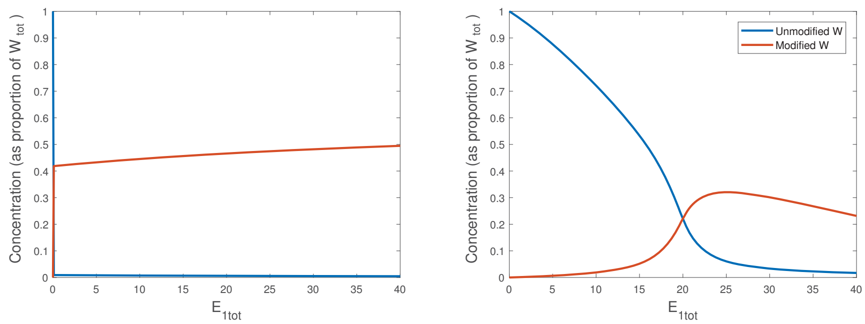

System 2 System 3

Figure 28: Base cases with all rate constants set to unity. We observe that in System 2, the profile has a trivial M-value and decreased conversion potential. For System 3 we have a decrease in sensitivity and conversion potential. We also observe that the concentration of the modified substrate decreases after the conversion potential is achieved. The system parameters were chosen such that $W_{tot} = 100$, $E_{2tot} = 20$, and $E_{1tot} \in [0, 40]$.

We are then interested in selecting a different parameter regime that can obtain features more similar to those of the G-K mechanism whilst using comparable rate constants to the G-K mechanism. By altering the rate constants associated with the added reactions that are not found in the G-K mechanism we maintain the same regime for the reactions that are found in all systems. Through trial and error we identified a more useful reference parameter set for thi multi-system comparison. These parameter regimes and their associated profiles can be found in Figure 29. Based on this figure we observe that we are now able to achieve similar levels of conversion potential and ultrasensitivity as the G-K mechanism.

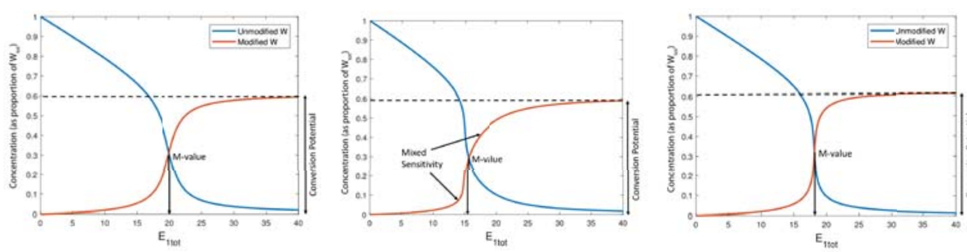

G-K Mechanism System 2 System 3

Figure 29: Optimised base cases for Systems 2 and 3 alongside the G-K mechanism. We now observe a conversion potential of approximately 0.6 for System 2 and the G-K mechanism and 0.62 for System 3. The M-value for the three systems is located at $E_{1tot} = 20$ for the G-K mechanism, $E_{1tot} \approx 15$ for System 2 and $E_{1tot} \approx 18$ for System 3. We also observe mixed sensitivity for System 2, but not for System 3 or the G-K mechanism. The system parameters were chosen such that $W_{tot} = 100$, $E_{2tot} = 20$, and $E_{1tot} \in [0, 40]$. For the three systems the rate constants for the forward and reverse reactions were set as $a_1 = a_2 = d_1 = d_2 = k_1 = k_2 = 1$. For System 2 we then set $a_3 = 0.01$ and $d_3 = k_3 = 1$. For System 3 we set $a_3 = 0.01$, $a_4 = 2$, $d_4 = 1$, and $d_3 = k_4 = 10$.

With a new reference parameter set for each system, we can now examine how alterations to these parameters affect these systems. We do this using the same procedure as in Chapter 2.3 by focusing on (i) the effect of substrate abundance, (ii) the role of the Michaelis constants, and (iii) the role of the individual rate constants. Detailed results of these investigations can be found in Appendices B.2 and B.3 along with a summary of the findings in Appendix B.4.

Introducing PAR into the reversible covalent-modification cycle increases the complexity of this system quite dramatically. Therefore using analytic methods, like what was used for the G-K mechanism, to understand how these systems behave is much more difficult. Instead we use the simulated results of altering these parameters and the knowledge that we have gained from analysing the G-K mechanism to investigate how the implementations of PAR affect the behaviour of our system. We are also interested in understanding how these affect a number of key characteristics in the concentration profiles. Namely we are interested in the conversion potential, mid-conversion stimulus (M-value), sensitivity, and mixed sensitivity.

We also discover that these two new models are capable of a response that was not possible for the original G-K mechanism: bistability. In these systems bistable behaviour refers to when the concentrations of substrate change discontinuously as the input increases i.e. they "jump" from one value to another. In the following simulations we do not observe discontinuities in the profile at the occurrence of the bistability due to the plotting method used. Instead we observe a bistable response as a sharp change as opposed to the smooth curves that we will associate with a continuous, ultrasensitive response. This can be seen in Figure 30 where we observe the sharp change in W^*. This plot also demonstrates the second set of steady states for the bistable response (dashed line). We emphasise that there is a clear and important distinction between bistable and ultrasensitive responses. We discuss this, along with the explanation for the occurrence of bistability, in detail in regards to the analytic solution to System 2 in Chapter 3.4.

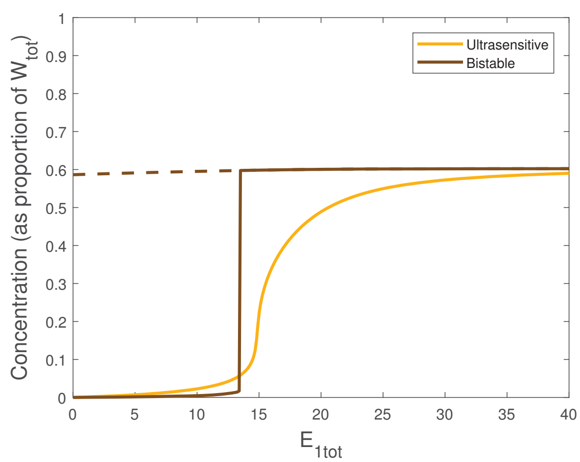

Figure 30: Comparison of an ultrasensitive and bistable response for the unmodified substrate in System 2. The ultrasensitive response is characterised by its smooth profile. A bistable response is then distinguished by the sharp change in the profile as we essentially "jump" from one value to the next. The dashed line represents the second set of steady states for the bistable response. The system parameters are set as $W_{tot} = 100$, $E_{2tot} = 20$, and $E_{1tot} \in [0, 40]$. The ultrasensitive response is created with the rate constants set to be $a_1 = a_2 = d_1 = d_2 = d_3 = k_1 = k_2 = k_3 = 1$, and $a_3 = 0.01$. The bistable response is created with the rate constants set to be $a_1 = a_2 = d_3 = k_3 = 5$, $d_1 = d_2 = k_1 = k_2 = 1$ and $a_3 = 0.05$.

3.2.1 The Role of Substrate Abundance

We first examine the effect of the relative concentrations of substrate and enzyme in the two new models. To do this we increase the value of W_{tot} ten-fold and one hundred fold whilst holding the total enzyme concentrations constant. The increase in substrate abundance is represented by the change in line type: solid, dashed, dotted. Detailed results of these investigations can be found in Appendices B.2 and B.3 along with a summary of the findings in Appendix B.4.

In the G-K mechanism, increasing the value of W_{tot} increased the sensitivity, conversion potential and, when the Michaelis constants were not equal, increased the M-value.

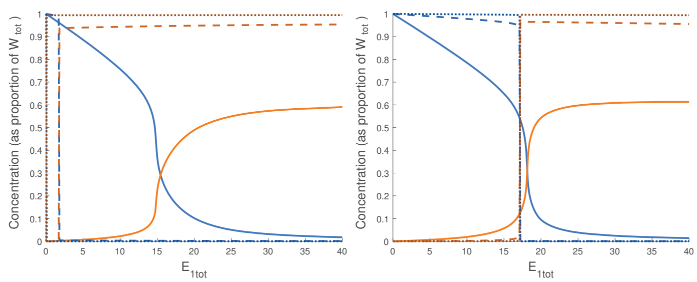

Figure 31: Investigation 1: Test 1. Profiles are created with the same parameters as the base cases for each system, but with $W_{tot} = \{100, 1000, 10000\}$. The increase in total substrate is represented by the line type: solid, dashed, dotted i.e. the smallest value for W_{tot} is represented by a solid line and the largest value is represented by a dotted line.

Much like in the G-K mechanism, Figure 31 demonstrates that increasing the relative abundance of substrate increases the conversion potential and the sensitivity of the modified systems. Since the concentrations of the complexes contribute a smaller percentage to the increased total substrate. This follows from the conservation equations for the total substrate for Systems 2 and 3 given by equations (53) and (56) respectively. Since in System 3 all of the complexes are bound by the total concentrations of the enzymes, E_{1tot} and E_{2tot}, increasing W_{tot} will decrease the complex concentrations in proportion and hence increase the conversion potential. For System 2, the complexes C_1 and C_2 are bound by the total enzyme, but C_3 is only bound by W_{tot}. However due to the small association constant that governs the creation of this complex, the concentration remains relatively small. Hence an increase in W_{tot} results in an increased conversion potential.

However we now find that both new systems are capable of a bistable response for some values of E_{1tot}. We observe this response in Figure 31 when $W_{tot} = 10^3$ (dashed line) and $W_{tot} = 10^4$ (dotted line).

We also begin to observe clear shifts in the mid-conversion stimulus as we increase the total substrate. This occurs even when the Michaelis constants are equal. This is unlike the G-K mechanism where the Michaelis constants had to be different in order for the total substrate to have some effect on the M-value. By increasing W_{tot} the M-value in both systems is decreased. This was much like the G-K mechanism when $K_{m1} < K_{m2}$, which could be caused by the extra affinity for the forward reaction as a result of the added reactions. In System 3 this shift is not dramatic and changed very little after the base case (solid line). System 2 however has a dramatic shift from the base case (solid line) as we increase W_{tot} and finally approaches a trivial M-value when $W_{tot} = 10^4$ where the conversion of the modified substrate occurs immediately with any input to the system. This change in the M-value is most likely due to the increased affinity for the added reactions in Systems 2 and 3. Since these reactions have a higher affinity, we observe a higher sensitivity and a decreased M-value. In the G-K mechanism, when the Michaelis constants were equal, this had no effect as increasing W_{tot} increased the affinity for both reactions equally. When these values were different, we were able to relate this back to a well-defined function for the M-value, but it could also be linked to a difference in affinities.

3.2.2 The Role of Michaelis Constants

We now investigate the effect that altering the Michaelis constants have on the modified systems by increasing the Michaelis constants associated with each reaction individually. This was done by decreasing and increasing the value of the associative constants, a_*, by five-fold which respectively increases and decreases the value of the associated Michaelis constant, K_{m*}. These Michaelis constants exist for all reactions, bar one in System 3, such that there were three Michaelis constants for System 2 and three for System 3. For System 3, the set of reactions that define the creation of C_3 only involves an associative and dissociative reaction, and therefore will not have a catalytic rate constant, k_3. We therefore refer to this as a "dissociation rate" and it represents the ratio of the two rate constants given by $K_d = \frac{d_3}{a_3}$. We increase and decrease this value by decreasing and increasing, respectively, the value of a_3 by five-fold. The decrease in the Michaelis constants and K_d is represented by the line type: solid, dashed, dotted. Detailed results of these investigations can be found in Appendices B.2 and B.3 along with a summary of the findings in Appendix B.4.

In the G-K mechanism, altering the Michaelis constants led to a number of effects on the substrate concentration profiles. We observed that decreasing the Michaelis constant, K_{m1}, or increasing K_{m2} resulted in shifting the M-value to the left and increasing the conversion potential. By decreasing K_{m1}, K_{m2} or both, we observed an increase in sensitivity of the profile. Finally, when the Michaelis constants were not equal, we observed a profile which had mixed sensitivity behaviour whereby the profile was asymmetric and appeared to be more sensitive on one side of the M-value than the other.

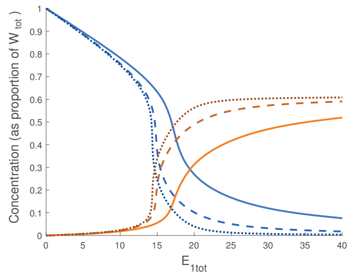

Altering K_{m1}: Test 2

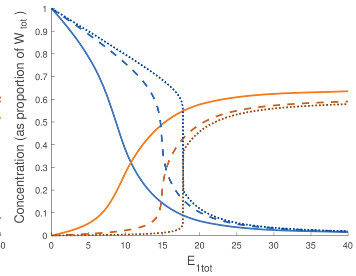

Altering K_{m2}: Test 3

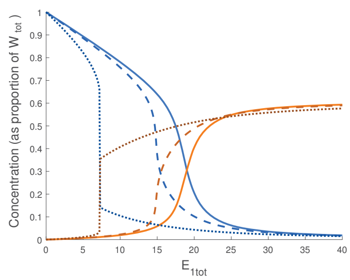

Altering K_{m3}: Test 4

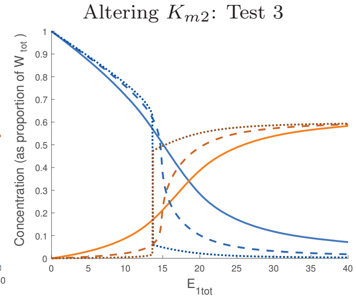

Altering K_{m1}, K_{m2} and K_{m3}: Test 5

Figure 32: System 2 Investigation 2: Altering Michaelis constants. The system parameters are set as $W_{tot} = 100$, $E_{2tot} = 20$, and $E_{1tot} \in [0, 40]$ with the rate constants set to be $d_1 = d_2 = k_1 = k_2 = d_3 = k_3 = 1$. To alter the Michaelis constants we set $a_1 = \{0.2, 1, 5\}$ in Test 2, $a_2 = \{0.2, 1, 5\}$ in Test 3, $a_3 = \{0.002, 0.01, 0.05\}$ in Test 4, and $a_1 = \{0.2, 1, 5\}$, $a_2 = \{0.2, 1, 5\}$, and $a_3 = \{0.002, 0.01, 0.05\}$ in Test 5. The increase in rate constants is represented by the line type: solid, dashed, dotted i.e. the smallest value for a is represented by a solid line and the largest value is represented by a dotted line.

For System 2 we find that when we examine the Michaelis constants associated with the original reactions, K_{m1} and K_{m2}, altering these values have the same effect as what was observed with the G-K mechanism (see Tests 2, and 3 in Figure 32). It is worth noting that we do obtain asymmetric behaviour i.e. mixed sensitivity, when altering these Michaelis constants, but unlike the G-K mechanism, this was already present in the base case. We could consider this to be a result of having unbalanced affinities for the creation and removal of the modified substrate as this system now has two reactions creating more W^* and only one reaction for its removal. However this may be specific to this implementation of PAR as we do not observe this in the indirect PAR implementation.

When decreasing the value of K_{m3} we observe similar behaviours to K_{m1} whereby we shift the M-value left and increase the sensitivity (see Test 4 in Figure 32). We also find that, more like K_{m2}, increasing K_{m3} increases the conversion potential. This effect is fairly minimal in comparison to the effect of the other Michaelis constants, but this is most likely due to the already large magnitude of this constant. We could link this behaviour to the observation made in the G-K mechanism whereby increasing the Michaelis constant was observed to decrease the creation of the complexes, which increases conversion potential, but also decreases the sensitivity.

When we examine these profiles in detail, we actually find that decreasing K_{m3} increases the mixed sensitivity of the profiles. This means that whilst the profiles may appear to increase in sensitivity, the Hill coefficient actually decreases from 9.5701 (solid line) to 4.2559 (dotted line). This highlights the Hill coefficients incapability to effectively measure the sensitivity of an asymmetric profile. It is also worth noting that when $K_{m3} = 10^3$ (solid line) we achieve a profile which appears to be symmetric. This can be observed when we are modifying K_{m3} by itself and when altering all Michaelis constants. This is possibly a result of the third reaction having such little effect, due to such a small association constant, that the profile appears to behave the same as the G-K mechanism.

When decreasing all three Michaelis constants we find that the profile increases in sensitivity as occurred in the G-K mechanism (see Test 5 in Figure 32). However we also shift the M-value left and obtain a bistable response for the smallest parameter regime (dotted line). This bistable response is also found for small values of K_{m1}, K_{m2} and K_{m3} when we continue to decrease this value past what is demonstrated here.

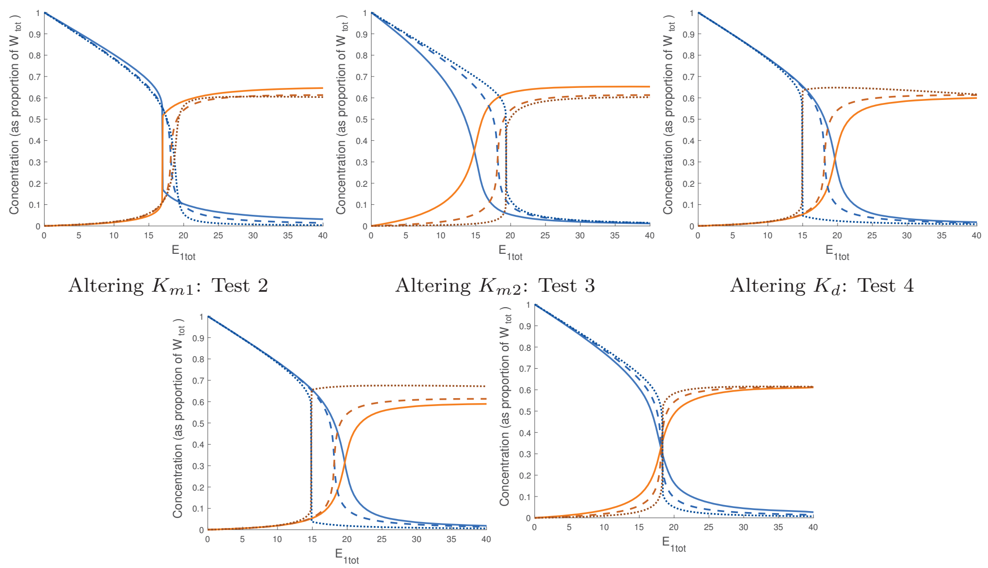

Altering K_{m1}: Test 2 — Altering K_{m2}: Test 3 — Altering K_d: Test 4

Altering K_{m4}: Test 5 — Altering K_{m1}, K_{m2} and K_{m4}: Test 6

Figure 33: System 3 Investigation 2: Altering Michaelis constants. The system parameters are set as $W_{tot} = 100$, $E_{2tot} = 20$, and $E_{1tot} \in [0, 40]$ with the rate constants set to be $d_1 = d_2 = k_1 = k_2 = d_4 = 1$, and $d_3 = k_4 = 10$. To alter the Michaelis constants we set $a_1 = \{0.2, 1, 5\}$ in Test 2, $a_2 = \{0.2, 1, 5\}$ in Test 3, $a_3 = \{0.002, 0.01, 0.05\}$ in Test 4, $a_4 = \{0.4, 2, 10\}$ in Test 5 and $a_1 = \{0.2, 1, 5\}$, $a_2 = \{0.2, 1, 5\}$, $a_3 = \{0.002, 0.01, 0.05\}$, and $a_4 = \{0.4, 2, 10\}$ in Test 6. The increase in rate constants is represented by the line type: solid, dashed, dotted i.e. the smallest value for a is represented by a solid line and the largest value is represented by a dotted line.

In System 3, we begin to observe some variation to the G-K mechanism, namely the effect of the Michaelis constant, K_{m1}. We now observe that an increase in K_{m1} increases the conversion potential and sensitivity and decreases the M-value (see Test 2 in Figure 33). This parameter now has the opposite effect to what it did in the G-K mechanism. In fact the added reactions now appear to take the role of altering K_{m1} in the G-K mechanism, whereby decreasing K_d or K_{m4} will increase the conversion potential and sensitivity and decreases the M-value (see Tests 4 and 5 in Figure 33). This dramatic change in the effect of K_{m1} could be linked to the introduced competition that the forward reaction now has with both the third and fourth reactions.

It is worth noting that altering K_{m2} has the same behaviour as it did in the G-K mechanism (see Test 3 in Figure 33). We also find that altering each of the Michaelis constants individually will result in mixed sensitivity which matches behaviour observed in the G-K mechanism, but now we also obtain bistability for some regimes. Also similar to the G-K mechanism, when altering all Michaelis constants simultaneously, we do not obtain mixed sensitivity, but we do obtain bistable profiles for smaller Michaelis constants (see Test 6 in Figure 33).

3.2.3 The Role of Individual Rate Constants

We now aim to understand the role that the individual rate constants (i.e. a_i, d_i, and k_i) play in the new systems. As was discussed in Section 2.3.3, of the three rate constants associated with the first reaction (W to W^*), only the catalytic constant k_1 had any effect on the dose-response profile of the G-K mechanism without also altering the value of the Michaelis constant. This is also applied to the modified systems whereby we investigate the effect of the catalytic constants by increasing all of the rate constants associated with a certain reaction by two-fold. This is done to ensure that the Michaelis constant remains unchanged throughout the investigation and only the magnitude of the rate constants are altered. This is equivalent to examining the result of increasing the affinity for a reaction by increasing all of the rate constants associated with that reaction. As stated in Section 3.2.2, System 3 includes a reaction that does not involve a catalytic constant. For this reaction we still increase both rate constants two-fold. The increase in the rate constants is represented by the line type: solid, dashed and dotted. The quantitative results of these investigations can be found in Appendices B.2 and B.3 along with a summary of the findings in Appendix B.4.

Much like the G-K mechanism when k_1 is increased or k_2 is decreased, the M-value is decreased, and the sensitivity and conversion potential are increased for both of the modified systems. It is also worth noting that for Systems 2 and 3 changes in k_2 have a larger effect on these features than k_1 does e.g. a larger decrease in the M-value is achieved by increasing k_2 then by decreasing k_1 (see Figures 34 and 35). For the G-K mechanism, this effect was the same. This result is most likely caused by the higher affinity for the production of W^* in the modified systems. We also find that when altering all catalytic constants, as observed in the G-K mechanism, there is no change in any of the systems (see Test 9 in Figure 34 and Test 11 in Figure 35).

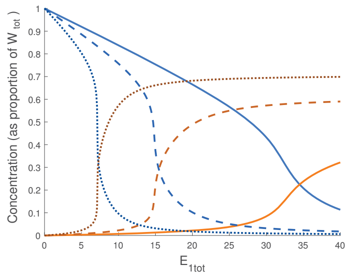

Increased affinity for forward reaction: Test 6

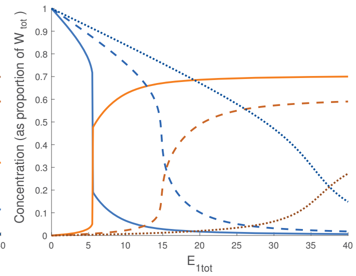

Increased affinity for reverse reaction: Test 7

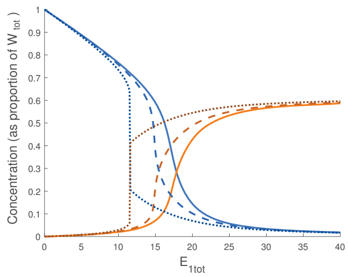

Increased affinity for third reaction: Test 8

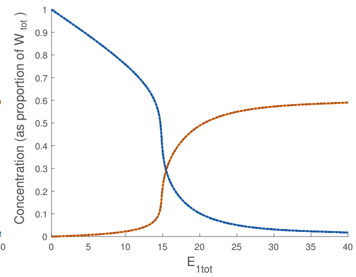

Increased affinity for all reactions: Test 9

Figure 34: System 2 Investigation 3: Altering all catalytic constants. The system parameters are set as $W_{tot} = 100$, $E_{2tot} = 20$, and $E_{1tot} \in [0, 40]$ with the rate constants set to be $a_1 = a_2 = d_1 = d_2 = k_1 = k_2 = d_3 = k_3 = 1$, and $a_3 = 0.01$. To alter the affinity of the reactions we alter the rate constants to be $a_1 = d_1 = k_1 = \{0.5, 1, 2\}$ for Test 6, $a_2 = d_2 = k_2 = \{0.5, 1, 2\}$ for Test 7, and $a_3 = \{0.005, 0.01, 0.02\}$, and $d_3 = k_3 = \{0.5, 1, 2\}$ for Test 8. Altering all rate from the base case by two-fold gives the regimes used in Test 9. The increase in rate constants is represented by the line type: solid, dashed, dotted i.e. the smallest set of values are represented by a solid line and the largest values are represented by a dotted line.

When examining the added reaction of System 2 we find that altering k_3 acts in much the same way as k_1 since this reaction takes a similar form as the forward reaction (see reactions 31 and 33). We observe that the magnitude of the effect on the sensitivity is similar to that observed when altering k_1. However the magnitude of the effect on the M-value and, in particular, the conversion potential, decreases in comparison (see Tests 6, and 8 in Figure 34). The profiles obtained for this system remain asymmetric and we find that we obtain bistable responses for larger values of k_2 and smaller values of k_1 and k_3.

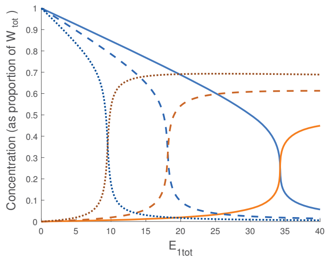

Increased affinity for forward reaction: Test 7

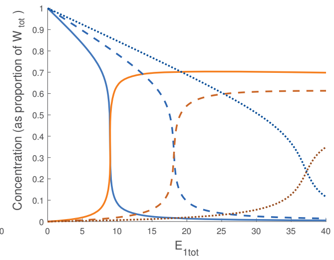

Increased affinity for reverse reaction: Test 8

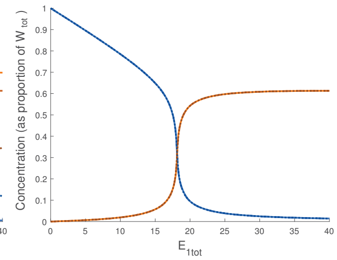

Increased affinity for third reaction: Test 9

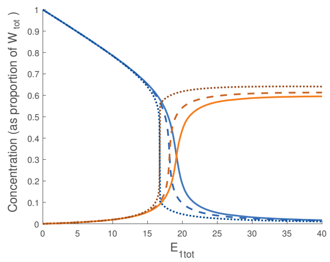

Increased affinity for fourth reaction: Test 10

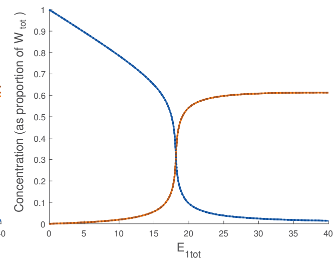

Increased affinity for all reactions: Test 11

Figure 35: System 3 Investigation 3: Altering all catalytic constants. The system parameters are set as $W_{tot} = 100$, $E_{2tot} = 20$, and $E_{1tot} \in [0, 40]$ with the rate constants set to be $a_1 = a_2 = d_1 = d_2 = k_1 = k_2 = d_4 = 1$, $a_3 = 0.01$, $a_4 = 2$ and $d_3 = k_4 = 10$. To alter the affinity of the reactions we alter the rate constants to be $a_1 = d_1 = k_1 = \{0.5, 1, 2\}$ in Test 7, $a_2 = d_2 = k_2 = \{0.5, 1, 2\}$ in Test 8, $a_3 = \{0.002, 0.01, 0.02\}$, and $d_3 = \{0.5, 1, 2\}$ in Test 9, and $a_4 = \{1, 2, 4\}$, $d_4 = \{0.5, 1, 2\}$, and $k_4 = \{5, 10, 20\}$ in Test 10. Altering all rates from the base case by two-fold gives the regimes used in Test 11. The increase in rate constants is represented by the line type: solid, dashed, dotted i.e. the smallest set of values are represented by a solid line and the largest values are represented by a dotted line.

For System 3 we observed that the effect of altering k_4 matches the effect of k_1 but again with a much smaller magnitude (see Tests 7,and 10 in Figure 35). This means that increasing k_4 also increases sensitivity and conversion potential and decreases the M-value. This similarity is most likely due to this reaction being very similar in form to the first reaction (see reactions 34 and 37). For larger values of k_4 we do however achieve a bistable response.

When examining the effect of altering d_3 we find that there is no change in the profile. We can relate this to the concentration of C_3 at steady state, whereby by manipulating the Mass-Action equations (51) and (51) gives the following expression,

$$C_3 = \frac{a_3}{d_3} W^* E_1.$$

From this we note that altering a_3 and d_3 simultaneously, and by the same amount, will not have any effect on the creation of the complex. Hence we do not observe any change in the profile.

3.3 Comparison to G-K Mechanism

We are now interested in directly comparing the modified systems with the G-K mechanism to understand how the features of the profiles compare. As previously discussed, we have defined a reference parameter set for Systems 2 and 3 whereby the first two reactions, which are present in all systems (including the G-K mechanism), have the same value for all rate constants.

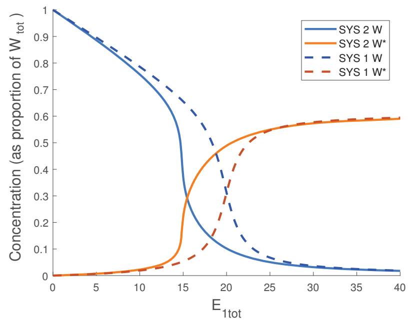

System 2

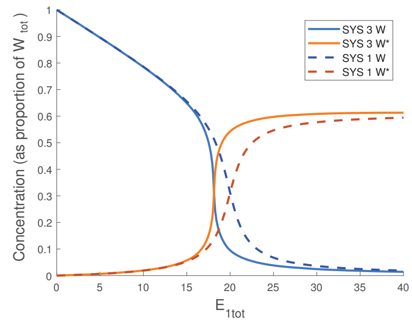

System 3

Figure 36: Direct comparison of modified systems (solid lines) and the G-K mechanism (dashed lines). The system parameters are set as $W_{tot} = 100$, $E_{2tot} = 20$, and $E_{1tot} \in [0, 40]$. For all systems the rate constants for the forward and reverse reactions were set as $a_1 = a_2 = d_1 = d_2 = k_1 = k_2 = 1$. For System 2 we then set $a_3 = 0.01$ and $d_3 = k_3 = 1$. For System 3 we set $a_3 = 0.01$, $a_4 = 2$, $d_4 = 1$, and $d_3 = k_4 = 10$.

Both of the two new systems produce different profiles to that obtained by the G-K mechanism. As shown in Figure 36, in System 2 we observe that the profile is able to achieve the same level of conversion potential as the G-K mechanism. However we observe that the M-value is decreased and we obtain the asymmetric behaviour associated with mixed sensitivity. We find that the Hill coefficient which could be considered to be like an average sensitivity measurement demonstrates that the G-K mechanism is more sensitive than System 2, but we can observe that System 2 is clearly more sensitive prior to the M-value. When we examine System 3 we observe similar behaviour with a shifted crossover, but now with a clear increase in sensitivity, supported by the Hill coefficient, and an increased conversion potential (see Figure 36).

We now consider the effect that the added reactions have on the new systems in comparison to the G-K mechanism. Firstly we note that we are able to decrease the M-value as the added reactions allow us to create the modified substrate at a faster rate. Secondly this increased rate of production, along with the effect of positive autoregulation, is most likely the reasoning for an increased sensitivity (at least prior to the M-value for System 2).

A reduced conversion potential occurs when there is a non-negligible concentration of complexes at steady state. For this reason we would expect that adding more reactions, and hence more complexes, would immediately decrease the conversion potential. However what we observe in both systems is that we are either able to match the conversion potential or improve upon it under these parameter regimes. When we examine the behaviour of the complexes in System 2 the concentration of the added complex, C_3, is only able to achieve a relatively low concentration. As we continue to increase the input, the complexes mainly consist of C_1 and C_2 at concentrations almost identical to those observed in the G-K mechanism. This results in the conversion potential being the same in the two profiles. When we examine System 3, we again find that the added complexes are almost insignificant in concentration. However we observe two differing features, namely that C_1 is now at a much lower concentration than in the G-K mechanism, and that as we continue to increase the input to the system, C_3 begins to increase in concentration. As C_1 is at a lower concentration, we are able to achieve an increased conversion potential. As we have observed earlier in this chapter (see Figure 28 for a clear example), the concentration of modified substrate begins to decrease after the conversion potential is achieved, as C_3 increases in concentration. This behaviour continues whilst we increase the input until all of the remaining free modified substrate, is contained in this complex.

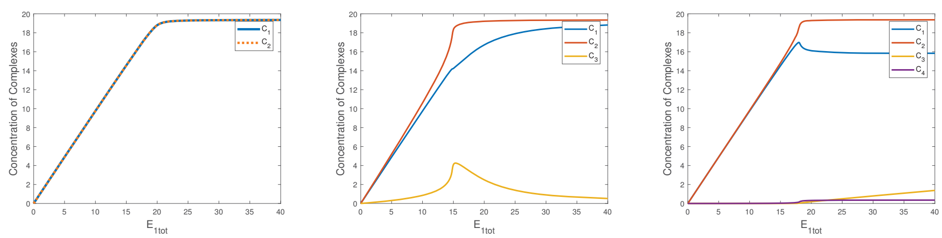

System 1 System 2 System 3

Figure 37: Complex concentrations for System 2 and 3 using the same parameter regimes as Figure 36. In System 1 the complexes are represented by: C_1 is the WE_1 complex (blue), and C_2 is the W^*E_2 complex (orange dashed). In System 2 the complexes are represented by: C_1 is the WE_1 complex (blue), C_2 is the W^*E_2 complex (red), and C_3 is the WW^* complex (yellow). In System 3 the complexes are represented by: C_1 is the WE_1 complex (blue), C_2 is the W^*E_2 complex (red), C_3 is the W^*E_1 complex (yellow), and C_4 is the WC_3 complex (purple).

We are also interested in examining the "robustness" of these parameter regimes. Here, a robust profile refers to the minimal effect on a systems profile when altering the systems parameters. When we are examining biological systems we would expect some variation in the parameters that govern the system. In some cases having a large effect to a small perturbation in parameters may have a positive effect, such as a large increase in sensitivity, or negative such as a decrease in conversion potential. We may also be interested in having a system which is robust to changes in the parameters.

By analysing the simulations of the three systems when changing the parameters for the shared reactions, we were able to gather information about which parameters effect which systems more (see Appendices B.2 and B.3). When examining System 2, we found that the sensitivity and M-value of the profiles were affected more by changes in the total substrate and by alterations in the Michaelis constants than was observed for the G-K mechanism. In addition, altering the Michaelis constant, K_{m2}, and the catalytic constant, k_2 had a larger effect on the M-value for System 2 than for the G-K mechanism. However if we alter k_1, the sensitivity and M-value for the G-K mechanism are altered more than for System 2. It is worth noting that all of the common parameters affect the conversion potential of these systems by a similar amount.

When examining System 3 on the other hand, we find that altering the total substrate has a larger effect on the sensitivity and M-value than the G-K mechanism, but the conversion potential is affected more in the G-K mechanism. We also find that the sensitivity is effected more in System 3 when altering all of the Michaelis constants simultaneously. However altering K_{m1} by itself or the catalytic constants, k_1 or k_2, effected the sensitivity and M-value more in the G-K mechanism. Similarly, altering k_1 or k_2 also had a greater effect on the conversion potential of the G-K mechanism.

It is also worth noting that altering some of these parameters can cause Systems 2 and 3 to exhibit bistable behaviour rather than ultrasensitivity. Depending on how these systems are embedded into a larger network structure, it could be functionally important that the system not be bistable.

3.4 Analytic Solutions

To better understand how these two new auto-regulatory models behave, we have attempted to derive analytic solutions for W and W^* at steady state in these models using similar methods to those used for the G-K mechanism. Through this method we obtained an analytic solution for the direct PAR system (System 2), but not for the indirect PAR system (System 3). In System 3 we find that the complexes at steady state are too strongly dependent on the two forms of substrate. Due to this dependence we were unable to successfully uncouple these variables using the same approach used for the other systems (see Appendix B.6 for attempted derivation). In future work systematic elimination methods (e.g. via Groebner bases [41]) could be used to uncouple these variables, although it is possible that no such uncoupling exists.

The analytic solution for W in System 2 is a quintic given by

$$\begin{aligned}
&W^5\big[k_3(K_{m3}-\gamma_3 K_{m2})\big] + W^4\big[\sigma_2(K_{m3}-\gamma_3 K_{m2}) - k_2\sigma_1 + \gamma_3 k_2 E_{2T} K_{m3}\big] \\
&+ W^3\big[-\sigma_3(K_{m3}-\gamma_3 K_{m2}) + \gamma_3\sigma_6 - \sigma_1\sigma_2 - k_3\sigma_4 + k_2 E_{2T} K_{m3}^2\big] \\
&+ W^2\big[\gamma_3\sigma_5 - \sigma_2\sigma_4 + \sigma_6 K_{m3} + \sigma_1\sigma_3\big] + W\big[\sigma_5 K_{m3} + \sigma_3\sigma_4 - \gamma_3 k_2 E_{2T} K_{m1}^2 K_{m3} W_T\big] \\
&- k_2 E_{2T} K_{m1}^2 K_{m3}^2 W_T = 0,
\end{aligned}$$

where

$$\sigma_1 = K_{m3}W_T - K_{m1}K_{m3} + K_{m2}K_{m3} - \gamma_1 E_{1T} K_{m3} = \gamma_3 K_{m1}K_{m2},$$
$$\sigma_2 = k_3(K_{m1} - W_T + \gamma_1 E_{1T}) - \gamma_3 k_1 E_{1T},$$
$$\sigma_3 = k_1 E_{1T} K_{m3} + k_3 K_{m3} W_T,$$
$$\sigma_4 = K_{m1}K_{m2}K_{m3} + K_{m1}K_{m3}W_T,$$
$$\sigma_5 = \sigma_7 k_2 E_{2T} K_{m1} - k_2 E_{2T} K_{m1} K_{m3} W_T,$$
$$\sigma_6 = \sigma_7 k_2 E_{2T} + k_2 E_{2T} K_{m1} K_{m3},$$
$$\sigma_6 = K_{m1}K_{m3} - K_{m3}W_T + \sigma_1 E_{1T} K_{m3}.$$

A detailed derivation of this solution is given in Appendix B.5.

The roots of this quintic polynomial are then found numerically using Matlab's built-in solver, *roots*. We found that when we use a parameter set that produces a continuous response to the input, E_{1tot}, such as the base case for this system (see Section 3.1), there exists only one valid root for each value of input that meets the physical requirements implied by our system, namely the conservation equations (Equations (53),(54), and (55)) and the concentrations of all molecules must be real values between zero and W_{tot} (see Figure 38). When the system has a parameter set that gives rise to a bistable response, we obtain a bifurcation. An example of how the analytic solution compares with the numeric solution for an ultrasensitive, continuous parameter regime can be found below.

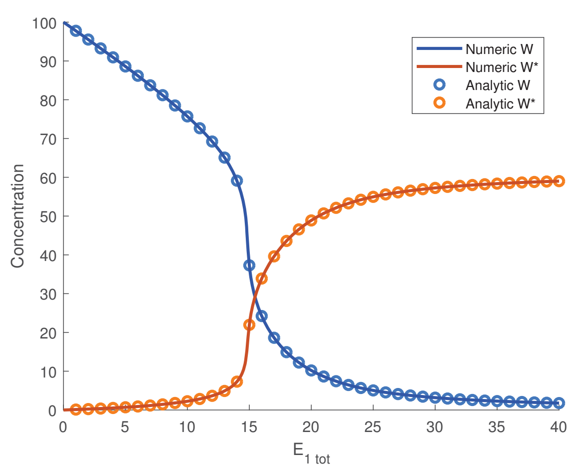

Figure 38: Comparison of analytic solution with numerical results from the ODEs. This confirms the validity of numeric solution. The system parameters are set as $W_{tot} = 100$, $E_{2tot} = 20$, and $E_{1tot} \in [0, 40]$ with the rate constants set to be $a_1 = a_2 = d_1 = d_2 = k_1 = k_2 = d_3 = k_3 = 1$, and $a_3 = 0.01$ for both the analytic and numeric results.

An example of the solution to System 2 using a parameter regime which gives rise to a bistable response is found in Figure 39. We observe that for low input values ($E_{1tot} \approx [0, 2.5]$) our numerical root solvers find three valid roots to the cubic solution in W. Beyond a threshold value in input ($E_{1tot} > 2.5$), we find that there is only one root. When we perform a linear stability analysis on these solutions we find that for these low input values, there is one unstable root between two stable roots. This relates to the bistable behaviour whereby a stable solution for W will jump from a large concentration state to a low concentration state as soon as its concentration passes under the unstable state. This also means that unlike the parameter regime that gives an ultrasensitive response, it is possible for this system to have no M-value if the initial concentration of W is located under the unstable solutions. This is demonstrated in Figure 39 whereby we obtain two profiles of the same bistable parameter regime using two different initial conditions. The first initial condition has our system starting with all free substrate found in the unmodified form, W. The second initial condition has all substrate initially in the modified form, W^*. We see that in the latter scenario the system will then remain in the high concentration state as we increase the input. This is also why if we begin to remove the input, we remain in this state as opposed to changing back into the low concentration state, like we would in a continuous, ultrasensitive regime. In the continuous parameter regime above (Figure 38) we only have one solution to the cubic in W, which is also stable, so we always approach this value regardless of the initial condition.

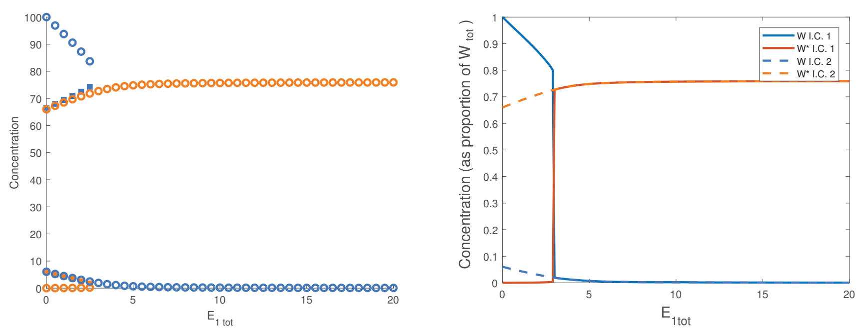

Analytic Solution Numeric Solutions

Figure 39: Demonstration of bistability using analytic solution (left) and numeric solutions to a bistable system under different initial conditions (right). Here empty circles represent a stable solution whilst solid squares represent an unstable solution. Note that a blue marker represents the concentration of the unmodified substrate, W, whilst an orange marker represents the concentration of the modified substrate, W^*. The initial conditions (I.C.) that the numeric solutions are subject to involved: I.C. 1 where all free substrate is initially found in the unmodified form such that $W_{init} = W_{tot}$ and I.C. 2 where all free substrate is initially found in the modified form such that $W^*_{init} = W_{tot}$. The system parameters are set as $W_{tot} = 100$, $E_{2tot} = 20$, and $E_{1tot} \in [0, 40]$ with the rate constants set to be $a_1 = a_2 = 20$, $d_1 = d_2 = k_2 = 1$, $k_1 = d_3 = k_3 = 5$, and $a_3 = 0.1$ for both the analytic and numeric solutions.

3.5 Stochastic Simulations of the Models

We are also interested in examining how these systems behave in a stochastic framework. This gives us the opportunity to examine cell-to-cell variability in the signalling responses generated by our models and is able to more accurately encode the behaviour of the system when molecular concentrations become very low. To do this we have found solutions to both systems by implementing reactions 31-33 for System 2 and reactions 34-37 for System 3 into Gillespie's Stochastic Simulation Algorithm. In the G-K mechanism we observed that increasing the sensitivity of our system, resulted in an increased variability of our solutions. We are then interested in examining whether this finding is also observed in the modified systems. We now examine an ultrasensitive parameter regime which uses the reference parameter sets defined in Section 3.2 and a graded regime. A graded response refers to when we decrease the sensitivity and approach a Michaelian response. Due to the complexity of the new systems it was not feasible to find a parameter regime which achieved a true Michaelian response as was achieved in the G-K mechanism.

When we examine System 3, with indirect positive autoregulation, we continue to observe the same behaviours as the G-K mechanism. As seen in Figure 40, for a graded response, we observe a similar, normal distribution of the modified substrate that shifts to the right as we increase the input to the system. As the sensitivity increases, we observe that this distribution changes dramatically as the input alters. Much like the G-K mechanism, when the input is either side of the M-value ($E_{1tot} = 18$), the distribution becomes skewed towards the center. As we approach the M-value, the variability increases dramatically so that the distribution now spans the range of modified substrate concentrations.

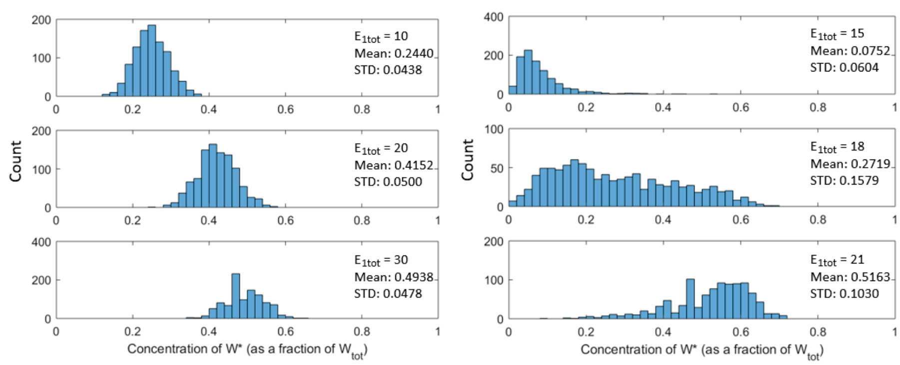

Graded Response

Ultrasensitive Response

Figure 40: Stochastic simulations of System 3 using Gillespie's Stochastic Simulation Algorithm. Distributions were created by simulating results over 1000 iterations for an increasing input centered around the M-value ($E_{1tot} \approx 20$ for graded and $E_{1tot} \approx 18$ for ultrasensitive). The system parameters are set as $W_{tot} = 100$, and $E_{2tot} = 20$. The graded response was created by setting the rate constants to be $a_1 = a_2 = a_3 = a_4 = 0.1$, $d_1 = d_2 = k_1 = k_2 = d_4 = k_4 = 5$, and $d_3 = 10$ with $E_{1tot} = \{10, 20, 30\}$. The ultrasensitive response was created by setting the rate constants to be $a_1 = a_2 = d_1 = d_2 = k_1 = k_2 = d_4 = 1$, $a_3 = 0.01$, $a_4 = 2$ and $d_3 = k_4 = 10$ with $E_{1tot} = \{15, 18, 21\}$.

When examining System 2, we can observe that for a graded profile, we obtain similar distributions as what was observed for System 3 and the G-K mechanism (see Figure 41). When examining the ultrasensitive reference parameter set of System 2, we are still able to observe the skewed behaviour of the system as we approach the M-value ($E_{1tot} = 12$) from the left, and the increased variability at the M-value. However instead of observing the skewed behaviour after the M-value, we observe the normally distributed behaviour of a graded profile. This is due to the mixed sensitivity that we observed in this profile, whereby the system is initially very sensitive for lower input values and then the sensitivity decreases dramatically after the M-value.

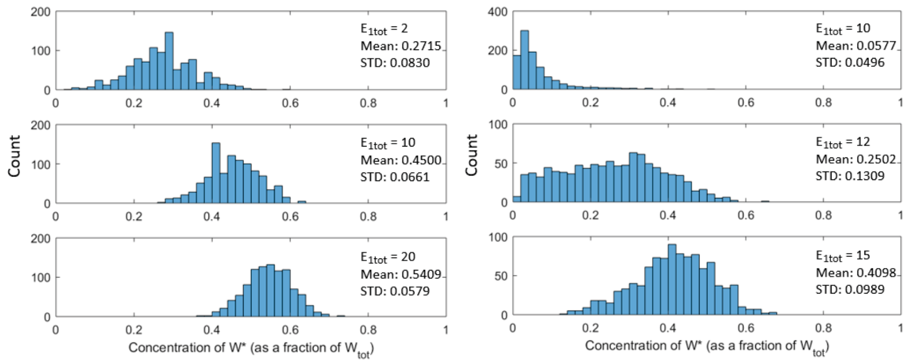

Graded Response   Ultrasensitive Response

Figure 41: Stochastic simulations of System 2 using Gillespie's Stochastic Simulation Algorithm. Distributions were created by simulating results over 1000 iterations for an increasing input centered around the M-value ($E_{1tot} \approx 10$ for graded and $E_{1tot} \approx 12$ for ultrasensitive). The system parameters are set as $W_{tot} = 100$, and $E_{2tot} = 20$. The graded response was created by setting the rate constants to be $a_1 = a_2 = 0.1$, $d_1 = d_2 = k_1 = 5$, $k_2 = 9$, $d_3 = k_3 = 10$, and $a_3 = 0.01$ for $E_{1tot} = \{2, 10, 20\}$. The ultrasensitive response was created by setting the rate constants to be $a_1 = a_2 = d_1 = d_2 = k_1 = k_2 = d_3 = k_3 = 1$, and $a_3 = 0.01$ for $E_{1tot} = \{10, 12, 15\}$.

We can also investigate how bistability behaves using stochastic methods as shown in Figure 42. Unlike some instances of the deterministic solvers where it was difficult to observe the discontinuity, we can now clearly observe the two possible states that the system can be in. When the input is less than or greater than the M-value, we tend to have a single Normal distribution which has a smaller variability. This is particularly clear in System 3. At values of input around the M-value, we observe bimodal distributions as the modified substrate begins transferring into the larger steady state. These distributions no longer demonstrate the skewed behaviour or high variability previously observed in an ultrasensitive parameter regime.

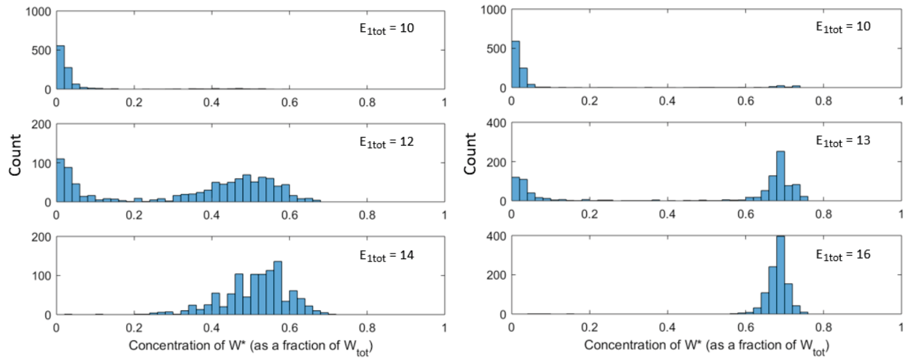

System 2 System 3

Figure 42: Stochastic simulations of models with bistable behaviour using Gillespie's Stochastic Simulation Algorithm. We observe that both systems achieve bimodal distributions. Distributions were created by simulating results over 1000 iterations for an increasing input centered around the M-value ($E_{1tot} \approx 12$ for System 2 and $E_{1tot} \approx 13$ for System 3). The system parameters are set as $W_{tot} = 100$, and $E_{2tot} = 20$. System 2 was created by setting the rate constants to be $a_1 = a_2 = 2$, $d_1 = d_2 = k_1 = k_2 = 1$, $d_3 = k_3 = 5$, and $a_3 = 0.01$ for $E_{1tot} = \{10, 12, 14\}$. System 3 was created by setting the rate constants to be $a_1 = a_2 = d_4 = 2$, $d_1 = d_2 = k_1 = k_2 = 1$, $a_3 = 0.1$, $d_3 = 10$, $a_4 = 4$, and $k_4 = 20$ with $E_{1tot} = \{10, 13, 16\}$.

We can also compare a selection of stochastic simulations of the time-dependent behaviour of System 2 in order to provide a further illustration of the qualitative differences between ultrasensitive and bistable responses. In Figure 43 we examine ten simulations using a parameter regime consistent with ultrasensitivity, as used for Figure 41, and ten simulations using a regime consistent with bistability, as used for Figure 42. This shows that while both cases exhibit a high degree of variability in W^* by the end of the simulation, the values separate into two distinct clusters for the bistable case. By contrast, the values at the end-time exhibit a single, large cluster for the ultrasensitive case.

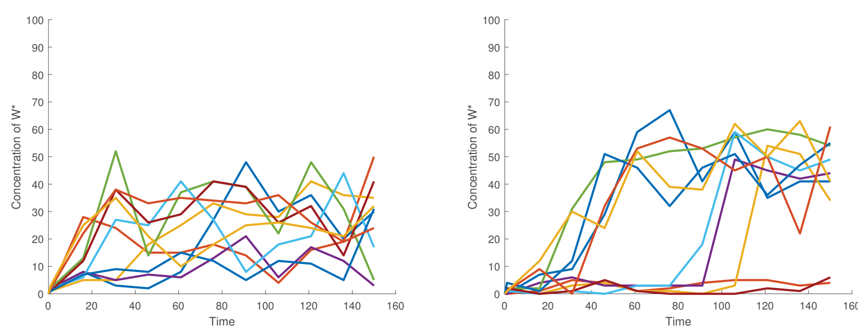

Ultrasensitive Response Bistable Response

Figure 43: Comparison of individual stochastic simulations of System 2 with ultrasensitive and bistable behaviours using Gillespie's Stochastic Simulation Algorithm. The system parameters are set as $W_{tot} = 100$, $E_{2tot} = 20$, and $E_{1tot} = 12$. The ultrasensitive response was created by setting the rate constants to be $a_1 = a_2 = d_1 = d_2 = k_1 = k_2 = d_3 = k_3 = 1$, and $a_3 = 0.01$. The bistable response was created by setting the rate constants to be $a_1 = a_2 = 2$, $d_1 = d_2 = k_1 = k_2 = 1$, $d_3 = k_3 = 5$, and $a_3 = 0.01$.

It is worth noting that the parameter regimes chosen in Figures 42 and 43 promote bistability over a significant range of E_{1tot} values. For parameter regimes which only admit bistability for a very narrow interval of E_{1tot} values on the other hand, we cannot distinguish between ultrasensitive and bistable responses from stochastic simulations alone. In these cases, the clusters that typically characterise bistability will exhibit a high degree of overlap, thus closely resembling the variability associated with ultrasensitivity.

3.6 Summary

Preliminary work (Appendix B.1) suggested that the addition of positive autoregulation to the basic G-K mechanism may allow us to obtain ultrasensitivity in a reversible covalent-modification cycle. We proposed two possible forms: direct and indirect PAR. We are particularly interested in investigating whether it is possible to increase the sensitivity and conversion potential of the G-K mechanism through these novel modifications.

For the system with direct PAR (System 2) we introduced a third reaction whereby the modified form of substrate could act as an enzyme and catalyse the unmodified substrate. In this system we were able to achieve a similar level of conversion potential as the G-K mechanism. This system also tends to produce mixed sensitivity whereby two different sensitivities were obtained on the two sides of the M-value. Now the Hill coefficient acts as an average sensitivity measurement. This indicated that the G-K mechanism was more sensitive than System 2.

The system with indirect PAR (System 3) was created by introducing two reactions to the reversible covalent-modification cycle. The first reaction allowed the modified substrate to form a complex with the free enzyme, E_1. This complex could then be used in a fourth reaction to catalyse the unmodified substrate and create more of the modified substrate. In comparison with the G-K mechanism, we are now able to increase the conversion potential and sensitivity without the mixed sensitivity found in the direct PAR implementation. This system also demonstrates another behaviour associated with the third reaction, whereby once the substrate has been fully converted into the modified form, the concentration of the modified substrate begins to decrease as we increase the input. This was directly related to the ratio of rate constants associated with this third reaction and decreasing this ratio allows us to essentially remove this effect.

We also found that both of these systems are prone to bistability. This behaviour restricts how the system can behave and whilst the change in states occurs almost simultaneously, we do not refer to this as ultrasensitivity. This behaviour was investigated via numerical simulations of the Mass-Action equations, but also via an analytic solution that was developed for System 2 and stochastic simulations for both Systems 2 and 3. These other methods clearly highlighted the discontinuous nature of bistability as opposed to the continuous behaviour that we require for ultrasensitivity.

By including these added reactions, the complexity of the system was greatly increased and it became difficult to investigate the behaviour of these systems through the analytic methods used for the G-K mechanism. However by examining numerical simulations we found that in most cases these systems perform almost identically to the G-K mechanism in terms of the effect of altering the substrate abundance, Michaelis constants and the individual rate constants. The most obvious exception to this is the effect of K_{m1} in System 3 whereby it now has the complete opposite effect to what was observed in the G-K mechanism. This could be linked to the introduced competition that the forward reaction has with both the third reaction, for E_1, and the fourth reaction, for W. For the added reactions we found that the third reaction in System 2 and the fourth in System 3 behave much like the forward reaction in the G-K mechanism as these added reactions take a very similar form. We also used stochastic simulations to investigate the behaviour of these systems. This showed that these systems display the same increased variability with ultrasensitivity that we observed in the G-K mechanism. We were also able to observe the mixed sensitivity behaviour of System 2 through this method which showed that the variability in this system actually decreases as we increase the input and the system becomes much more graded.

Overall, our results clearly show that by implementing positive autoregulation into a reversible covalent-modification cycle we can obtain improvements in sensitivity and conversion potential whilst maintaining similar behaviours to the G-K mechanism and while able to better support comparable concentrations of substrate and enzyme. Our results also show that these improvements came at the expense of introducing the potential for bistability in these new models.

4 Conclusion

4.1 Summary and Discussion

In their 1981 paper [26], Goldbeter and Koshland defined zero-order ultrasensitivity in a reversible covalent-modification cycle. This system, which we refer to as the G-K mechanism, achieved an ultrasensitive response when under the condition that the concentration of substrate was present in vast excess over the concentration of enzyme. It is now known that intracellular signalling networks involve enzyme-substrate combinations that exist at more comparable concentrations [11]. Our work has demonstrated the detrimental effect that having such comparable concentrations of enzyme and substrate has on ultrasensitivity, and key features of the steady-state substrate concentration profiles. We have defined these key features throughout our analysis of this system in order to differentiate effects on the profiles that could be crucial for later implementations of this system into larger network mechanisms. These new terms include the conversion potential, the mid-conversion stimulus (M-value), and mixed sensitivity.

We also investigated the effects of substrate concentration on sensitivity. When we examined these features we found that the substrate abundance had a key role in altering sensitivity and conversion potential. This effect, particularly on the conversion potential, could be linked to high concentrations of complexes that made up a significant proportion of the system when we introduced comparable concentrations of enzyme and substrate. We also investigated the importance of the Michaelis constants and the catalytic rate constants have in effecting the above profile features. Goldbeter and Koshland showed that increasing the Michaelis constants decreases sensitivity [26], but as we have shown, also increases the conversion potential. Altering these constants individually also resulted in a profile which shifts the M-value, and alters conversion potential. When altering the rate constants we found that, if the Michaelis constant is unchanged, only the catalytic constant has an effect on the profile. In particular, if we increase k_1, or decrease k_2, both the sensitivity and conversion potential increase, and the M-value decreases. Understanding how these parameters can alter the profile allows us to obtain some insight into the limits of ultrasensitivity in covalent modification cycles. This will be of particular use when studying the embedding of these covalent modification cycles into larger signalling networks. As we have seen here, having comparable concentrations of enzyme and substrate generally has a significant negative effect on the conversion potential and sensitivity.

This is the first study, to our knowledge, that highlights the potential for mixed sensitivity in covalent modification cycles. This is important because, for these models, the Hill coefficient can only capture the average sensitivity in the neighbourhood of the M-value, and results in a misleading measure of ultrasensitivity in these systems.

In this work we have also proposed two possible positive autoregulation (PAR) strategies into the G-K mechanism. PAR refers to a mechanism whereby the output of a system increases its own production. This was integrated into the reversible covalent-modification system by two possible implementations: indirect and direct PAR. The direct implementation (System 2), added a third reaction whereby the modified substrate now acted as an enzyme to modify the unmodified substrate. For the indirect implementation (System 3), we introduced two new reactions. The third reaction enabled the creation of a new complex, C_3, which combines the modified substrate and the forward catalysing enzyme, E_1. This complex can then catalyse W to create more modified substrate in the fourth reaction.

We then compared both of these new models with the G-K mechanism under similar parameter regimes. We first examined parameter regimes where each rate constant was set to unity, but this resulted in profiles which had very poor features, particularly in terms of the conversion potential and M-value. By only altering the rate constants for the reactions which were not also present in the G-K mechanism, we were able to "optimise" parameter regimes for the modified systems. For System 2 the profile was able to match the conversion potential of the G-K mechanism and had a small decrease (left shift) in the M-value. Most important was the sensitivity of this dose-response profile. This system tended to create a profile which had mixed sensitivity where the sensitivity was significantly higher prior to the M-value. This meant that in comparison to the G-K mechanism we were able to improve on the sensitivity prior to the M-value, but the average sensitivity, as given by the Hill coefficient, was higher in the G-K mechanism. For System 3 the profile was able to improve upon both the conversion potential and the sensitivity of the G-K mechanism.

When we examined the behaviours of these systems we also found that in the majority of cases, altering substrate abundance, the Michaelis constants and the magnitude of the individual rate constants for the reactions present in the three systems, had the same effects on the dose-response profile. When examining the added reactions for Systems 2 and 3 we also observed that these behaved much like when altering the Michaelis constant or rate constants associated with the forward reaction in the G-K mechanism. When we examined these systems using stochastic simulations we found that, in all cases, increasing the sensitivity of a system also increased the variability of its output. Of particular interest was examining the mixed sensitivity of System 2 which demonstrated both the high variability of an ultrasensitive profile, and the low variability of a graded profile depending on whether the input was before or after the M-value.

A particular concern of the modified systems was the possibility of bistability for some parameter regimes. This behaviour involved the substrate concentrations essentially jumping from a low state to a high state, or vice versa, as the input crossed a threshold value. Thus, unlike ultrasensitivity (which involves a highly sensitive, but continuous, dose-response profile), this dose-response profile involves a discontinuity. In stochastic solutions this discontinuity gave rise to a bimodal concentration distribution as opposed to the single distribution for the continuous (ultrasensitive) cases.

We can consider the possible implementations of these modified systems in which they will be able to improve upon the performance of the G-K mechanism. In a mechanism which requires a lower concentration of the modified substrate to be achieved rapidly, and with less input, System 2 is able to achieve improvements on the performance of the G-K mechanism. System 3 may be particularly suited to a signalling network that requires a higher concentration of the modified substrate and a more ultrasensitive response than the G-K mechanism can provide. However, due to the potential for bistability, these new systems may have important limitations in comparison with the G-K mechanism.

4.2 Direction of Future Work

There are a number of possible extensions of our thorough analysis of covalent-modification cycles for future work.

As discussed a number of times throughout this report, the Hill coefficient which is long established as a measure of sensitivity, does not allow us to capture the asymmetric dose-response profiles that were observed for many parameter regimes. For these profiles the Hill coefficient acts as an average sensitivity measurement. For this reason we are interested in developing a more flexible measure of sensitivity that accommodates both symmetric (uniform ultrasensitivity) and asymmetric (mixed ultrasensitivity) profiles. This is particularly important when comparing the sensitivity of the new systems presented in this work.

There is also potential for analytical (or computational, if need be) work on identifying the precise location of the M-value (for continuous dose-response profiles) or bifurcation point (for bistable profiles). We are then interested in understanding which parameters, or groupings of parameters, can "tune" these features.

In addition, noting the requirement for embedded ultrasensitivity in many robust perfect adaptation (RPA) capable network modules [8], a potential major extension of this work is to investigate implementations of the G-K mechanism and the modified systems into larger signalling networks. RPA is found in a large array of biological systems [55, 33, 9, 4, 30, 46, 15, 10, 16], from large scale organism development [10, 16], to cellular level signal transduction and gene regulation [4, 30, 46]. The ability to alter the dose-response profiles of the systems investigated throughout this report allows for an investigation into how the behaviour and features of ultrasensitivity may effect these larger mechanisms and allow us to achieve the RPA behaviours.

Appendices

A Goldbeter-Koshland Mechanism

A.1 Michaelis-Menten Equation

Here we derive the Michaelis-Menten equation from the mass-action equations corresponding to (2) in Chapter 1. This system of equations is given by,

$$\frac{\mathrm{d}E}{\mathrm{d}t} = -k_1 ES + k_2 C + k_3 C, \tag{59}$$
$$\frac{\mathrm{d}S}{\mathrm{d}t} = -k_1 ES + k_2 C, \tag{60}$$
$$\frac{\mathrm{d}C}{\mathrm{d}t} = k_1 ES - k_2 C - k_3 C, \tag{61}$$
$$\frac{\mathrm{d}P}{\mathrm{d}t} = k_3 C, \tag{62}$$

with the conservation equations given by,

$$S_{tot} = S_{free} + C + P \tag{63}$$
$$E_{tot} = E_{free} + C \tag{64}$$

To begin with we define v to be the initial velocity of the reaction, i.e. the production rate of P,

$$v = \frac{\mathrm{d}P}{\mathrm{d}t} = k_3 C \tag{65}$$

We now make the assumptions that $P \ll S$ and $E \ll S$. This simplifies equation (63) to

$$S_{tot} = S \tag{66}$$

For our final solution we require equation (65) to be strictly in terms of measurable variables i.e. S and E_{tot}. Therefore it is required that C be replaced by some function of these variables by examining the quasi-steady state of C. The steady state is achieved when the production and removal rates are equal, i.e.

$$k_1 SE = (k_2 + k_3)C \tag{67}$$

Rearranging this gives

$$\frac{k_2 + k_3}{k_1} = \frac{SE}{C} \tag{68}$$

We now need to remove the dependence on E. We can do this by rearranging equation (64) to get

$$E = E_{tot} - C. \tag{69}$$

Substituting this into equation (68) and setting $K_m = \frac{k_2+k_3}{k_1}$,

$$K_m = \frac{S(E_{tot} - C)}{C} \tag{70}$$

Rearranging this equation to have C as the subject gives,

$$C = \frac{E_{tot}S}{K_m + S} \tag{71}$$

Substitute equation (71) into (65) to now obtain an expression for v that is only in terms of measurable quantities,

$$v = \frac{k_3 E_{tot} S}{K_m + S} \tag{72}$$

Using equation (71) it can also be noted that, when the enzyme is saturated ($C = E_{tot}$), the maximum velocity occurs, and is given by

$$V_{max} = k_3 E_{tot}. \tag{73}$$

Substituting this into equation (72) gives the Michaelis-Menten equation,

$$v = \frac{V_{max} S}{K_m + S}. \tag{74}$$

A.2 Characterisation of a Michaelian Enzyme

Here we prove that the Michaelis-Menten equation requires an 81-fold increase in input to increase from 10% to 90% of the maximum output. These values first need to be expressed in terms of the Michaelis-Menten equation whereby 10% of the maximum output (i.e. $0.1V_{\max}$) is given by,

$$0.1V_{\max} = \frac{V_{\max} S_1}{K_m + S_1}, \tag{75}$$

where S_1 is the input at which 10% of the maximum output is achieved. Rearranging and expanding this expanding this expression gives,

$$0.1K_m = 0.9S_1 \tag{76}$$

We then obtain a similar expression for 90% of the maximum output(i.e. $0.9V_{\max}$).

$$0.9V_{\max} = \frac{V_{\max}S_2}{K_m + S_2} \tag{77}$$

Expanding and rearranging gives,

$$0.9K_m = 0.1S_2 \tag{78}$$

We can now take the ratio of these two equations to give,

$$\frac{0.1K_m}{0.9K_m} = \frac{0.9S_1}{0.1S_2} \tag{79}$$

Rearranging this can now remove the dependence on the Mihcaelis constants and gives the final expression,

$$S_2 = 81S_1 \tag{80}$$

This demonstrates that the input required to achieve 90% of the maximum output, S_2, is 81-fold the input to achieve 10% of the maximum output, S_1.

A.3 Analytic Solution to a Reversible Covalent-Modification System Under the Assumption of Negligible Enzyme-Substrate Complexes

Here we derive the quadratic solution to the G-K mechanism. This system is described by the system of equations (7)-(13) developed in Section 2.2. These are also included below.
Mass action equations:

$$\frac{\mathrm{d}W}{\mathrm{d}t} = d_1C_1 + k_2C_2 - a_1WE_1, \tag{81}$$
$$\frac{\mathrm{d}W^*}{\mathrm{d}t} = d_2C_2 + k_1C_1 - a_2W^*E_2, \tag{82}$$
$$\frac{\mathrm{d}C_1}{\mathrm{d}t} = a_1WE_1 - d_1C_1 - k_1C_1, \tag{83}$$
$$\frac{\mathrm{d}C_2}{\mathrm{d}t} = a_2W^*E_2 - d_2C_2 - k_2C_2. \tag{84}$$

Conservation equations:

$$W_{tot} = W + W^* + C_1 + C_2, \tag{85}$$
$$E_{1tot} = E_1 + C_1, \tag{86}$$
$$E_{2tot} = E_2 + C_2. \tag{87}$$

We now introduce the assumption that the total concentration of substrate is much larger than the concentration of enzyme. This now allows us to exclude the dependence on the complexes, C_1 and C_2, in the conservation equation for the total substrate. Equation (85) can then be re-written as

$$W_{tot} = W + W^*. \tag{88}$$

For this system to be at steady state we require the production of the modified substrate to be equal to the production of the unmodified substrate i.e.

$$k_1 C_1 = k_2 C_2. \tag{89}$$

To then develop a solution for the substrates we need to express C_1 and C_2 as a function of measurable quantities. This follows a process identical to that used in Appendix A.1. For C_1 we use equation (83) at quasi-steady state to examine when the production is equal to the removal of complex.

$$k_1 W E_1 = (d_1 + k_1) C_1$$

Rearranging this we obtain

$$K_{m1} = \frac{W E_1}{C_1}, \tag{90}$$

where $K_{m1} = \frac{d_1 + k_1}{a_1}$. We need to remove the dependence on the enzyme as this is not a measurable quantity. We can do this by using the rearranged equation (86)

$$E_1 = E_{1tot} - C_1.$$

Substituting this into equation (90) we can rearrange to obtain an expression for C_1. This is in the same form of the Michaelis-Menten equation.

$$C_1 = \frac{E_{1tot} W}{K_{m1} + W} \tag{91}$$

We can also apply this process to C_2 to obtain the following expression

$$C_2 = \frac{E_{2tot} W^*}{K_{m2} + W^*}, \tag{92}$$

where $K_{m2} = \frac{d_2 + k_2}{a_2}$. We can now substitute equations (91) and (92) into equation (89).

$$\frac{k_1 E_{1tot} W}{K_{m1} + W} = \frac{k_2 E_{2tot} W*}{K_{m2} + W^*} \tag{93}$$

We now wish to remove the dependence on both W and W^*. We do this by rearranging equation (88) to obtain $W = W_{tot} - W^*$. We can then substitute this into equation (93).

$$\frac{k_1 E_{1tot}(W_{tot} - W^*)}{K_{m1} + w_{tot} - W^*} = \frac{k_2 E_{2tot} W^*}{K_{m2} + W^*} \tag{94}$$

Rearranging this gives

$$\frac{V_1}{V_2}(K_{2m} + W^*)(W_{tot} - W^*) = W^*(K_{1m} + W_{tot} - W^*) \tag{95}$$

where $V_1 = k_1 E_{1tot}$ and $V_2 = k_2 E_{1tot}$. We now expand this expression and collect to obtain a quadratic in W^*. We also non-dimensionalise this result by dividing through by W_{tot}^2 to obtain

$$\bar{W^*}^2(1 - \frac{V_1}{V_2}) + \bar{W^*}\left[\left(\frac{V_1}{V_2} - 1\right) - K_2\left(\frac{V_1}{V_2} + \frac{K_1}{K_2}\right)\right] + \frac{V_1}{V_2}K_2 = 0 \tag{96}$$

where $\bar{W^*} = \frac{W^*}{W_{tot}}$, $K_1 = \frac{K_{m1}}{W_{tot}}$ and $K_2 = \frac{K_{m2}}{W_{tot}}$. We are then able to obtain a solution by solving this with the quadratic formula.

$$\bar{W^*} = \frac{\left[\left(\frac{V_1}{V_2} - 1\right) - K_2\left(\frac{V_1}{V_2} + \frac{K_1}{K_2}\right)\right] - \pm\sqrt{\left[\left(\frac{V_1}{V_2} - 1\right) - K_2\left(\frac{V_1}{V_2} + \frac{K_1}{K_2}\right)\right]^2 + 4K_2\left(\frac{V_1}{V_2} - 1\right)\frac{V_1}{V_2}}}{2\left(\frac{V_1}{V_2} - 1\right)} \tag{97}$$

Since we are not able to accept negative values solutions as a protein concentration, we take the positive roots as the solution for $\bar{W^*}$

$$\bar{W^*} = \frac{\left[\left(\frac{V_1}{V_2} - 1\right) - K_2\left(\frac{V_1}{V_2} + \frac{K_1}{K_2}\right)\right] + \sqrt{\left[\left(\frac{V_1}{V_2} - 1\right) - K_2\left(\frac{V_1}{V_2} + \frac{K_1}{K_2}\right)\right]^2 + 4K_2\left(\frac{V_1}{V_2} - 1\right)\frac{V_1}{V_2}}}{2\left(\frac{V_1}{V_2} - 1\right)} \tag{98}$$

We have now obtained expressions for W^* (using equation (98)) and W (using a non-dimensionalised equation (88)).

$$W^* = \frac{\left[\left(\frac{V_1}{V_2} - 1\right) - K_2\left(\frac{V_1}{V_2} + \frac{K_1}{K_2}\right)\right] + \sqrt{\left[\left(\frac{V_1}{V_2} - 1\right) - K_2\left(\frac{V_1}{V_2} + \frac{K_1}{K_2}\right)\right]^2 + 4K_2\left(\frac{V_1}{V_2} - 1\right)\frac{V_1}{V_2}}}{2\left(\frac{V_1}{V_2} - 1\right)}$$

$$W = 1 - W^*$$

A.4 Analytic Solution to a Reversible Covalent-Modification System Accounting For Non-Negligible Complex Formation

Here we derive the cubic equation in W for the G-K mechanism at steady state. This system uses the same set of equations as outlined in Appendix A.3 as outlined below.
Mass action equations:

$$\frac{\mathrm{d}W}{\mathrm{d}t} = d_1 C_1 + k_2 C_2 - a_1 W E_1, \tag{99}$$
$$\frac{\mathrm{d}W^*}{\mathrm{d}t} = d_2 C_2 + k_1 C_1 - a_2 W^* E_2, \tag{100}$$
$$\frac{\mathrm{d}C_1}{\mathrm{d}t} = a_1 W E_1 - d_1 C_1 - k_1 C_1, \tag{101}$$
$$\frac{\mathrm{d}C_2}{\mathrm{d}t} = a_2 W^* E_2 - d_2 C_2 - k_2 C_2. \tag{102}$$

Conservation equations:

$$W_{tot} = W + W^* + C_1 + C_2, \tag{103}$$
$$E_{1tot} = E_1 + C_1, \tag{104}$$
$$E_{2tot} = E_2 + C_2. \tag{105}$$

We can now follow an identical procedure to that in Appendix A.3 to obtain the following expression for when the production of W is equal to the production of W^* (see up to equation (93) in Appendix A.3)

$$\frac{k_1 E_{1tot} W}{K_{m1} + W} = \frac{k_2 E_{2tot} W*}{K_{m2} + W^*}, \tag{106}$$

where the constants, $K_{m1} = \frac{d_1 + k_1}{a_1}$ and $K_{m2} = \frac{d_2 + k_2}{a_2}$ are the Michaelis constants associated with each reaction. We also obtain steady state expressions for C_1 and C_2 as given by the respective equations (91) and (92) in Appendix A.3,

$$C_1 = \frac{E_{1tot} W}{K_{m1} + W}, \tag{107}$$
$$C_2 = \frac{E_{2tot} W^*}{K_{m2} + W^*}, . \tag{108}$$

We now wish to remove the dependence on both W and W^*. We do this by rearranging equation (103) to obtain $W^* = W_{tot} - W - C_1 - C_2$. We can then substitute this into equation (106).

$$\frac{k_1 E_{1tot} W}{K_{m1} + W} = \frac{k_2 E_{2tot}(W_{tot} - W - C_1 - C_2)}{K_{m2} + (W_{tot} - W - C_1 - C_2)} \tag{109}$$

Rearranging this gives

$$\frac{V_1}{V_2}W(K_{2m} + W_{tot} - W - C_1 - C_2) = (K_{1m} + W)(W_{tot} - W - C_1 - C_2) \tag{110}$$

where $V_1 = k_1 E_{1tot}$ and $V_2 = k_2 E_{1tot}$.

By removing the dependence on W^* we have now reintroduced C_1 and C_2 back into the expression. Since C_1 is only dependent on W we are able to use equation (107) to remove the dependence on C_1. However we find that C_2 is dependent on W^* so we are not able to use equation (108) to remove this dependence. Instead we now examine the mass action equations (99) and (101). At steady state, adding these equations gives,

$$0 = k_2 C_2 - k_1 C_1 \tag{111}$$

Rearranging this gives an expression for the relationship between C_2 and C_1,

$$C_2 = \frac{k_1}{k_2} C_1 \tag{112}$$

By using equations (107) and (112) we can remove the dependence on C_1 and C_2 in equation (110) to obtain,

$$\frac{V_1}{V_2}W\left(K_{2m} + W_{tot} - W - \frac{E_{1tot}W}{K_{1m} + W}(1 + \frac{k_1}{k_2})\right) = (K_{1m} + W)\left(W_{tot} - W - \frac{E_{1tot}W}{K_{1m} + W}(1 + \frac{k_1}{k_2})\right)$$

By multiplying through by $K_{1m} + W$ to remove the denominator that has now been introduced, and expanding, this takes the form of the cubic,

$$\begin{aligned} W^3\left[1 - \frac{V_1}{V_2}\right] + W^2\left[\frac{V_1}{V_2}\left(K_{2m} - K_{1m} + W_{tot} - E_{1tot}\left(1 + \frac{k_1}{k_2}\right)\right) - W_{tot} + E_{1tot}\left(1 + \frac{k_1}{k_2}\right) + 2K_{1m}\right] \\ +W\left[\frac{V_1}{V_2}\left(K_{1m}K_{2m} + K_{1m}W_{tot}\right) + K_{1m}^2 + K_{1m}E_{1tot}\left(1 + \frac{k_1}{k_2}\right) - 2K_{1m}W_{tot}\right] - K_{1m}^2 = 0 \end{aligned}$$

This equation can then be non-dimensionalised by dividing through by W_{tot}^3. To match the notation of the original analytical solution, the non-dimensionalised form of W will be continued to be written as W. Non-dimensionalised constants are rewritten as $K_1 = \frac{K_{1m}}{W_{tot}}$, $K_2 = \frac{K_{2m}}{W_{tot}}$, $\epsilon_1 = \frac{E_{1tot}}{W_{tot}}$ and $\epsilon_2 = \frac{E_{2tot}}{W_{tot}}$. To simplify this equation the ratio of inputs can be rewritten as $\alpha = \frac{V_1}{V_2}$. It is also important to note the use of epsilon in regards to the non-dimensionalised form of the total enzymes are this is typically reserved for small values. Rearranging the non-dimensionalised form to match that of the original gives,

$$\begin{aligned} W^3\{1 - \alpha\} + W^2\left\{(K_1 + K_2\alpha) + (1 - \alpha)(K_1 + \epsilon_1\left(1 + \frac{k_1}{k_2}\right) - 1)\right\} \\ +K_1 W\left\{(K_1 + K_2\alpha) + (\alpha - 2) + \epsilon_1\left(1 + \frac{k_1}{k_2}\right)\right\} - K_1^2 = 0 \end{aligned}$$

By noting that $\epsilon_2\alpha = \frac{E_{2tot}}{W_{tot}}\frac{k_1 E_{1tot}}{k_2 E_{2tot}} = \frac{k_1}{k_2}\epsilon_1$, a matching solution to the original found by Goldbeter and Koshland can be achieved,

$$W^3\{1-\alpha\} + W^2\{(K_1 + K_2\alpha) + (1-\alpha)(K_1 + \epsilon_1 + \epsilon_2\alpha - 1)\} \tag{113}$$

$$+K_1W\{(K_1 + K_2\alpha) + (\alpha - 2) + (\epsilon_1 + \epsilon_2\alpha)\} - K_1^2 = 0 \tag{114}$$

We have now obtained a cubic equation in W. By solving for the roots of this equations we obtain the concentration of W at steady state. This can then be used to calculate the concentrations of W^*, C_1, and C_2 using non-dimensionalised versions of equations (103), (107), and (108) respectively.

$$C_1 = \frac{\epsilon_1 W}{K_1 + W} \tag{115}$$

$$C_2 = \frac{k_1}{k_2}C_1 \tag{116}$$

$$W^* = 1 - W - C_1 - C_2 \tag{117}$$

A.5 Detailed Results of G-K Mechanism Tests

The following table includes the results for the Hill coefficient and conversion potential for the tests as described in Chapter 2 Figures 14, 15, 16, and 17.

	Hill Coefficient			Conversion Potential		
Line Type	Solid	Dashed	Dotted	Solid	Dashed	Dotted
Test 1	17.4859	293.6902	881.0852	0.59691	0.95904	0.9959
Test 2	9.6593	17.4859	27.48	0.55876	0.59691	0.60457
Test 3	7.1461	17.4859	29.1955	0.62118	0.59691	0.59142
Test 4	5.2016	17.4859	80.0787	0.58858	0.59691	0.59934
Test 5	17.4859	17.4859		0.59691	0.59691	
Test 6	17.4859	19.6934		0.59691	0.73495	
Test 7	17.4859	18.314		0.59691	0.6667	
Test 8	12.333	17.4859	19.1177	0.21343	0.59691	0.70095
Test 9	19.1177	17.4859	12.333	0.70095	0.59691	0.21343
Test 10	17.4859	17.4859	17.4859	0.59691	0.59691	0.59691

A.6 Mid-Conversion Stimulus (M-value) Function Derivation

Here we derive the equation that governs the occurrence of the M-value. In order to obtain this expression we examine the system at steady state. This process is covered in detail in Appendix A.3. The steady state is given by the balancer equation where the production of W is equal to the production of W^*.

$$k_1C_1 = k_2C_2$$

We must now express the concentration of these complexes as function of measurable quantities. As shown in Appendix A.3 the steady state concentration of these complexes are given by,

$$C_1 = \frac{E_{1tot}W}{K_{m1} + W}$$

$$C_2 = \frac{E_{2tot}W^*}{K_{m2} + W^*}$$

By then substituting this in to the balancer equation, we get that

$$\frac{k_1 E_{1tot} W}{K_{m1} + W} = \frac{k_2 E_{2tot} W^*}{K_{m2} + W^*}$$

We now set $W = W^*$ as this is defined as when the M-value occurs. We then rearrange to obtain an expression for E_{1tot},

$$\begin{aligned}
\frac{k_1 E_{1tot} W}{K_{m1} + W} &= \frac{k_2 E_{2tot} W}{K_{m2} + W} \\
k_1 E_{1tot} W (K_{m2} + W) &= k_2 E_{2tot} W (K_{m1} + W) \\
k_1 E_{1tot} (K_{m2} + W) &= k_2 E_{2tot} (K_{m1} + W) \\
E_{1tot} &= E_{2tot} \frac{k_2 (K_{m1} + W)}{k_1 (K_{m2} + W)}
\end{aligned}$$

Since the M-value is the input value when the substrate concentrations are equal, we can set $E_{1tot} =$ M-value. We therefore have obtained an expression for the M-value.

$$\text{M-value} = E_{2tot} \frac{k_2 (K_{m1} + W)}{k_1 (K_{m2} + W)}$$

B Simulation Data For Positive Autoregulation Models

B.1 Analytical Investigation of Covalent Modification Cycle with Positive Autoregulation

Here we investigate the effect of including positive autoregulation (PAR) on ultrasensitivity. We first use the Michaelis-Menten equation for each of the two independent reactions in the reversible covalent modification cycle. We introduce PAR to this approximation by including W^*. It's the term associated with its own creation.

$$\frac{\mathrm{d}W^*}{\mathrm{d}t} = \frac{k_1 E_1 W W^*}{K_1 + W} - \frac{k_2 E_2 W^*}{K_2 + W^*}$$

We then investigate the case when $K_1 \ll W_{tot} - W^*$ and $K_2 \gg W^*$. The rate of change in W^* then becomes

$$\begin{aligned}\frac{\mathrm{d}W^*}{\mathrm{d}t} &\approx k_1 E_{1tot} W^* - \frac{k_2}{K_2} E_{2tot} W^* \\ &= W^* \left(k_1 E_1 - \frac{k_2}{K_2} E_2 \right)\end{aligned}$$

We now examine the system at steady state so that there is no longer any change in W^* i.e. $\frac{\mathrm{d}W^*}{\mathrm{d}t} = 0$.

$$\begin{aligned}0 &\approx W^* \left(k_1 E_1 - \frac{k_2}{K_2} E_2 \right) \\ 0 &\approx k_1 E_1 - \frac{k_2}{K_2} E_2 \\ k_1 E_1 &\approx \frac{k_2}{K_2} E_2\end{aligned}$$

This demonstrates that at steady state E_1 is approximately a constant for all values of W^*. We can then conclude that since we obtain approximately all values of W^* for a constant E_1, then this system, with PAR, must be able to achieve an ultrasensitive response.

B.2 Comparing the G-K Mechanism and System 2

The following table includes the results for the Hill coefficient and conversion potential for the tests as described in Chapter 3 applied to System 2 and the G-K Mechanism (Figures 31, 32, 34).

G-K Mechanism

	Hill Coefficient			Conversion Potential		
Line Type	Solid	Dashed	Dotted	Solid	Dashed	Dotted
Test 1	9.8638	125.8568	881.0852	0.59428	0.95809	0.9958
Test 2	6.6617	9.8638	14.6908	0.52188	0.59428	0.60897
Test 3	4.5311	9.8638	17.3281	0.6389	0.59428	0.583
Test 4	9.8638	9.8638	9.8638	0.59428	0.59428	0.59428
Test 5	3.5466	9.8638	39.9092	0.58399	0.59428	0.59871
Test 6	7.4569	9.8638	10.7294	0.22454	0.59428	0.70189
Test 7	10.7294	9.8638	7.4569	0.70189	0.59428	0.22454
Test 8	9.8638	9.8638	9.8638	0.59428	0.59428	0.59428
Test 9	9.8638	9.8638	9.8638	0.59428	0.59428	0.59428

System 2

	Hill Coefficient			Conversion Potential		
Line Type	Solid	Dashed	Dotted	Solid	Dashed	Dotted
Test 1	8.4336	Inf	Inf	0.5901	0.95351	0.99449
Test 2	6.2489	8.4336	11.8022	0.51901	0.5901	0.6079
Test 3	3.5222	8.4336	15.1279	0.63528	0.5901	0.57865
Test 4	9.5701	8.4336	4.2559	0.59341	0.5901	0.57671
Test 5	3.4099	8.4336	15.7781	0.58305	0.5901	0.5934
Test 6	9.4351	8.4336	7.8237	0.32162	0.5901	0.69871
Test 7	7.0988	8.4336	8.4036	0.69992	0.5901	0.27256
Test 8	8.378	8.4336	8.9059	0.58693	0.5901	0.59605
Test 9	8.4336	8.4336	8.4336	0.5901	0.5901	0.5901

B.3 Comparing the G-K Mechanism and System 3

The following table includes the results for the Hill coefficient and conversion potential for the tests as described in Chapter 3 applied to System 3 and the G-K Mechanism (Figures 31, 33, 35).

G-K Mechanism

	Hill Coefficient			Conversion Potential		
Line Type	Solid	Dashed	Dotted	Solid	Dashed	Dotted
Test 1	9.8638	125.8568	881.0852	0.59428	0.95809	0.9958
Test 2	6.6617	9.8638	14.6908	0.52188	0.59428	0.60897
Test 3	4.5311	9.8638	17.3281	0.6389	0.59428	0.583
Test 4	9.8638	9.8638	9.8638	0.59428	0.59428	0.59428
Test 5	9.8638	9.8638	9.8638	0.59428	0.59428	0.59428
Test 6	3.5466	9.8638	39.9092	0.58399	0.59428	0.59871
Test 7	7.4569	9.8638	10.7294	0.22454	0.59428	0.70189
Test 8	10.7294	9.8638	7.4569	0.70189	0.59428	0.22454
Test 9	9.8638	9.8638	9.8638	0.59428	0.59428	0.59428
Test 10	9.8638	9.8638	9.8638	0.59428	0.59428	0.59428
Test 11	9.8638	9.8638	9.8638	0.59428	0.59428	0.59428

System 3

	Hill Coefficient			Conversion Potential		
Line Type	Solid	Dashed	Dotted	Solid	Dashed	Dotted
Test 1	15.2754	Inf	Inf	0.61301	0.96545	0.99614
Test 2	20.6222	15.2754	16.5252	0.64599	0.61301	0.60591
Test 3	5.5735	15.2754	44.1278	0.6527	0.61301	0.60314
Test 4	10.6688	15.2754	91.952	0.59929	0.61301	0.64788
Test 5	10.838	15.2754	128.7449	0.58922	0.61301	0.67545
Test 6	7.579	15.2754	46.6242	0.61106	0.61301	0.61529
Test 7	17.0548	15.2754	13.7993	0.44931	0.61301	0.69306
Test 8	18.6425	15.2754	10.9772	0.70327	0.61301	0.3488
Test 9	15.2754	15.2754	15.2754	0.61301	0.61301	0.61301
Test 10	12.0157	15.2754	32.3093	0.5952	0.61301	0.64157
Test 11	15.2754	15.2754	15.2754	0.61301	0.61301	0.61301

B.4 Summary Table of Parameter Effects

Goldbeter-Koshland Mechanism

Increased Variable	Effects
W_{tot}	increased conversion potential, increased sensitivity, (can) shift M-value
K_{m1}	decreased conversion potential, decreased sensitivity, increased M-value, mixed sensitivity
K_{m2}	increased conversion potential, decreased sensitivity, decreased M-value, mixed sensitivity
K_{m1} and K_{m2}	decreased sensitivity
k_1	increased conversion potential, increased sensitivity, decreased M-value
k_2	decreased conversion potential, decreased sensitivity, increased M-value
k_1 and k_2	no change

System 2

Increased Variable	Effects
W_{tot}	increased conversion potential, increased sensitivity, decreased M-value, bistability
K_{m1}	decreased conversion potential, decreased sensitivity, increased M-value, mixed sensitivity, removes bistability
K_{m2}	increased conversion potential, decreased sensitivity, decreased M-value, mixed sensitivity, removes bistability
K_{m3}	increased conversion potential, decreased sensitivity, increased M-value, removes mixed sensitivity, removes bistability
K_{m1}, K_{m2} and K_{m3}	decreased conversion potential, decreased sensitivity, increased M-value, mixed sensitivity, removes bistability
k_1	increased conversion potential, increased sensitivity, decreased M-value, mixed sensitivity, bistability
k_2	decreased conversion potential, decreased sensitivity, increased M-value, mixed sensitivity, removes bistability
k_3	increased sensitivity, decreased M-value, mixed sensitivity, bistability
k_1, k_2 and k_3	no change

System 3

Increased Variable	Effects
W_{tot}	increased conversion potential, increased sensitivity, decreased M-value, bistability
K_{m1}	increased conversion potential, increased sensitivity, decreased M-value, mixed sensitivity, bistability
K_{m2}	increased conversion potential, decreased sensitivity, decreased M-value, mixed sensitivity, removes bistability
K_d	decreased conversion potential, decreased sensitivity, increased M-value, mixed sensitivity, removes bistability, removes decrease in W^* after conversion potential
K_{m4}	decreased conversion potential, decreased sensitivity, increased M-value, mixed sensitivity, removes bistability
K_{m1}, K_{m2} and K_{m4}	decreases sensitivity
k_1	increased conversion potential, increased sensitivity, decreased M-value
k_2	decreased conversion potential, decreased sensitivity, increased M-value
d_3	no change
k_4	increased conversion potential, increased sensitivity, decreased M-value, bistability
k_1, k_2, d_3 and k_4	no change

B.5 Derivation of Analytic Solution to System 2

Here we derive the analytic solution to System 2. This system is described by the system of equations (38)-(44) and (53)-(55) in Section 3.1. These are also included below.

Mass action equations:

$$\frac{\mathrm{d}W}{\mathrm{d}t} = d_1C_1 + d_3C_3 + k_2C_2 - a_1WE_1 - a_3WW^*, \tag{118}$$
$$\frac{\mathrm{d}W^*}{\mathrm{d}t} = d_2C_2 + d_3C_3 + k_1C_1 + 2k_3C_3 - a_2W^*E_2 - a_3WW^*, \tag{119}$$
$$\frac{\mathrm{d}E_1}{\mathrm{d}t} = d_1C_1 + k_1C_1 - a_1WE_1, \tag{120}$$
$$\frac{\mathrm{d}E_2}{\mathrm{d}t} = d_2C_2 + k_2C_2 - a_2W^*E_2, \tag{121}$$
$$\frac{\mathrm{d}C_1}{\mathrm{d}t} = a_1WE_1 - d_1C_1 - k_1C_1, \tag{122}$$
$$\frac{\mathrm{d}C_2}{\mathrm{d}t} = a_2W^*E_2 - d_2C_2 - k_2C_2, \tag{123}$$
$$\frac{\mathrm{d}C_3}{\mathrm{d}t} = a_3WW^* - d_3C_3 - k_3C_3. \tag{124}$$

Conservation equations:

$$W_{tot} = W + W^* + C_1 + C_2 + C_3, \tag{125}$$
$$E_{1tot} = E_1 + C_1, \tag{126}$$
$$E_{2tot} = E_2 + C_2. \tag{127}$$

For this system to be at steady state we require the production of the modified substrate to be equal to the production of the unmodified substrate i.e.

$$k_1C_1 + k_3C_3 = k_2C_2. \tag{128}$$

To then develop a solution for the substrates we need to express C_1, C_2, and C_3 as a function of measurable quantities. The equations for C_1 and C_2 are obtained using the same method as Appendix A.3 for equations (91) and (92) to get

$$C_1 = \frac{E_{1tot}W}{K_{m1} + W}, \tag{129}$$
$$C_2 = \frac{E_{2tot}W^*}{K_{m2} + W^*}. \tag{130}$$

For C_3 we use equation (124) at quasi-steady state to examine when the production is equal to the removal of the complex.

$$(d_3 + k_3)C_3 = a_3WW^* \tag{131}$$

This equation is dependent on both W and W^*. We can remove the dependence on W^* by rearranging equation (125) to obtain

$$W^* = W_{tot} - W - C_1 - C_2 - C_3 \tag{132}$$

This equations includes C_2 which is still dependent on W^*. To remove the dependence of W^* we can use equation (128). By applying this to equation (125) we obtain a new equation for W^*

$$W^* = W_{tot} - W - \gamma_1 C_1 - \gamma_3 C_3 \tag{133}$$

where $\gamma_* = 1 + \frac{k_*}{k_2}$. This can then be substituted back into equation (131) and then rearranged to get

$$C_3 = \frac{W(W_{tot} - W - \gamma_1 C_1)}{K_{m3} + \gamma_3 W}, \tag{134}$$

where $K_{m3} = \frac{d_3+k_3}{a_3}$. Substituting in equation 129 for C_1 and rearranging to obtain a single fraction gives the following equation for C_3.

$$C_3 = \frac{W[(W_{tot} - W)(K_{m1} + W) - \gamma_1 E_{1tot} W]}{(K_{m3} + \gamma_3 W)(K_{m1} + W)} \tag{135}$$

This can then be used, along with the equation for C_1, to complete an equation for W^* in terms of W. Substituting these results into equation (133) and rearranging gives,

$$W^* = \frac{K_{m3}(W_{tot} - W)(K_{m1} + W) - \gamma_1 E_{1tot} K_{m3} W}{(K_{m3} + \gamma_3 W)(K_{m1} + W)} \tag{136}$$

We are now able to substitute in for C_1, C_2, and C_3 using equations (129), (130), and (135) respectively into equation (128),

$$\frac{k_1 E_{1tot} W}{K_1 + W} + \frac{k_3 W[(W_{tot} - W)(K_{m1} + W) - \gamma_1 E_{1tot} W]}{(K_{m3} + \gamma_3 W)(K_{m1} + W)} = \frac{k_2 E_{2tot} W^*}{K_2 + W^*}$$

By then substituting in the equation for W^* and rearranging, we obtain the equation,

$$\begin{aligned}
&\Big[k_1 E_{1tot} W(K_3 + \gamma_3 W) + k_3 W[(W_{tot} - W)(K_{m1} + W) - \gamma_1 E_{1tot} W]\Big] \times \\
&\Big[K_{m2}(K_{m1} + W)(K_{m3} + \gamma_3 W) + K_{m3}(W_{tot} - W)(K_{m1} + W) - \gamma_1 E_{1tot} K_{m3} W\Big] \\
&- k_2 E_{2tot}(K_{m1} + W)(K_{m3} + \gamma_3 W)\big[K_{m3}(W_{tot} - W)(K_{m1} + W) - \gamma_1 E_{1tot} K_{m3} W\big] = 0
\end{aligned}$$

We then expand this equation and collect the powers of W to obtain the following quintic,

$$
\begin{aligned}
&W^5\big[k_3(K_{m3}-\gamma_3 K_{m2})\big] + W^4\big[\sigma_2(K_{m3}-\gamma_3 K_{m2}) - k_2\sigma_1 + \gamma_3 k_2 E_{2tot}K_{m3}\big]\\
&+W^3\big[-\sigma_3(K_{m3}-\gamma_3 K_{m2}) + \gamma_3\sigma_6 - \sigma_1\sigma_2 - k_3\sigma_4 + k_2 E_{2tot}K_{m3}^2\big]\\
&+W^2\big[\gamma_3\sigma_5 - \sigma_2\sigma_4 + \sigma_6 K_{m3} + \sigma_1\sigma_3\big] + W\big[\sigma_5 K_{m3} + \sigma_3\sigma_4 - \gamma_3 k_2 E_{2tot}K_{m1}^2 K_{m3}W_{tot}\big]\\
&-k_2 E_{2tot}K_{m1}^2 K_{m3}^2 W_{tot} = 0
\end{aligned}
$$

where

$$
\begin{aligned}
\sigma_1 &= K_{m3}W_{tot} - K_{m1}K_{m3} + K_{m2}K_{m3} - \gamma_1 E_{1tot}K_{m3} = \gamma_3 K_{m1}K_{m2}\\
\sigma_2 &= k_3(K_{m1} - W_{tot} + \gamma_1 E_{1tot}) - \gamma_3 k_1 E_{1tot}\\
\sigma_3 &= k_1 E_{1tot}K_{m3} + k_3 K_{m3}W_{tot}\\
\sigma_4 &= K_{m1}K_{m2}K_{m3} + K_{m1}K_{m3}W_{tot}\\
\sigma_5 &= \sigma_7 k_2 E_{2tot}K_{m1} - k_2 E_{2tot}K_{m1}K_{m3}W_{tot}\\
\sigma_6 &= \sigma_7 k_2 E_{2tot} + k_2 E_{2tot}K_{m1}K_{m3}\\
\sigma_6 &= K_{m1}K_{m3} - K_{m3}W_{tot} + \sigma_1 E_{1tot}K_{m3}
\end{aligned}
$$

This polynomial can be solve to obtain the steady state concentration of W. This can then be used to calculate the concentrations of W^*, C_1, C_2, and C_3 using equations (132), (129), (128), and (134) respectively.

$$W^* = W_{tot} - W - C_1 - C_2 - C_3 \tag{137}$$

$$C_1 = \frac{E_{1tot}W}{K_{m1}+W} \tag{138}$$

$$C_2 = \frac{k_1}{k_2}C_1 + \frac{k_3}{k_2}C_3 \tag{139}$$

$$C_3 = \frac{W(W_{tot}-W-\gamma_1 C_1)}{K_{m3}+\gamma_3 W} \tag{140}$$

B.6 Derivation of Analytic Solution to System 3

Here we include the attempt at the derivation of an analytic solution to System 3. This system is described by the system of equations (45)-(52) and (56)-(58) in Section 3.1. These are also included below.

Mass action equations:

$$\frac{\mathrm{d}W}{\mathrm{d}t} = d_1C_1 + k_2C_2 + d_4c_4 - a_1WE_1 - a_4WC_3, \tag{141}$$
$$\frac{\mathrm{d}W^*}{\mathrm{d}t} = k_1C_1 + d_2C_2 + d_3C_3 + k_4C_4 - a_2W^*E_2 - a_3W^*E_1, \tag{142}$$
$$\frac{\mathrm{d}E_1}{\mathrm{d}t} = d_1C_1 + k_1C_1 + d_3C_3 - a_1WE_1 - a_3W^*E_1, \tag{143}$$
$$\frac{\mathrm{d}E_2}{\mathrm{d}t} = d_2C_2 + k_2C_2 - a_2W^*E_2, \tag{144}$$
$$\frac{\mathrm{d}C_1}{\mathrm{d}t} = a_1WE_1 - d_1C_1 - k_1C_1, \tag{145}$$
$$\frac{\mathrm{d}C_2}{\mathrm{d}t} = a_2W^*E_2 - d_2C_2 - k_2C_2, \tag{146}$$
$$\frac{\mathrm{d}C_3}{\mathrm{d}t} = a_3W^*E_1 + d_4C_4 + k_4C_4 - d_3C_3 - a_4WC_3 \tag{147}$$
$$\frac{\mathrm{d}C_4}{\mathrm{d}t} = a_4WC_3 - d_4C_4 - k_4C_4. \tag{148}$$

Conservation equations:

$$W_{tot} = W + W^* + C_1 + C_2 + C_3 + C_4, \tag{149}$$
$$E_{1tot} = E_1 + C_1 + C_3 + C_4, \tag{150}$$
$$E_{2tot} = E_2 + C_2. \tag{151}$$

For this system to be at steady state we require the production of the modified substrate to be equal to the production of the unmodified substrate i.e.

$$k_1C_1 + k_4C_4 = k_2C_2 \tag{152}$$

To then develop a solution for the substrates we need to express C_1, C_2, and C_4 as a function of measurable quantities. The equation for C_2 is obtained using the same method as Appendix A.3 for equation (92) to get

$$C_2 = \frac{E_{2tot}W^*}{K_{m2} + W^*} \tag{153}$$

where $K_{m2} = \frac{d_2+k_2}{a_2}$. For C_1 we are unable to use the same method as we have altered the conservation equation for E_{1tot}. When we examine equation (148), in order to acquire an expression for C_4, we require an expression for C_3 first. To obtain this expression we examine equations (147) and (148) at steady state to obtain,

$$K_dC_3 = W^*E_1 \tag{154}$$

where $K_d = \frac{d_3}{a_3}$ is the dissociation rate. We must now remove the dependence on E_1 by using equation (150) to obtain $E_1 = E_{1tot} - C_1 - C_3 - C_4$. Substituting this in gives,

$$K_d C_3 = W^*(E_{1tot} - C_1 - C_3 - C_4) \tag{155}$$

At this point we can observe that C_1 and C_4 are dependent on W and C_2 and C_3 are dependent on W^*. We want to remove this dependence on both forms of substrate. We begin by trying to remove the dependence on W. We can do this by starting to remove the complexes that are dependent i.e. C_1 and C_4 by using equation (152) to obtain an expression for C_1, $C_1 = \alpha_2 C_2 - \alpha_4 C_4$, where $\alpha_* = \frac{k_*}{k_1}$. Substituting this in to equation (155) gives

$$K_d C_3 = W^*(E_{1tot} - \alpha_2 C_2 - C_3 - \gamma_4 C_4) \tag{156}$$

where $\gamma_4 = 1 - \alpha_4 = 1 - \frac{k_4}{k_1}$. By now substituting in the function for C_2 (equation (153)) and rearranging this we can obtain an expression for C_3.

$$C_3 = \frac{W^*[(E_{1tot} - \gamma_4 C_4)(K_{2m} + W^*) - \alpha_2 E_{2tot} W^*]}{(K_d + W^*)(K_{2m} + W^*)} \tag{157}$$

To now obtain an expression for C_4 we need to investigate equation (148) at steady state.

$$K_{m4} C_4 = W C_3$$

where $K_{m4} = \frac{d_4 + k_4}{a_4}$.

To remove the dependence on W we use equation (149), $W = W_{tot} - W^* - C_1 - C_2 - C_3 - C_4$, and the rearranged form of equation (152), $C_1 = \frac{k_2}{k_1} C_2 - \frac{k_4}{k_1} C_4$, to obtain,

$$K_{m4} C_4 = (W_{tot} - W^* - \gamma_2 C_2 - C_3 - \gamma_4 C_4) C_3$$

where $\gamma_2 = 1 + \alpha_2 = 1 + \frac{k_2}{k_1}$. We can now substitute in for C_3 using equation (157), and rearrange to obtain,

$$\begin{aligned}
0 = &\big[(W_{tot} - W^* - \gamma_4 C_4)(K_{2m} + W^*)(K_d + W^*) - \gamma_2 E_{2tot} W^*(K_d + W^*) \\
&- W^*[(E_{1tot} - \gamma_4 C_4)(K_{2m} + W^*) \\
&- \alpha_2 E_{2tot} W^*]\big] W^*[(E_{1tot} - \gamma_4 C_4)(K_{2m} + W^*) - \alpha_2 E_{2tot} W^*] \\
&- K_{4m} C_4 (K_d + W^*)^2 (K_{2m} + W^*)^2
\end{aligned}$$

This can then be rearranged to obtain a quadratic in C_4 whereby the roots of that quadratic will give the concentrations of C_4. These are found by using Matlab solvers to ensure that this is still a function of W^* and other measurable quantities. By further analysis it is found that there is a common denominator between these roots. To attempt an simplify the process for later on, the roots of C_4 are used by,

$$C_4 = \frac{C_4^*}{2K_d W^* \gamma_4^2 (K_{2m} + W^*)} \tag{158}$$

where $C_4^* = \bar{C}_4[2K_d W^* \gamma_4^2 (K_{2m} + W^*)]$ to remove the W^* from the denominator of the calculated roots, $\bar{C}_4$.

We now want to find an expression for C_1 using equation (145) at steady state.

$$K_{m1} C_1 = W E_1$$

where $K_{m1} = \frac{d_1 + k_1}{a_1}$. Using equations (149) and(152), for W and E_1 respectively, we obtain,

$$K_{m1} C_1 = (W_{tot} - W^* - C_1 - C_2 - C_3 - C_4)(E_{1tot} - C_1 - C_3 - C_4)$$

We now substitute in the functions for C_2, C_3 and C_4 from equations (153), (157) and (158) and rearrange to obtain,

$$\begin{aligned}
0 = \\
&\Big[2K_d W^* \gamma_4^2 (K_{2m} + W^*)^2 (K_d + W^*)(W_{tot} - W^* - C_1) - E_{2tot} {W^*}^2 2K_d \gamma_4^2 (K_{2m} + W^*)(K_d + W^*) \\
&- W^*[(2E_{1tot} K_d W^* \gamma_4^2 (K_{2m} + W^*) - \gamma_4 C_4^*)(K_{2m} + W^*) - 2\alpha_2 K_d {W^*}^2 \gamma_4^2 E_{2tot}(K_{2m} + W^*)] \\
&- C_4^*(K_{2m} + W^*)(K_d + W^*)\Big]\Big[(E_{1tot} - C_1) 2K_d W^* \gamma_4^2 (K_{2m} + W^*)^2 (K_d + W^*) \\
&- W^*[(2E_{1tot} K_d W^* \gamma_4^2 (K_{2m} + W^*) - \gamma_4 C_4^*)(K_{2m} + W^*) - 2\alpha_2 K_d {W^*}^2 \gamma_4^2 E_{2tot}(K_{2m} + W^*)] \\
&- C_4 * (K_{2m} + W^*)(K_d + W^*)\Big] - 4K_{1m} C_1 K_d^2 {W^*}^2 \gamma_4^4 (K_{2m} + W^*)^4 (K_d + W^*)^2
\end{aligned}$$

This can then be expanded and rearranged to obtain a quadratic in C_1. Since these roots are dependent on the value of C_4^*, we have to find roots for based on the two possible values of C_4^* separately, which will give four possible roots of $\bar{C}_1$. Similar to C_4 the roots still have a dependence on W^*. These roots will once again all have a common denominator so C_1 can be expressed by,

$$C_1 = \frac{C_1^*}{2K_d W^* \gamma_4^2 (K_{2m} + W^*)} \tag{159}$$

where $C_1^* = (2K_d W^* \gamma_4^2 (K_{2m} + W^*))\bar{C}_1$.

We can now find an expression for W^* by substituting in the equations for C_1, C_2 and C_4 (equations (159), (153) and (158)) into equation (152) and rearranging to obtain,

$$0 = (k_1 C_1^* + k_4 C_4^*)(K_{2m} + W^*) - 2k_2 K_d E_{2tot} \gamma_4^2 {W^*}^2 (K_{2m} + W^*) \tag{160}$$

By solving this equation with the four possible combinations of values for C_1^* and C_4^* we obtain an expression for W^* that is not a polynomial. Plotting this has shown that there is at most two roots within the domain of W^*. The roots are then found by using 'fzero'.

We then calculate the other variables using the functions for C_2, and C_3 and recalculating the roots for C_4. To obtain a result for C_1 we use the rearranged version of equation (152) whereby $C_1 = \frac{k_2}{k_1} C_2 - \frac{k_4}{k_1} C_4$. We then obtain a value for W, E_1 and E_2 using the conservation equations associated with those concentrations.

5 Bibliography

References

[1] M Abiola, M Favier, E Christodoulou-Vafeiadou, A-L Pichard, I Martelly, and I Guillet-Deniau. Activation of Wnt/β-Catenin Signaling Increases Insulin Sensitivity Through a Reciprocal Regulation of Wnt10b and SREBP-1c in Skeletal Muscle Cells. *PloS one*, 4(12):e8509, 2009.

[2] GS Adair. The Hemoglobin System vi. The Oxygen Dissociation Curve of Hemoglobin. *Journal of Biological Chemistry*, 63(2):529–545, 1925.

[3] U Alon. *An Introduction to Systems Biology: Design Principles of Biological Circuits*. Chapman and Hall/CRC, 2006.

[4] U Alon, MG Surette, N Barkai, and S Leibler. Robustness in bacterial chemotaxis. *Nature*, 397(6715):168, 1999.

[5] E Altszyler, A Ventura, A Colman-Lerner, and A Chernomoretz. Impact of upstream and downstream constraints on a signaling module's ultrasensitivity. *Physical Biology*, 11(6):066003, 2014.

[6] NL Anderson, AD Matheson, and S Steiner. Proteomics: applications in basic and applied biology. *Current Opinion in Biotechnology*, 11(4):408–412, 2000.

[7] RP Araujo and LA Liotta. A control theoretic paradigm for cell signaling networks: a simple complexity for a sensitive robustness. *Current Opinion in Chemical Biology*, 10(1):81–87, 2006.

[8] RP Araujo and LA Liotta. The topological requirements for robust perfect adaptation in networks of any size. *Nature Communications*, 9(1):1757, 2018.

[9] N Barkai and S Leibler. Robustness in simple biochemical networks. *Nature*, 387(6636):913, 1997.

[10] N Ben-Zvi, Dand Barkai. Scaling of morphogen gradients by an expansion-repression integral feedback control. *Proceedings of the National Academy of Sciences*, 107(15):6924–6929, 2010.

[11] N Blüthgen, FJ Bruggeman, S Legewie, H Herzel, HV Westerhoff, and BN Kholodenko. Effects of sequestration on signal transduction cascades. *The FEBS Journal*, 273(5):895–906, 2006.

[12] GE Briggs and JBS Haldane. A Note on the Kinetics of Enzyme Action. *Biochemical Journal*, 19(2):338, 1925.

[13] PB Chock and ER Stadtman. Superiority of interconvertible enzyme cascades in metabolic regulation: Analysis of multicyclic systems. *Proceedings of the National Academy of Sciences*, 74(7):2766–2770, 1977.

[14] MP Czech. PIP2 and PIP3: Complex Roles at the Cell Surface. *Cell*, 100(6):603–606, 2000.

[15] H El-Samad, JP Goff, and M Khammash. Calcium Homeostasis and Parturient Hypocalcemia: An Integral Feedback Perspective. *Journal of Theoretical Biology*, 214(1):17–29, 2002.

[16] A Eldar, R Dorfman, D Weiss, H Ashe, B-Z Shilo, and N Barkai. Robustness of the bmp morphogen gradient in drosophila embryonic patterning. *Nature*, 419(6904):304, 2002.

[17] V Espina, AI Mehta, ME Winters, V Calvert, J Wulfkuhle, EF Petricoin III, and LA Liotta. Protein microarrays: molecular profiling technologies for clinical specimens. *Proteomics*, 3(11):2091–2100, 2003.

[18] JE Ferrell and SH Ha. Ultrasensitivity Part II: Multisite phosphorylation, stoichiometric inhibitors, and positive feedback. *Trends in Biochemical Sciences*, 39(11):556–569, 2014.

[19] JE Ferrell Jr. Building a cellular switch: more lessons from a good egg. *Bioessays*, 21(10):866–870, 1999.

[20] JE Ferrell Jr and SH Ha. Ultrasensitivity Part I: Michaelian responses and zero-order ultrasensitivity. *Trends in Biochemical Sciences*, 39(10):496–503, 2014.

[21] JE Ferrell Jr and SH Ha. Ultrasensitivity Part III: Cascades, bistable switches, and oscillators. *Trends in Biochemical Sciences*, 39(12):612–618, 2014.

[22] D Figeys. Novel approaches to map protein interactions. *Current opinion in biotechnology*, 14(1):119–125, 2003.

[23] EH Fischer and EG Krebs. Conversion of Phosphorylase b to Phosphorylase a in Muscle Extracts. *Journal of Biological Chemistry*, 216(1):121–132, 1955.

[24] R Gesztelyi, J Zsuga, A Kemeny-Beke, B Varga, B Juhasz, and A Tosaki. The Hill equation and the origin of quantitative pharmacology. *Archive for History of Exact Sciences*, 66(4):427–438, 2012.

[25] DT Gillespie. Exact stochastic simulation of coupled chemical reactions. *The journal of physical chemistry*, 81(25):2340–2361, 1977.

[26] A Goldbeter and DE Koshland Jr. An amplified sensitivity arising from covalent modification in biological systems. *Proceedings of the National Academy of Sciences*, 78(11):6840–6844, 1981.

[27] CM Guldberg and P Waage. *Studier over Affiniteten, I, II, og III.* NTH-Trykk, 1864.

[28] CM Guldberg and P Waage. *Etudes sur les affinités chimiques.* Brøgger & Christie, 1867.

[29] J Gunawardena. Some lessons about models from Michaelis and Menten. *Molecular Biology of the Cell*, 23(4):517–519, 2012.

[30] Y Hart, D Madar, J Yuan, A Bren, AE Mayo, JD Rabinowitz, and U Alon. Robust control of nitrogen assimilation by a bifunctional enzyme in e. coli. *Molecular cell*, 41(1):117–127, 2011.

[31] AV Hill. The Possible Effects Of The Aggregation Of The Molecules Of Haemoglobin On Its Dissociation Curves. *J. Physiol.*, 40:4–7, 1910.

[32] AV Hill. The Combinations of Haemoglobin with Oxygen and with Carbon Monoxide. I. *Biochemical Journal*, 7(5):471, 1913.

[33] O Hoeller, D Gong, and OD Weiner. How to understand and outwit adaptation. *Developmental cell*, 28(6):607–616, 2014.

[34] B Horowitz. What are Enzymes? *The Scientific Monthly*, 6(3):253–259, 1918.

[35] C-Y Huang and JE Ferrell. Ultrasensitivity in the mitogen-activated protein kinase cascade. *Proceedings of the National Academy of Sciences*, 93(19):10078–10083, 1996.

[36] KA Johnson and RS Goody. The Original Michaelis Constant: Translation Of The 1913 Michaelis–Menten Paper. *Biochemistry*, 50(39):8264–8269, 2011.

[37] C-M Kim, K Koike, I Saito, T Miyamura, and G Jay. Hbx gene of hepatitis b virus induces liver cancer in transgenic mice. *Nature*, 351(6324):317, 1991.

[38] EC Kohn, Y Lu, H Wang, Q Yu, S Yu, H Hall, DL Smith, F Meric-Bernstam, GN Hortobagyi, and GB Mills. Molecular therapeutics: promise and challenges. In *Seminars in oncology*, volume 31, pages 39–53. Elsevier, 2004.

[39] DE Koshland Jr, G Némethy, and D Filmer. Comparison of Experimental Binding Data and Theoretical Models in Proteins Containing Subunits. *Biochemistry*, 5(1):365–385, 1966.

[40] EG Krebs and EH Fischer. The Phosphorylase b to a Converting Enzyme of Rabbit Skeletal Muscle. *Biochimica et biophysica acta*, 20:150–157, 1956.

[41] D Lazard. Gröbner bases, gaussian elimination and resolution of systems of algebraic equations. In *European Conference on Computer Algebra*, pages 146–156. Springer, 1983.

[42] H Li, L Zhao, Z Yang, JW Funder, and J-P Liu. Telomerase is controlled by protein kinase cα in human breast cancer cells. *Journal of Biological Chemistry*, 273(50):33436–33442, 1998.

[43] LA Liotta, V Espina, AI Mehta, V Calvert, K Rosenblatt, D Geho, PJ Munson, L Young, J Wulfkuhle, and EF Petricoin III. Protein microarrays: meeting analytical challenges for clinical applications. *Cancer cell*, 3(4):317–325, 2003.

[44] L Michaelis and ML Menten. *Die Kinetik der Invertinwirkung*. Universitätsbibliothek Johann Christian Senckenberg, 2007.

[45] JD Murray. Mathematical Biology. I, Volume 17 of Interdisciplinary Applied Mathematics, 2002.

[46] D Muzzey, CA Gómez-Uribe, JT Mettetal, and A van Oudenaarden. A systems-level analysis of perfect adaptation in yeast osmoregulation. *Cell*, 138(1):160–171, 2009.

[47] L Pauling. The Oxygen Equilibrium of Hemoglobin And Its Structural Interpretation. *Proceedings of the National Academy of Sciences*, 21(4):186–191, 1935.

[48] R Speer, JD Wulfkuhle, LA Liotta, and EF Petricoin. Reverse-phase protein microarrays for tissue-based analysis. *Current opinion in molecular therapeutics*, 7(3):240–245, 2005.

[49] ER Stadtman and PB Chock. Superiority of interconvertible enzyme cascades in metabolic regulation: Analysis of monocyclic systems. *Proceedings of the National Academy of Sciences*, 74(7):2761–2765, 1977.

[50] K Taketa and BM Pogell. Allosteric Inhibition of Rat Liver Fructose 1, 6-Diphosphatase by Adenosine 5'-Monophosphate. *Journal of Biological Chemistry*, 240(2):651–662, 1965.

[51] AC Ventura, J-A Sepulchre, and SD Merajver. A Hidden Feedback in Signaling Cascades is Revealed. *PLoS Computational Biology*, 4(3):e1000041, 2008.

[52] B Vogelstein and KW Kinzler. Cancer genes and the pathways they control. *Nature medicine*, 10(8):789, 2004.

[53] EO Voit, HA Martens, and SW Omholt. 150 Years of the Mass Action Law. *PLoS Computational Biology*, 11(1):e1004012, 2015.

[54] Peter Waage and Cato Maximilian Gulberg. Studies concerning affinity: Translation by henry i. brash. *Journal of Chemical Education*, 63(12):1044, 1986.

[55] A Wagner. *Robustness and evolvability in living systems*, volume 24. Princeton university press, 2007.

[56] DA Walsh, JP Perkins, and EG Krebs. An Adenosine 3', 5'-Monophosphate-Dependant Protein Kinase From Rabbit Skeletal Muscle. *Journal of Biological Chemistry*, 243(13):3763–3765, 1968.

[57] J Wulfkuhle, V Espina, L Liotta, and E Petricoin. Genomic and proteomic technologies for individualisation and improvement of cancer treatment. *European Journal of Cancer*, 40(17):2623–2632, 2004.